Dissertation

submitted to the
Combined Faculties for the Natural Sciences and for Mathematics
of the Ruperto-Carola University of Heidelberg, Germany
for the degree of
Doctor of Natural Sciences

Presented by

Master of Technology (Biotechnology)
Venkata Sai Badireenath, Konkimalla
Born in
Jaggayyapeta, India

Oral-examination :

Studies on the optimization of expression and purification
&
Functional characterization of Class C – GPCRs

Refrees:

Prof. Dr. Irmgard Sinning
Prof. Dr. Felix Wieland

Contents

III.RESULTS

Acknowledgments

❖ First of all I would like to thank Prof. Dr. Irmi Sinning for giving me the opportunity to work for my doctoral thesis in her lab in the Biochemie Zentrum Heidelberg (BZH)/Centre for Biochemistry in the Faculty of Biology of the Ruprecht-Karls University of Heidelberg.

❖ I am extremely grateful to her for supervising me during my period in her lab. I am also indebted to Prof. Dr. Felix Wieland for being my second supervisor, and also to Prof. Dr. Nils Metzler-Nolte for his invaluable help and suggestions during the preparation of this thesis.

❖ I am thankful to Valerie for her guidance in the project, Bernd for his excellent technical assistance and Marion for helping me with all paper work. Astrid, Oliver, Christina and other lab members for their constant encouragement.

❖ I am grateful to Prof. Dr. Rohini Kuener for her timely help and to the lab members for a pleasant environment. I am thankful to Rose for clearing all my bugging questions regarding the paper work.

❖ I am extremely grateful to my German family, Mrs & Mr. Graf, for the care and help.

❖ My special thanks to another GPCR, multigene family, my Indian family (HISA group). I am extremely grateful to everyone for helping and supporting me in all possible ways (Unfortunately, both the list of people and the help rendered is inexhaustible so couldn't mention anyone in particular).

❖ And last but not the least, I am grateful to my family and all the friends back home for their affection, support and love.

Abbreviations

BSA   Bovine serum albumin

cDNA   Complementary DNA

cGH   Chicken growth hormone

DmGluRA   Drosophila metabotropic glutamate receptor A

DRMs   Detergent resistant membranes

ECD   Extracellular domain

GABA   Gamma amino butyric acid

GBR1bNT   Metabotropic $GABA_B$1b receptor

GPCR   G protein coupled receptor

GPI   Glycosyl-phosphatidyl inositol

GST   Glutathione S-transferase

IC50   Inhibitory concentration at 50%

kDa   Kilo Dalton

LBD   Ligand binding domain

LIVbp   Leucine, Isoleucine, Valine binding protein

MOI   Multiplicity of infection

MβCD   Methyl β̃-cyclo dexrin

pCBM   Putative cholesterol binding motif

PCR   Polymerase chain reaction

PERL   Practical Extraction and Report Tool

PMSF   Para-methyl sulphonate

RBV   Recombinant baculovirus

RMSD   Root mean square deviation

SDS   Sodium dodecyl sulphate

SEM   Standard Error of Mean

TEV   Tobacco etch virus

TM   Transmembrane

VS   Viral stocks

Summary

G-protein coupled receptor (GPCRs) is a multigene family consisting of more than 1000 genes. They are the most abundant membrane proteins found on a cell surface and are involved in several signaling pathways. In a cell, the signal is transduced by diverse activating endogenous ligands binding on the extracellular surface. This results in the uncoupling of G-proteins from the cytoplasmic loops, leading to the activation of the second messengers. GPCRs have enormous therapeutic importance due to their involvement in basic physiological processes including sensory perception, neurotransmission, metabolism, hormonal balance, etc. Structural and biochemical data are the pre-requisites for designing the drugs involving GPCRs.

The current study was focused on the optimization of expression, purification and functional characterization of class-C GPCRs involved in neurotransmission. The first part of the study was aimed at optimizing the expression and purification of the ligand binding extracellular domain (ECD) of rat metabotropic $GABA_B1b$ receptor (GBR1bNT) in the recombinant baculovirus (RBV) and *E.coli* expression systems. GBR1bNT was modeled based on the crystal structure coordinates of ECD of metabotropic glutamate receptor (mGluR). Depending on this GBR1bNT model, molecular cloning strategies were developed for the expression of GBR1bNT. In both systems, GBR1bNT was well expressed and purified.

The second part of the study was aimed at biochemical characterization of a putative cholesterol binding motif (pCBM) in Drosophila metabotropic glutamate receptor (DmGluRA). This pCBM might be involved in regulating the binding of DmGluRA to glutamate with high affinity. During the study, it was inferred that a 12-amino-acid amphipathic peptide containing the pCBM might be crucial for the activity of the receptor. Upon conducting [^{3}H]-glutamate binding and detergent-resistant-membrane (DRM) association studies on different truncation constructs of DmGluRA (1-910 amino acids), the N-terminal construct (1-624 amino acids) containing the ECD with one single pCBM was found to be capable of binding glutamate in high affinity state as observed with the full length DmGluRA.

Together this study shows that 1) Using an interdisciplinary approach (computational and experimental strategies) GBR1bNt was efficiently expressed and purified in both *E.coli* and RBV expression systems and 2) the role of pCBM was studied in DmGluRA receptor regulation.

Zusammenfassung

G-Protein gekoppelte Rezeptoren (GPCRs) gehören zu einer Multigen-Familie mit mehr als 1000 Genen. Sie bilden die größte Gruppe der Membranproteine auf der Zelloberfläche und sind an einer Vielzahl von Signaltransduktions-Wegen beteiligt. In einer Zelle wird ein Signal übertragen, indem aktivierende endogene Liganden extrazellulär an die GPCRs binden. Dies führt zu einer Abspaltung von G-Proteinen von den cytoplasmatischen loops des Rezeptors und damit zur Aktivierung von sekundären Signalmolekülen (second messengers), welche die Signalkaskade fortsetzen. GPCRs sind an grundlegenden physiologischen Prozessen beteiligt und spielen somit eine wichtige Rolle bei therapeutischen Ansätzen. Die Aufklärung der Struktur und das Sammeln biochemischer Daten der GPCRs sind Voraussetzung für die Entwicklung von Medikamenten, die diese Prozesse beeinflussen.

Der Schwerpunkt dieser Studie lag auf der Optimierung der Expression, Aufreinigung und der funktionellen Charakterisierung von GPCRs der Klasse C welche an der neuronalen Signalübertragung beteiligt sind. Der erste Teil der Studie zielte auf die Optimierung der Expression und Aufreinigung der extrazellulären Ligandenbindungsstelle (extracellular domain, ECD) des $GABA_B1B$-Rezeptors (Rattus norvegicus) (GBR1bNT) in rekombinanten Baculovirus- (RBV) und E.coli-Expressionssystemen. Basierend auf den Daten der Kristallstruktur der ECD des Glutamatrezeptors mGluR wurde ein Modell für GBR1bNT generiert. Dieses Modell war Grundlage für die Entwicklung molekularer Klonierungsstrategien für die Expression von GBR1bNT. In beiden Systemen konnte GBR1bNT gut exprimiert und aufgereinigt werden.

Der zweite Teil der Studie befasste sich mit der funktionellen Charakterisierung eines putativen Cholesterin-Bindemotivs (putative cholesterol binding motif, pCBM) des Drosophila Glutamat-Rezeptors DmGluRA. Dieses Bindemotiv scheint an der Regulation der Bindung zwischen DmGluRA und Glutamat beteiligt zu sein. Während der Studie konnte ein 12 Aminosäure langes, amphipatisches Peptid identifiziert werden, welches das pCBM enthält und eine entscheidende Rolle bei der Aktivierung des Rezeptors zu spielen scheint. Basierend auf Studien über [^{3}H]-Glutamat-Bindung und Detergenz-resistente Membranassoziation (DRM) für verschiedene verkürzte Formen des DmGluRA (1-910 Aminosäuren) fand man heraus, dass die N-terminale Form (1-624 Aminosäuren), welche die ECD und ein einziges pCBM enthält, mit hoher Affinität an Glutamat binden kann so wie dies auch bei der vollständigen Form des DmGluRA der Fall ist.

I. Introduction

I.1 G-Protein Coupled Receptors

G-protein coupled receptors or GTP-binding protein coupled receptors or GPCRs form a large and diverse multigene super-family of integral membrane proteins (receptors). They act as cell surface receptors responsible for the transduction of endogenous signals into cellular response *via* activation of G-proteins. In human, more than 1000 genes encode for GPCRs (Marinissen and Gutkind, 2001) and are classified into over 100 sub-families based on sequence homology, ligand structure and receptor functions. GPCRs are involved in the regulation of various physiological activities such as neurotransmission, vision, pain perception, hormone secretion, taste, smell and metabolism. There is an enormous therapeutic application for GPCRs in the field of drug discovery.

A number of diseases are known to be associated with mutations in GPCR genes. Such mutations induce one of two phenotypes caused by a loss-of-function or gain-of-function. The diseases caused by GPCR loss-of-function include color blindness, retinitis pigmentosa, Hirschsprung disease and diabetes mellitus. The diseases caused by GPCR gain-of-function include thyroid adenomas, cogenital eye blindness and hyperthyroidism (Spiegel and Weinstein, 2004).

By single-site directed mutagenesis experiments, it is possible to map the ligand-binding domain of these receptors, which would serve as a lead to design synthetic ligands based on knowledge of the structure of the receptor site.

So far, the molecular structure of GPCRs (except bovine rhodopsin) could not be defined by any structure determination techniques such as X-ray crystallography nor NMR. Molecular modelling approaches based on bovine rhodopsin as the structure template has given very few successes (Flower, 1999). Still there are limitations in these molecular modelling approaches such as defining the oligomeric state of the receptor to understand the mechanism of activation and in identifying the allosteric sites involved in the regulation to design ligands for the same.

I.1.1 General description of GPCRs and its classification

There are 2 main criteria for a protein to be classified as a GPCR ((Marinissen and Gutkind, 2001).

First criterion: All GPCRs have an extracellular N-terminal segment, seven transmembrane (TM) helices (that form the TM core), three exoloops, three cytoloops, and a C-terminal segment. A fourth cytoplasmic loop is formed when the C-terminal segment is palmitoylated at the Cysteine residue (Cys^{322} residue in bovine rhodopsin). Each of the seven TM helices is generally composed of characteristic sequence motif, consisting of 20-27 consecutive residues with a relatively high degree of hydrophobicity. These sequences form seven α-helices that span the plasma membrane in a counter-clockwise manner. Hydrogen bonds, salt bridges and disulphide bonds hold the TM core tightly. Moreover, to elicit diverse function, the N-terminal segments (7-595 amino acids), loops (5-230 amino acids), and C-terminal segments (12-359 amino acids) vary in size.

Second criterion: The second principle criterion is the ability of the receptor to interact with a G-protein using its cytoloops.
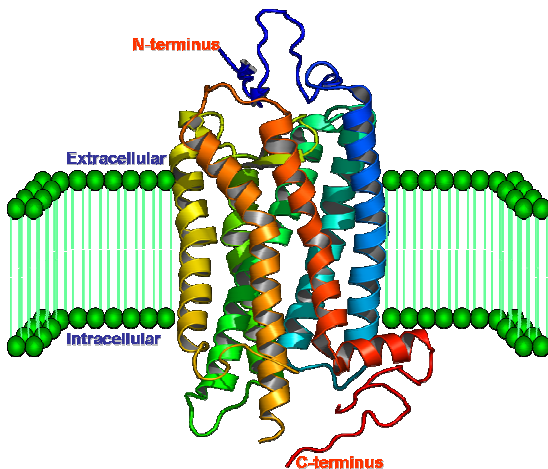
fig 1. **Crystal structure of bovine rhodopsin (PDB code: 1HZX) monomer prepared using PyMOL software; a representative structure of GPCR showing its orientation in the cell membrane.**

These evidences suggest that overall structure of GPCRs is similar to that of bovine rhodopsin (Palczewski et al., 2000). The structure of bovine rhodopsin has been solved experimentally and is composed of seven TM helices forming a flattened two-layered structure (*see fig. 1*). Despite a common pattern of hydrophobic residues and some similarity in function, there is no homology between bovine rhodopsin and GPCR sequences.

GPCRs are divided into Six distinct classes and into to several families within a particular class. There is considerable sequence homology between the members of family under one class, but were less between different classes (Horn et al., 2001).

Class A: Rhodopsin-like receptors

Family I: Olfactory receptors, adenosine receptors, melanocortin receptors, and others

Family II: Biogenic amine receptors

Family III: Vertebrate opsins and neuropeptide receptors

Family IV: Invertebrate opsins

Family V: Chemokine, chemotactic, somatostatin, opioids and others

Family VI: Melatonin receptors and others

Class B: Calcitonin and related receptors

Family I: Calcitonin, calcitonin-like, and CRF receptors

Family II: PTH/PTHrP receptors

Family III: Glucagon, secretin receptors and others

Family IV: Latrotoxin receptors and others

Class C: Metabotropic glutamate and related receptors

Family I: Metabotropic glutamate receptors

Family II: Calcium receptors

Family III: GABA-B receptors (metabotropic receptor)

Family IV: Putative pheromone receptors

Class D: Fungal Pheromone receptors

Family I: fungal pheromone A-factor like, B like, M- and P- factor

Class E: cAMP receptors (Dictyostelium)

Class F: Frizzled/smoothened family

Frizzled receptors
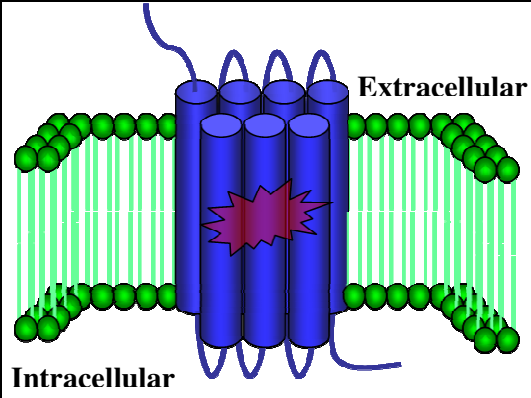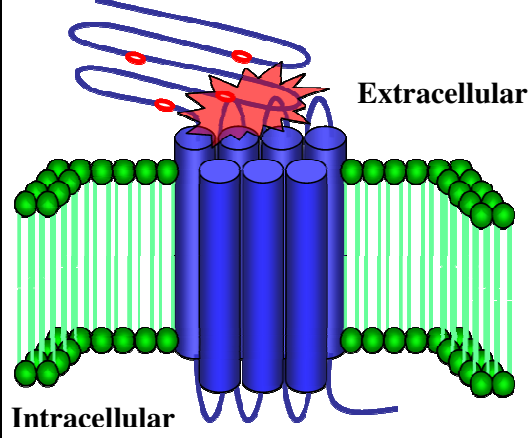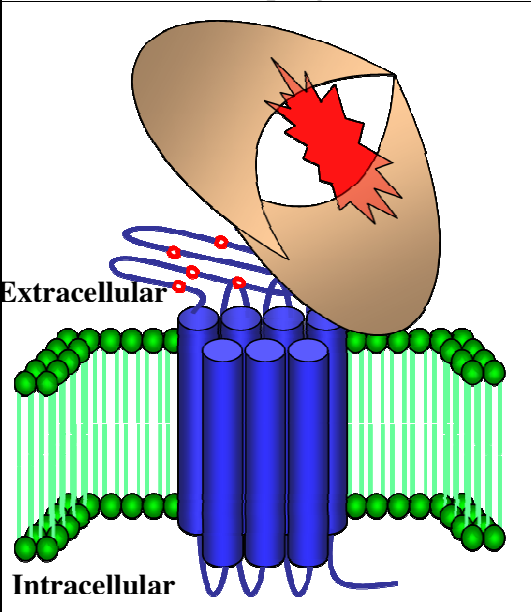
Class A: Rhodopsin-like receptors	
Extracellular **Intracellular**	Consists of a short N-terminal extracellular and C-terminal intracellular tails. Ligand binding occurs in the pocket formed by the transmembrane helices
Class B: Calcitonin and related receptors	
Extracellular **Intracellular**	Apart from the features of Class A GPCR topology, Class B GPCR consists of an N-terminal extracellular cysteine rich domain involved in ligand binding.
Class C: Metabotropic glutamate and related receptors	
Extracellular **Intracellular**	Consists of an N-terminal extracellular domain homologous to Leucine-isoleucine-valine binding proteins (LIVbp like domain) that contributes to ligand binding. Metabotropic glutamate receptors consist of cysteine rich domain between the ligand binding domain and the transmembrane domain on the extracellular domain.

fig 2. **Classification of GPCRs:** All GPCRs share a set of seven transmembrane helices which are weakly homologous to each other and span across the membrane.

I.1.2 Mechanism of GPCR activation, desensitization and internalisation

ß$_2$-adrenergic receptors are the first among the GPCR to be cloned and fully characterized. Site-directed mutagenesis experiments show that the long third cytoplasmic loop is the region of the molecule that couples to the G-protein. Any deletion or modification of this region results in receptors that are still capable of binding the ligand but cannot associate with G-proteins to produce any response.

In class A GPCRs (for example in the Histamine receptors) the receptor activation is achieved by binding of Histamine molecule to the cleft between the α-helical segments within the membrane and uncoupling of the G-protein in the cytoplasmic region.

I.1.3 G-proteins and GPCR activation

G-proteins are heterotrimeric proteins composed of three subunits, α, β and γ. Guanine nucleotides bind to the α-subunit, which possesses enzymatic activity, catalysing the conversion of GTP to GDP. The β- and γ- subunits remain together as a βγ-complex (*see fig 3*). The three subunits are anchored to the plasma membrane through a fatty acid modification, coupled to the G-protein through a reaction known as *prenylation*. G-proteins are diffusible in the plane of the membrane leading to an interaction of a single G-protein with several receptors and effectors involved in several signalling pathways.

fig 3. **Crystal structure of a G-protein heterotrimer.** G-protein heterotrimer is composed of 3 subunits Gα-subunit in yellow with bound GDP shown in ball and stick, Gβ-subunit in blue and Gγ-subunit in green. The figure was prepared using PyMOL PDB code : 1GP2 .
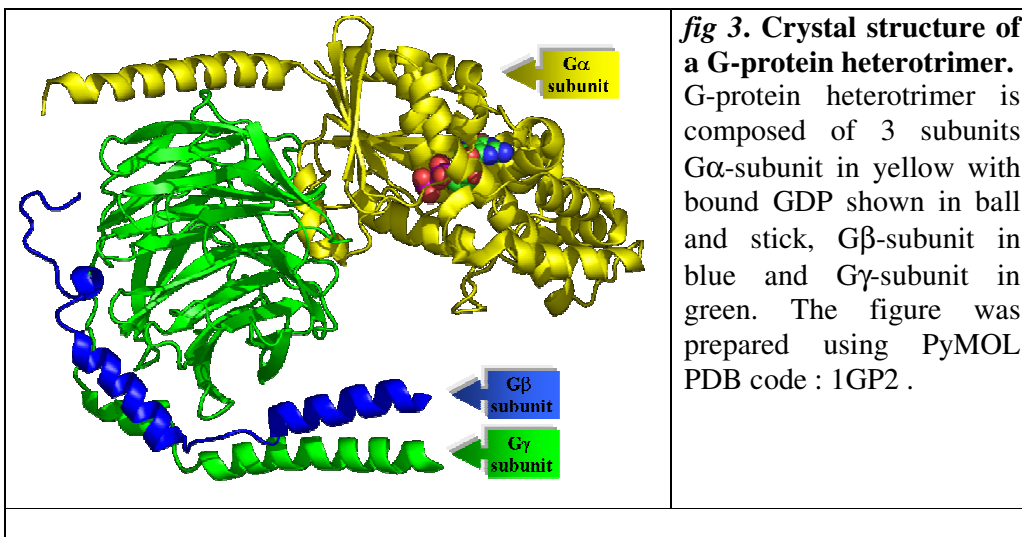
In the resting state, the G-protein exists as an unattached αβγ-trimer, with Gα-subunit in GDP bound state. When an agonist molecule binds to GPCR, a conformational change occurs involving the cytoplasmic domain of the receptor causing it to acquire high affinity for the G-protein αβγ-trimer. Association of αβγ-trimer with the receptor causes the bound GDP to dissociate and exchange with GTP followed by the dissociation of the trimeric complex, releasing the Gα-GTP complex and βγ-subunits; these are the active forms of the G-protein (Marinissen and Gutkind, 2001) (*see fig a*).
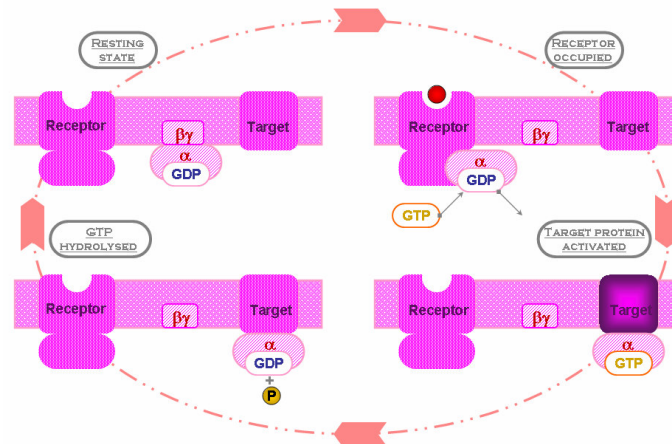
Fig. 4a. Mechanism of GPCR activation and effector systems of G-proteins.
G-proteins exist as unattached αβγ-trimer, with Gα-subunit in GDP bound state, in the resting state. Upon agonist molecule binds to GPCR, a conformational change occurs involving the cytoplasmic domain of the receptor causing it to acquire high affinity for the G-protein αβγ-trimer. Association of αβγ-trimer with the receptor causes the bound GDP to dissociate and exchange with GTP followed by the dissociation of the trimeric complex, releasing the Gα-GTP complex and βγ-subunits. (Adopted from Rang and Dale, Pharmacology, 5th ed.)

The Gα–GTP complex diffuse in the membrane and associate with various effector enzymes, such as adenylyl or guanylyl cyclase, phospholipase A2 or C, inhibiting or stimulating production of second messengers including cAMP, cGMP, diacyl glycerol, and IP3, which in turn cause downstream effects including the opening of Ca^{2+} or K^+ channels (Hamm, 1998) and generation of other messengers, such as arachidonic and phosphatidic acid (*see fig 4, bottom*).
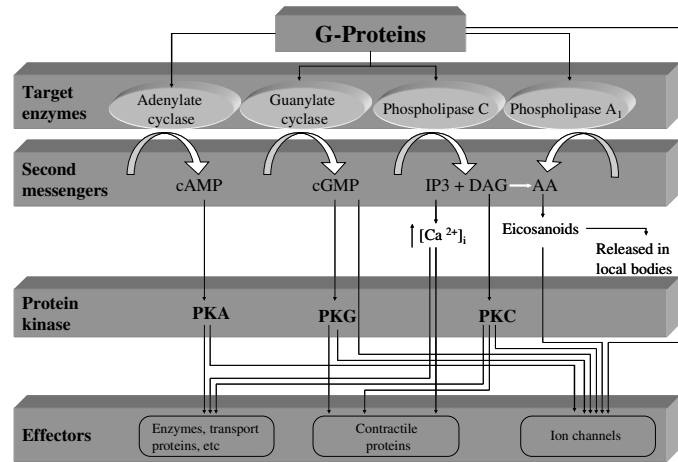
Fig. 4b. Various effector system associated with G-proteins.
The Gα–GTP complex triggers the signaling cascade by associating with the target enzymes; that further triggers the second messengers leading to the activation of protein kinases and finally reaching the effectors. (adopted from Rang and Dale, Pharmacology, 5th ed.)

Many GPCRs are also known to activate MAP kinase signalling pathways. This process is dependent upon GPCR endocytosis and involves a G-protein mediated pathway involving tyrosine kinase phosphorylation of a series of adaptor proteins. GPCR signaling is a complex system involving a variety of mechanisms that include regulatory feedback desensitization mediated by protein kinase phosphorylation of different types since a particular GPCR can interact with more than one kind of G-protein.

I.2 Class C G-Protein Coupled Receptor

Class C GPCRs have several characteristic features, which include a large extracellular N-terminus often referred to as *Venus flytrap* that plays a critical role in ligand binding, followed by seven closely spaced putative transmembrane domains, typical of GPCRs. The *metabotropic glutamate receptor (mGluR)* and the *metabotropic GABA$_B$ receptor (GABA$_B$R)* belong to this class of GPCRs. The third intracellular loop in this class of GPCR is short and highly conserved and known to be crucial for G-protein activation, whereas the second intracellular loop is crucial for G-protein coupling selectivity. The carboxy-terminal intracellular tail is the most variable region of these receptors and is subject to natural truncations by alternative splicing of the mRNA. Moreover, this region of mGluRs is shown to interact with multiple interacting proteins such as the Homer proteins. When compared with mGluRs, GABA$_B$R1 shares only 18-23% sequence similarity, but structural architecture indicates clear conservation between these receptors.

Sequence analysis by O'Hara and co-workers on the ligand binding domain (LBD) of mGluRs and GABA$_B$Rs showed that these domains possessed a considerable similarity with the *Leucine, Isoleucine, Valine binding protein (LIVbp)* (Olah et al., 1993). LIVbp is a bacterial periplasmic protein (PBP) capable of binding the amino acids leucine, isoleucine and valine. LIVbp is expressible in soluble form and the X-ray structure reveals a binding pocket that is made up by two globular lobes (lobes I and II) separated by a hinge region. The two lobes close upon ligand binding, similar to a Venus flytrap when touched by an insect (Quiocho and Ledvina, 1996). The crystal structure of LIVbp served as a template in the construction of a theoretical three-dimensional model for the LBD of mGluRs and GABA$_B$Rs. Thus, derived theoretical model gave considerable amount of information in understanding the architecture/scaffold of the receptor at the binding pockets and the key residues involved in the selectivity for binding the ligands, Glutamate and GABA to the LBD of mGluR and GABA1bR respectively.

I.2.1 GPCR dimerization- Dimers in class C GPCRs

For many years it was assumed that GPCRs exist and function in monomeric species. Studies on GPCR-GPCR interactions show that all GPCRs may not be

monomeric but can exist as dimers or higher order oligomers. There have been evidences reporting that GPCR-GPCR interactions occur initially during biosynthesis, get N-terminally glycosylated to form the mature form before being exported from the golgi apparatus (Robbins et al., 1999).

Modelling approaches in understanding the mechanism of activation and structural organisation of rhodopsin also support the fact that it exists as dimer. It is proposed that a dimer of rhodopsin would be required to bind single heterotrimeric G protein consisting of transducin α and β1 + γ1complex (Liang et al., 2003).

Class C GPCRs are classical examples of GPCRs that function as dimers. Metabotropic glutamate receptors exist as homodimers (*see fig. 5a*) formed by covalent and noncovalent interactions and that each dimeric unit can couple to two sets of G-proteins to trigger the signalling pathway. Romano et al were the first to show that mGlu5 receptor exist in a dimeric form not only in heterologous expression systems but also in the brain (Romano et al., 2001). Since then this has been confirmed with many other class-C GPCRs, including most other mGluRs, the Ca^{2+} sensing receptor, the $GABA_B$ receptor and the taste receptors.

A. Metabotropic $GABA_B$ receptor (Heterodimers)

B. Metabotropic Glutamate receptor (Homodimers)
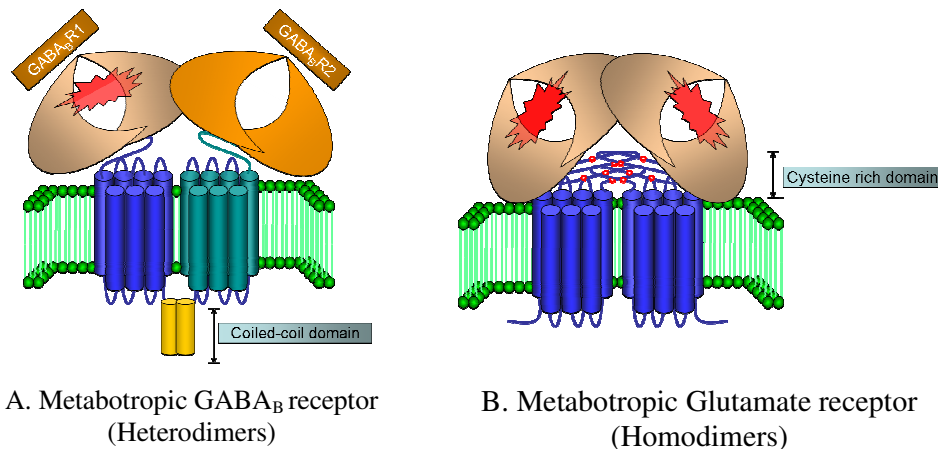
Fig 5. **Types of dimers observed in Class C GPCRs and the domains involved in the dimerzation.**

In many cases, only homodimers have been described, but the $GABA_B$ receptors as well as the taste receptors were found to form heteromers (see fig. 5b). In all class-C GPCRs except the $GABA_B$ receptor, the two subunits are linked by a disulfide

bridge at the extracellular level, which indicates that such dimers are likely to be constitutive. Mutation of the cysteines involved in the disulphide bridge does not prevent the receptors from dimerizing, indicating the other regions are involved in the formation of the dimer and that the disulphide bridge firmly stabilizes the dimer.

The functional heterodimeric metabotropic $GABA_B$ receptor unit is formed by interactions between the alternatively splice variants $GABA_B1b$ and $GABA_B2$ receptors. Chimeric and truncation constructs on $GABA_B1b$ and $GABA_B2$ show that the heterodimeric receptor is activated by a phenomenon called ***transactivation****,* wherein the ligand binds the extracellular domain (ECD) of the $GABA_B1b$ unit and the G-protein is uncoupled from the cytosolic loop region of the $GABA_B2$ subunit.

I.3 Metabotropic GABA$_B$ receptor

Gamma-amino butyric acid (GABA) is a primary inhibitory neurotransmitter in the mammalian central nervous system and mediates its action via distinct receptor systems, the ionotropic GABA$_A$ and metabotropic GABA$_B$ receptors. It exerts fast and powerful synaptic inhibition by acting on GABA$_A$ receptors. These receptors are directly coupled to an integral chloride channel and produce inhibition by increasing the membrane chloride conductance. This form of synaptic inhibition is critical for maintaining and shaping the neuronal communication.

However, like other neurotransmitters that activate fast, ionotropic responses lasting for milliseconds, GABA can also activate a second class of receptors that produce slow synaptic responses capable of lasting for seconds. The receptors producing these slow, metabotropic responses are called *GABA$_B$ receptor (GABA$_B$Rs)*. They play an important role in regulating neurotransmission, which makes them potentially important therapeutic targets in the treatment of a variety of neurological conditions including epilepsy, spasticity, pain and psychiatric illness.
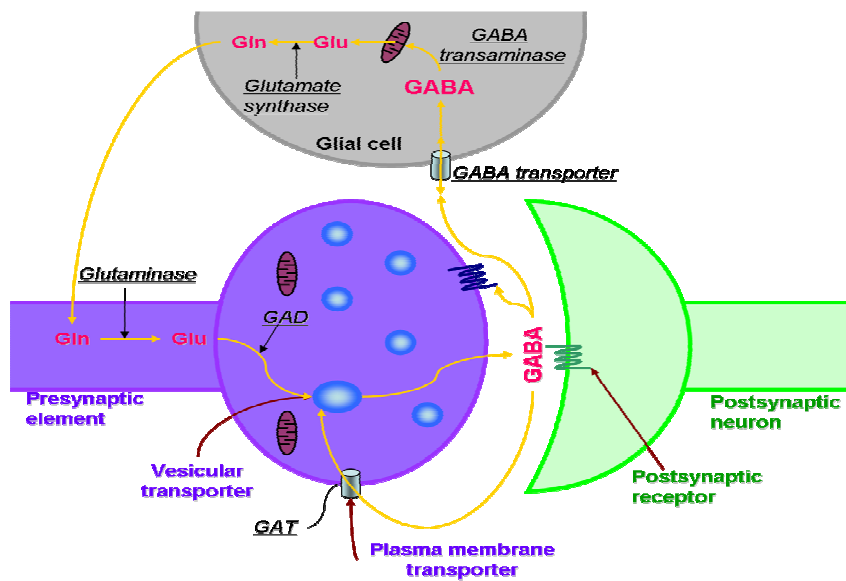
Fig.6.GABA is formed from glutamate by the action of *glutamic acid decarboxylase* (GAD), an enzyme found only in GABA-synthesizing neurons in the brain. GABA is destroyed by a transamination reaction, in which the amino group is transferred to α-oxoglutaric acid (to yield glutamic acid), with the production of succinic semialdehyde, and then succinic acid. This reaction is catalysed by *GABA transaminase*. GABA-ergic neurons and astrocytes take up GABA by specific transporters and *GABA transaminase* that removes the GABA after it is released. (Adopted from Fundamental neuroscience, 1999)

I.3.1 Discovery of the GABA$_B$ receptor

A high affinity GABA$_B$ antagonist [^{125}I] CGP64213 was developed (Kaupmann et al., 1997) and upon photoaffinity labelling resulted in two receptor proteins in the cortex, cerebellum and spinal cord of mammals. The 4.4 kb cDNA insert in a rat cortex were transfected into mammalian COS-1 cells by expression cloning leading to the identification of GABA$_B$1aR (100 kDa) and GABA$_B$1bR (130 kDa). GABA$_B$1aR and GABA$_B$1bR were the GABA$_B$R1 isoforms to be first discovered, which are pharmacologically identical with similar ligand binding affinities and differ only in the length of their N-terminal sequences. The primary protein sequences of GABA$_B$R1a and GABA$_B$R1b isoform shares no significant sequence similarity with either GABA$_A$ or GABA$_C$ receptors; and that it was distantly related to class C GPCRs (Bettler et al., 1998).

The first 147 amino acids of the mature GABA$_B$R1a isoform are replaced in GABA$_B$R1b with a sequence of 18 amino acids. GABA$_B$R1a and GABA$_B$R1b are not generated by N-terminal alternative splicing but result from the presence of an alternative transcription initiation site within the GABA$_B$R1a (Pfaff et al., 1999). Presumably, GABA$_B$1a and GABA$_B$1b use different promoters, with the GABA$_B$1b promoter being buried within GABA$_B$1a intron sequences. GABA$_B$1a and GABA$_B$1b primarily differ by the presence of a pair of sushi repeats in the GABA$_B$1a -specific domain. Sushi repeats, also known as short consensus repeats (SCRs) (Hawrot et al., 1998), were originally identified in complement proteins as a module that is involved in protein-protein interactions. They are mostly found in proteins that are involved in cell-cell adhesion and were never before observed in a neurotransmitter receptor. Sushi repeats have yet to exhibit a function in the context of the GABA$_B$ receptor.

I.3.2 Heterodimerization in GABA$_B$ receptors

While GABA$_B$R1 subunit displays binding and biochemical characterisation similar to those of native heterodimeric GABA$_B$ receptors, discrepancies were noted between these cloned receptors and native GABA$_B$ receptors (Marshall et al., 1999). There was a 100- to 150-fold lower affinity for agonists that is observed with recombinant GABA$_B$R1 subunits compared with native GABA$_B$ receptors (Kaupmann et al., 1997). When expressed in cell lines GABA$_B$R1 coupled only

weakly to adenylyl cyclase and did not couple to other effector systems, such as Ca^{2+} or K^+ channels. Moss and colleagues (Couve et al., 1998) examined the receptor using epitope tagged versions of $GABA_BR1$ subunit to study the cellular distribution of the receptor in a variety of cell types. The studies showed that the $GABA_BR1$ retained in the endoplasmic reticulum (ER) when expressed in the heterologous cells and therefore failed to reach the cell surface.

The failure of $GABA_BR1$ subunit alone to produce functional $GABA_B$ receptor, lead to the discovery of a second $GABA_B$ receptor gene $GABA_BR2$. This finding represented the first evidence for heteromerization among the GPCRs. Recombinant heteromeric $GABA_BR1$-$GABA_BR2$ receptors are known to couple to all prominent effector systems of native $GABA_B$ receptors, that is, adenylyl cyclase, Kir3-type K+ channels, and P/Q- and N-type Ca^{2+} channels (Easter and Spruce, 2002), (Filippov et al., 2000) and (Marshall et al., 1999). When the $GABA_BR2$ subunit was co-expressed with $GABA_BR1$, agonist potency more closely approximates that of native receptors (Marshall et al., 1999).

The reason for the intracellular retention of $GABA_BR1$ subunits is due to the presence of a four-amino acid motif RSRR, an Endoplasmic Retention (ER)-retention signal, in its cytoplasmic tail (Margeta-Mitrovic et al., 2000) and (Pagano et al., 2001). The other proteins were the ER-retention signals of the RXR type were observed are, the K_{ATP} channels (Zerangue et al., 1999) or N-methyl-D-aspartate (NMDA) (Scott et al., 2001) receptors. It was recently proposed that the sequence context of the RSRR motif in $GABA_BR1$ is crucial for ER retention, and the RSRR motif was extended to include the sequence QLQXRQQLRSRR (Grunewald et al., 2002). The ER-retention signal in $GABA_BR1$ is masked from its ER-anchoring mechanism through the interaction with the C-terminus of $GABA_BR2$, thus allowing for delivery of the $GABA_BR$ ($GABA_BR1$-$GABA_BR2$) complex to the cell surface. This ER retention mechanism is suggested to prevent incorrectly folded $GABA_B$ complex from reaching the cell surface and to represent a quality control mechanism. Thus, it was understood that a fully functional $GABA_B$ receptors require coupling between $GABA_BR1$ and $GABA_BR2$.

I.3.3 Extracellular domain of GABA$_B$R1 is crucial for ligand binding
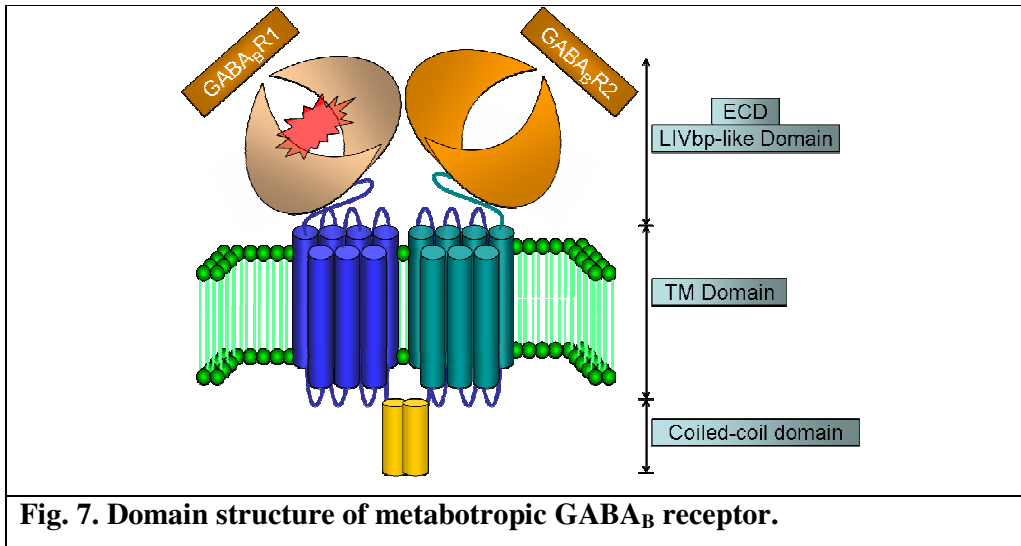
Fig. 7. Domain structure of metabotropic GABA$_B$ receptor.

The GABA$_B$R1 and GABA$_B$R2 subunits are consists of a large extracellular domain (ECD, around 50 kDa) that is homologous to leucine, isoleucine and valine binding protein (LIVbp, refered to as the V*enus fly trap*) and the seven transmembrane (TM) helix domain. The protein sequence of GABA$_B$R2 possessed a 35% identity with that of GABA$_B$R1 and exhibited many of the structural features of GABA$_B$R1, including a large molecular weight (110 kDa), an extended extracellular N-terminus and seven transmembrane spanning domains. In contrast, the intracellular carboxy-terminus of GABA$_B$R2 was longer than that of GABA$_B$R1.

All GABA$_B$ receptor agonists and competitive antagonists bind to the extracellular (ECD) of the GABA$_B$R1 subunit only and not to GABA$_B$R2 (Malitschek et al., 1999). The ECD of GABA$_B$R1 when expressed alone without its TM domain retains the binding properties of wild-type receptors, indicating that it folds independently from the transmembrane domains. Sequence analysis of the GABA$_B$R1 ECD reveals a weak sequence homology with LIVbp. In all GABA$_B$ subunits the LIVbp-like domain is linked to the first transmembrane domain via a short sequence that lacks the cysteine-rich region conserved between the other members of Class C GPCRs. In the mGlu receptors, this cysteine-rich region appears to be necessary for the LIVbp-like domain to bind glutamate (Okamoto et al., 1998b).

The inability of GABA$_B$R2 to bind antagonists results due to a single aminoacid difference in the binding pocket of GABA$_B$R2; the substitution of a proline in GABA$_B$R2 for a critical serine (S246) in GABA$_B$R1a.

I.4 Expression systems and overexpression of GPCRs

In recent years there have been several expression systems that are developed for the over-expression of GPCRs. the expression systems include *E.coli*, yeast, insect and mammalian cell system (Grisshammer and Tate, 1995). *E.coli* has an advantage of ease of handling, low cost and ease of scale up. The disadvantage of it being, prokaryotic, and lacking most of the targeting and post-translational modification machinery. There have been successes in the expression of 5HT4 receptor, when refolded from inclusion bodies (Baneres et al., 2005). Very recently, an NMR structure of Vasopressin V2 receptor was determined by refolding the protein from inclusion bodies (Tian, C., 2005). Yeast is yet another cheap and versatile expression system containing the machinery required for the post-translation modification. But the disadvantage of this system is that it possesses different post-translational patterns than that of mammalian system. It has also been reported that there is heterogeneity of GPCRs due to incomplete maturation of the protein (Reilander and Weiss, 1998).

The insect and mammalian systems have proven to be the most efficient system suitable for expression of the receptors. The insect cell system has been shown efficient in expressing several proteins.

I.1.5 Metabotropic Glutamate receptor (mGluR)

L-Glutamate is the principle neurotransmitter of the fast excitatory synapses in the mammalian CNS and plays an important role in a wide variety of CNS functions. Like other transmitters, glutamate is stored in synaptic vesicles and released by calcium dependent exocytosis; specific transporter proteins account for its uptake by neurons and other cells, and for its accumulation by synaptic vesicles (*see fig.8*). Glutamate taken up by astrocytes is converted to glutamine and recycled via transporters, back to the neurons, which convert the glutamine back to glutamate. Glutamine, which lacks the pharmacological activity of glutamate, thus serves as a pool of inactive transmitter under the regulatory control of the astrocytes. Until recently, the actions of glutamate in mammalian brain were thought to be mediated exclusively by activation of glutamate-gated cation channels termed ionotropic glutamate receptors (iGluRs).
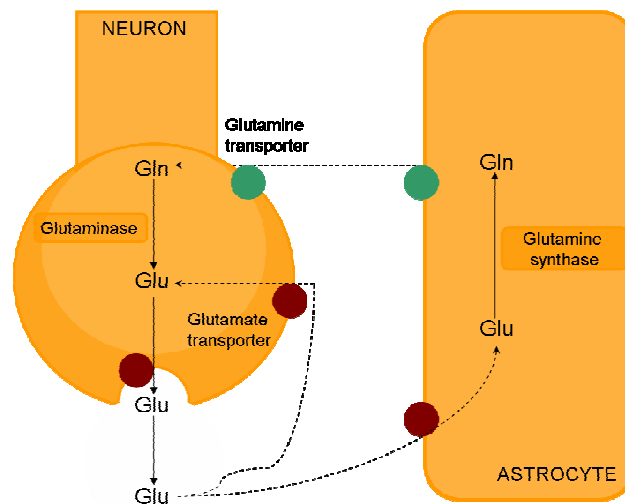
Fig. 8. Storage and release of glutamate in the neurons (adopted from Rang and Dale, Pharmacology, 5th ed.).

The excitatory neurotransmitter glutamate plays important roles in the mammalian brain, ranging from synaptic plasticity to memory. To mediate these functions, glutamate activates two types of receptors: ligand-gated channels and metabotropic receptors coupled to G-proteins (Tanabe et al., 1992). Both families of glutamate receptors share no homology and possess original structural features compared with other ligand-gated channels and G-protein coupled receptors, respectively. On the basis of studies with selective agonist and antagonists the ligand-channels can be divided into three main subtypes of EAA receptors, namely, NMDA; AMPA, and

kainite receptors. In the mid 1980s, however, evidence for the existence of glutamate receptors directly coupled to second messenger systems via G-proteins began to appear with the discovery of glutamate receptors coupled to activation of phosphoinositide hydrolysis (Nakanishi, 1994). Since that time, it has become clear that glutamate activates a large family of receptors, termed metabotropic glutamate receptors (mGluRs) that are coupled to effector systems through GTP-binding proteins.

The cloning of eight mGluR subtypes expanded the study of mGluRs as these were expressed in heterologous systems to determine coupling to second-messenger systems, establish pharmacological profiles with glutamate analogues, and screen for novel subtype-specific pharmacological agents (Houamed et al., 1991) and (Masu et al., 1991). Based on sequence homology, pharmacological profile and second messenger coupling, mGluR subtypes can be classified into three different groups. mGluRs of the same group show about 70% sequence identity, whereas between groups this percentage decreases to about 45% (Conn and Pin, 1997).
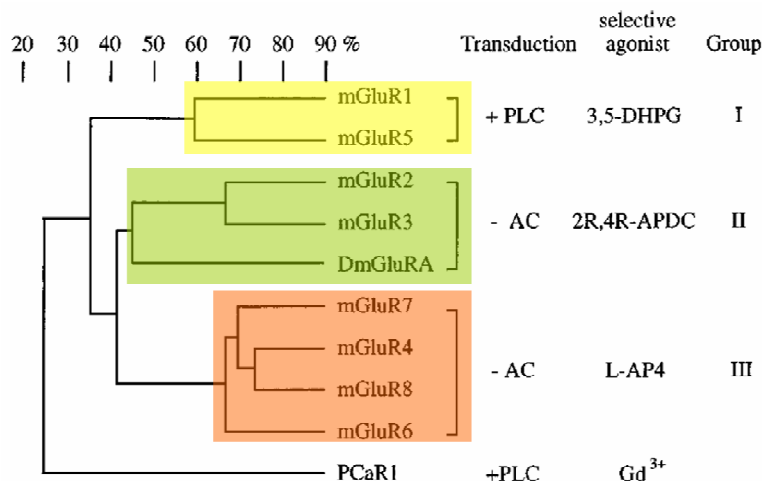
Fig. 9. Classification of mGluRs. Based on sequence homology, the mGluRs can be broadly classified into 3 groups. The classification gives more insight into the specificity of the agonist and the transduction elicited. Adapted from (Conn and Pin, 1997).

Group I mGluRs includes mGluR1 and mGluR5 are localized in the peripheral parts of postsynaptic densities and contribute to the regulation of synaptic plasticity (Baude et al., 1993). *Group II mGluRs* includes mGluR2 and mGluR3 are found in the presynaptic and glial cells. The presynaptic mGluRs negatively regulate

glutamate release whereas glial mGluR3 exerts neuroprotective effects through paracrine mechanism based on the production of neurotrophic factors. When expressed in mammalian cells, group II mGluRs (mGluR2 and mGluR3) inhibit cAMP formation stimulated by either forskolin or αG_S-coupled receptor. This effect is inhibited by pertussis toxin (PTX) treatment of the cells, which indicates the involvement of a Gi-type of G-protein. *Group III mGluRs* include mGluR4, mGluR7 and mGluR8 that are presynaptically localized and inhibit the release of glutamate or GABA, whereas mGluR6 receptors are exclusively expressed by optic nerve bipolar cells in the retina and play an important role in the amplification of visual inputs. Like group II mGluRs, all group III mGluRs inhibit adenylyl cyclase via a PTX-sensitive G-protein when expressed in CHO or BHK cells.

I.5.1 Domain structure of Metabotropic glutamate receptors

Metabotropic glutamate receptors (mGluRs) like the other receptors of the class C GPCRs possess a very large extracellular domain besides the characteristic seven transmembrane domains, separated by short intra- and extra-cellular loops, and a cytoplasmic carboxyl-terminal domain variable in length. Nineteen cysteine residues that are located in the N-terminal extracellular are conserved in all members of this receptor family, which suggests important roles for these residues either in the three dimensional structure of the molecule or in the intramolecular transduction. The agonist-binding site for small ligands in most GPCRs is located in a pocket defined by the seven transmembrane domain segments, but in the case of mGluRs it is found in the ECD.

The glutamate binding site is proposed to be equivalent to the known amino acid binding sites of LIVbp (O'Hara et al., 1993). This model allowed the identification of two residues, S165 and T188, in the extracellular domain of mGluR1, mutation of which affects glutamate affinity.

The extracellular domain (ligand binding domain) of mGluRs can be expressed as secreted receptors. The crystal structure from the glutamate-binding domain of mGluR1 has been solved, which confirms the predicted LIVbp-like fold (two globular domains separated by a hinge region often referred to as "venus trap"

(Kunishima et al., 2000) (*see fig. 10, left*). The structure of the soluble receptor revealed the fact that the receptor is present in equilibrium between two different conformations, 'open' (resting) and 'closed' (active), in ligand free form. Upon glutamate binding the receptor is stabilized in the 'closed' conformation. As predicted by the modeling studies, the α-amino acid moiety of glutamate interacts via hydrogen bonds with Ser165 and Thr188 from lobe I (*see fig. 10, right*), and the amino group interacts with Tyr236 and Asp308 from lobe II. These 4 residues are conserved in much class–C GPCRs and bacterial LIVbps. The distal carboxylic group of the glutamate interacts with Lys409 as well as with Arg78 via a water molecule.
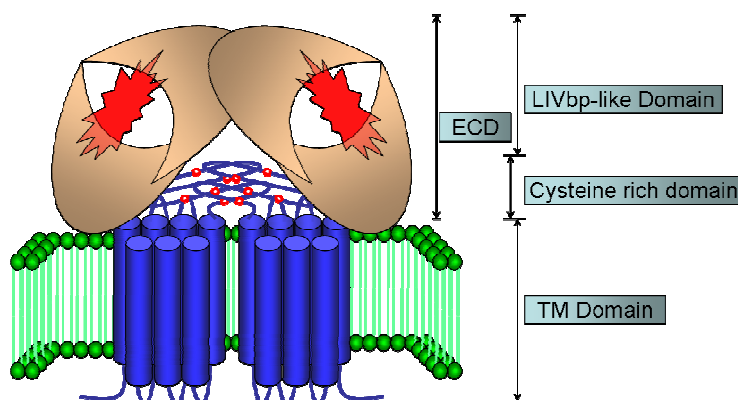
Fig. 10a. Domain structure of mGluR
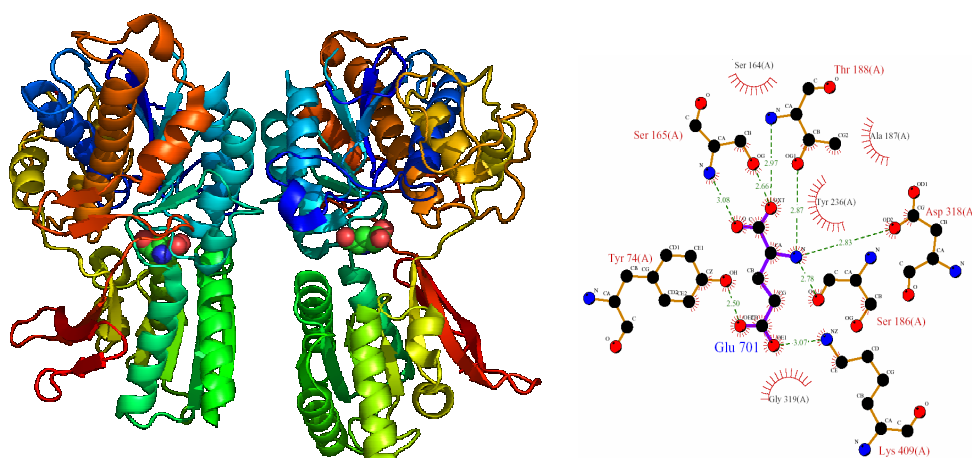
Fig. 10b. X-Ray crystal structure of the ligand binding domain of mGluR. *Left,*The X-ray crystal structure of mGluR1 represented as ribbons and the bound ligand glutamate in ball and stick representation. The figure prepared using PyMOL software (1EWK). *Right,* the residues involved in the glutamate binding to the ligand binding domain of mGluR. The figure prepared using LigPlot.

I.5.2 *Drosophila* **metabotropic glutamate receptor (DmGluRA)**

In arthropods, glutamate is well known as the most common transmitter at the neuromuscular junction ((Delgado et al., 1989). It is also recognized as a neurotransmitter in the CNS of invertebrates. Fast glutamatergic transmission is mediated by ionotropic glutamate receptors (iGluRs), but synaptically released glutamate also activates metabotropic glutamate receptors, which signal via slower G-protein coupled pathways. In vertebrates, several groups of metabotropic glutamate receptors (mGluRs) are known to modulate synaptic properties (Schuster et al., 1991). In contrast, the *Drosophila* genome encodes a single functional mGluR (DmGluRA), an ortholog of vertebrate group II mGluRs, greatly expediting the functional characterization of mGluR-mediated signalling in the nervous system. This receptor displays 45 and 43% amino acid sequence identity with its mammalian homologs mGluR3 and mGluR2, respectively. Moreover, its pharmacology and transduction mechanisms are surprisingly similar to those of mGluR2 and mGluR3. DmGluRA is expressed in the in the CNS of the late embryo.

DmGluRA is a 2.4 kilobase open reading frame encoding 977 amino acid protein (108 kDa) (Parmentier et al., 1996). It contains all the structural features characteristic of mammalian mGluRs such as the glutamate binding domain, cysteine rich domain with all of the cysteines observed conserved as in mammalian mGluRs and the seven transmembrane helical domains spanning the membrane. In one study, the DmGluRA was expressed in the fly system where in the receptor was expressed in the rhabdomeres of the fly eye (Eroglu et al., 2002). Biochemical characterisation of the receptor expressed in the fly eye and insect cells showed that the receptor had a 10 lower affinity for binding glutamate when expressed in the rhabdomeres. Lipid analysis data on the sterol content showed that the rhabdomeres contained ergosterol and the insect cell contained cholesterol. Further characterisation of the receptor showed that, the affinity of DmGluRA to glutamate can be regulated by the receptor association with specialised domains of the cell membranes, referred to as lipid microdomains or detergent resistant membranes (DRMs) dictated by the cholesterol content at the membrane (Eroglu et al., 2003).

I.6 Organisation of lipid membranes and regulation of membrane proteins

Cell membrane consists of more than 2000 species of lipid molecules, including sphingolipids and sterols. For many years, the lipid bilayer of the eukaryotic plasma membranes has been referred as a two-dimensional "fluid mosaic". Apart from glycerophospholipids that are sufficient to form bilayers, most eukaryotic cells contain two additional classes of lipids: sterols and sphingolipids.

The lipidic part of sphingolipids consists of a sphingoid base. Based on the type of headgroup attached, sphingolipids are classified as phosphosphingolipids or glycosphingolipids. The sterols are based on a rigid four-ring structure, with cholesterol being the principle form found in the vertebrates. Sterols and sphingolipids are present at low levels in internal membranes and synthesized in the endoplasmic reticulum (ER) and golgi respectively, but are at high levels in the plasma membrane (30-40 mol%) and endosomes.

In vivo approaches to understand the importance and specificity of phospholipids and sterols are studied by disrupting the pathway responsible for the synthesis of specific phospholipids. The other approach involves the reconstitution of the delipidated and purified membrane protein into proteoliposomes of a defined composition. Delipidation of membrane proteins leads to protein inactivation and can be reversed by addition of selective external lipids that can restore the activity of the membrane protein.

In a review, a list of membrane protein with a requirement of specific phospholipids for its activity was published as follows (

Membrane protein	Lipid	Effect/activity	Reference
P-glycoprotein	PC, PE	Restore activity of delipidated ATPase Headgroup and acyl chains affect drug binding affinity	(Sharom, 1997)
Ca2 + ATPase	PI-4 phosphate PE	2- to 4-fold increase in ATPase activity Stimulates catalytic activity	(Varsanyi et al., 1983) (Lee, 1998; Hunter et al., 1999)
Phosphate carrier-Mitochondria	CL	30-fold increase of specific activity	(Kadenbach et al., 1982) (Schlame et al., 2000)
Pyruvate carrier-Mitochondria		Requirement for activity and stability	(Schlame et al., 2000) (Nalecz et al., 1986)
ADP/ATP carrier Mitochondria-Mammals	CL	Strong effect on conformational transition and ADP binding	(Schlame et al., 2000) (Beyer and Nuscher, 1996)
Lac permease *E.coli*	PE	Required for H+-coupled transport, not for energy-independent translocation Acts as a molecular chaperone for correct folding and membrane topology	(Chen and Wilson, 1984) (Bogdanov and Dowhan, 1995) (Bogdanov and Dowhan, 1998) (Bogdanov and Dowhan, 1999; Bogdanov et al., 2002)
ABC-transporter OpuA-L.lactis	PG/PS	Osmotic stress sensed via alterations in ionic interaction with lipids	(van der Heide et al., 2001)
Pore protein PhoE-*E.coli*	PE	Required for trimerization of PhoE in vitro	(de Cock et al., 2001)
SecYEG translocase E. coli; B. subtilis	PG PE	Essential for preprotein translocation Stimulatory in E. coli; essential in B. subtilis	(van der Does et al., 2000) (Rietveld et al., 1995)
Hyaluronan synthase-Streptococcus	CL	Pore formation together with the protein postulated	(Tlapak-Simmons et al., 1999)
Monoglucosyl-diacylglycerol synthase A. laidlawii	PG, CL	Strong activation	(Berg et al., 2001)

Chitin synthase-S. cerevisiae	PS	Required for activity in vitro	(Duran and Cabib, 1978)
Plasma membrane ATPase-S. cerevisiae	PI, PG	Required for activity in reconstituted system	(Kruse et al., 2000)
Photosystem II Spinach-Synechocystis	PG	Involved in dimer –monomer interconversions essential for photosynthetic activity in vivo	(Hagio et al., 2000)

PC- Phosphatidyl choline; PE- Phosphatidiyl ethanolamine ; CL- Cardiolipin; PG- Phosphatidyl glycerol; PS- Phosphatidyl serine

Following biochemical experiments involving interactions between lipids and membrane proteins, the strongest evidence comes for highly specific protein-phospholipid and/or sterol interaction comes from 3D structures of membrane proteins (Adopted from.

Protein	Lipids	Remarks	Function	Reference
Cytochrome c oxidase Bovine	3 PE, 7 PG, 1 PC, 3 CL	5 molecules at the outer leaflet of the inner mitochondrial membrane, 9 at the matrix side	CL essential for activity	(Robinson, 1982)
Cytochrome c oxidase P. denitrificans	1 PC	Forms two ion pairs with Arg233 and Asp74 of subunit III		(Iwata et al., 1995)
Cytochrome bc1 S. cerevisiae	2 PE^a,1PI^a,1PC^a,1CL^a ^{a}-per monomer	1 PE interacts with both monomers PI is in interhelical position All lipids except PI are on the matrix side of the mitochondrial membrane	Dimer stabilization. Stabilizes complex via interaction with Lys272 One of the CL phosphodiesters may be part of the proton translocation path	(Lange et al., 2001)
Photosystem I Syn. elongatus	3 PG, 1 MGD	All located at the stromal side of the membrane Phosphodiester of one PG binds one antenna chorophyll α		(Jordan et al., 2001)
Reaction center R. sphaeroides	1 CL	One phosphodiester of CL interacts with His145 and Arg267 of subunit M		(McAuley et al., 1999)
K+ channel KcsA Strep. lividans	2 PG			
Bacteriorhodopsin H salinarum	6 dietherlipids/trimer [sulfated triglyceride lipid (S-TGA-1)] 1 squalene and 5 PGP/monomer 18 phytanyl lipids/trimer		Stabilization of BR-trimer 1 squalene and 1 PGP essential for normal photocycle characteristics Form annulus around trimer In part fill grooves of the proteins	(Joshi et al., 1998) (Luecke et al., 1999) (Belrhali et al., 1999)

1.6.1 Membrane phases and lipid rafts – Role of cholesterol

It is a very well known that lipid compositions of the two leaflets are not homogenous and are dynamic due to rapid flip-flop of sterols and lateral diffusion of the lipids. The outer leaftlet generally consists of sphingolipids, while the inner leaflet is composed of glycerophospholipids such as phosphatidylinositol, phosphatidylethanolamine and phosphatidylserine.

Studies relating to lipid biophysics, lipid sorting, and the effects of detergents on biological bilayer, shows existence of a particular type of microdomain that is rich in cholesterol and sphingolipids in the plasma membrane.

I.6.2 Role of cholesterol in maintaining the membrane fluidity

The importance of cholesterol in the functioning of cell membranes might be its ability to alter fundamental properties of the phospholipid bilayer and to interact directly with specific membrane proteins. Cholesterol is known to undergo spontaneous flipping between the two leaflets and preferentially interacts with sphingolipids in the outer leaflet rather than the unsaturated phospholipids in the inner leaflet. This way it plays a crucial role in segregating saturated phospholipids and sphingolipids from unsaturated phospholipids in bilayer membranes.
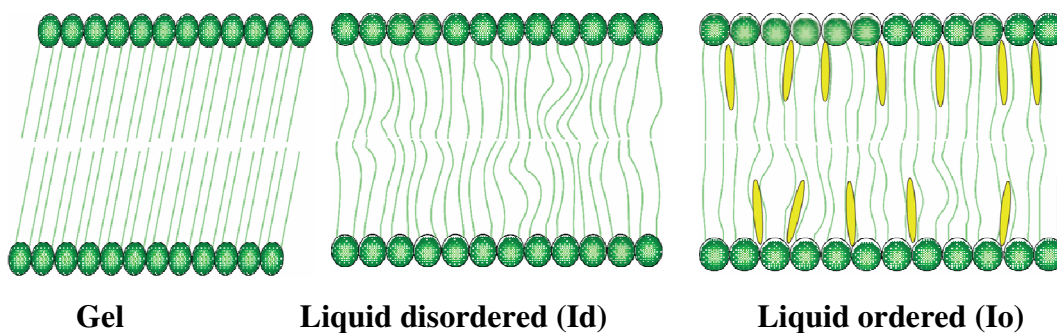
Gel   Liquid disordered (Id)   Liquid ordered (Io)
Fig 11. Different phases of the lipid bilayer (Brown and London, 1998)

The need for high levels of cholesterol in the plasma membranes and its effect on the physical properties of the lipid bilayers showed that the pure phospholipid bilayers can exist in two states, a solid or "gel" state, and a fluid or "liquid" state. The solid gel phase is not thought to be of physiological revelance. However, the fluid structure of liquid

bilayers is profoundly altered by the addition of high levels of cholesterol. The rigid sterol causes the lipid acyl chains to become closely packed or compacted, and the bilayer to be thickened. Because the long rigid cholesterol molecule is arranged perpendicular to the bilayer, this organizing effect is highly directional. The high cholesterol bilayer is thus termed "liquid-ordered" (Io), in contrast to the "liquid-disordered" (Id) state without cholesterol (Brown and London, 1998).

The insolubility of Io microdomains in non-ionic detergents at low temperatures has been extensively used for their isolation. The term "lipid raft" was introduced to refer to a sub-population of cellular membranes, isolated by their insolubility in non-ionic detergents at 4°C that are enriched in cholesterol, sphingomyelin, and glycolipids such as GM1 ganglioside and display a light buoyant density in sucrose gradients. The lipid raft model therefore proposes that the cholesterol and sphingolipids of the outer leaflet of the plasma membrane are not evenly distributed, but rather cluster into Io domains that float in an Id bilayer. In the liquid-crystalline state of lipid bilayers, packing is loose and lateral diffusion is relatively rapid which implies that all plasma membrane proteins are like "icebergs in a sea of lipid," uniformly dispersed in the lipid solvent, subjected to random mixing. Transmembrane proteins in the lipid bilayer would either reside in, or be excluded from, rafts depending on partitioning imparted by their physical properties. In the case of the outer leaflet of the bilayer, it is suggested that a major resident of rafts are proteins attached to the bilayer by covalent linkage to glycosylphosphatidylinositiol (GPI) lipid anchors.

I.6.3 Functional revelance of lipid rafts

The functional revelance of the raft model comes from the proposal that the sphingolipid and cholesterol-rich domains in the outer leaflet are connected to lipid domains in the inner leaflet. The components of signal transduction pathways, in particular G-proteins and nonreceptor tyrosine-kinases are anchored to the inner leaflet of the plasma membrane by virtue of multiple acyl chains, selectively partition into this inner leaflet part of the raft. This would allow rafts to act as "signalling platforms" that couple events on the outside of the cell with signalling pathways inside the cell, and indeed this has

been suggested to be their most important functions. Rafts have been proposed to play a role in signalling by, amongst others, T cell receptors, B cell receptors, IgE receptors, neurotrophic factors, growth factors, chemokines, interleukins and insulin.

fig 12.Composition of lipids observed in the plasma membrane of mammals, nematodes, insects and fungi.
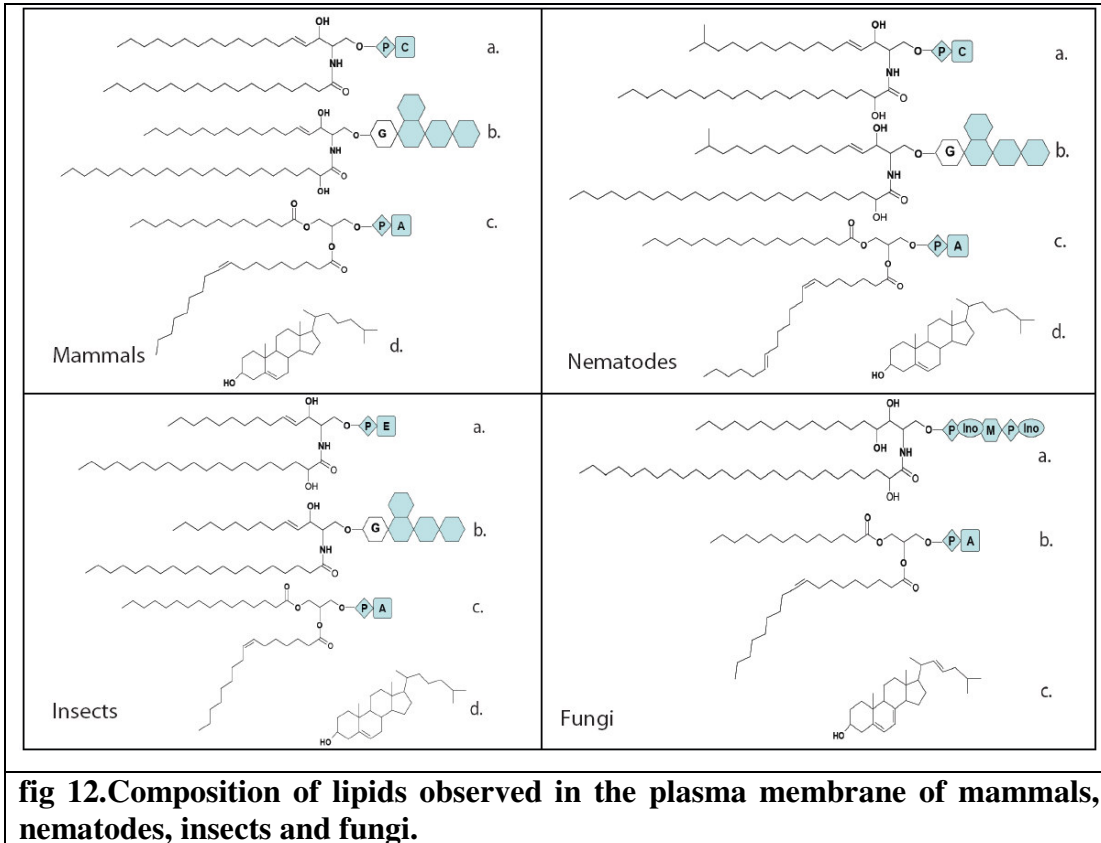
GPCRs localized in lipid raft or caveolae

Most of the receptors are localized in caveolae, as caveolae membranes are highly enriched in cholesterol and glycosphingolipids as rafts. Detergent extraction and density gradient centrifugation of the caveolae membranes results in the associated proteins in the same subcellular fractions as that of DRMs. The caveolar localisation is further verified by electron microscopy morphological appearance as 50-100nm diameter flask-shaped invaginations located at or near the plasma membrane of the cell. It has been reported that GPCRs co-immunoprecipite caveolin..

List of GPCRs localised to lipid rafts and/caveolae (adopted from (Chini and Parenti, 2004))

Receptor	Enrichment in DRMs	Enrichment in 'caveolar fractions'	Reference
Angiotensin AT1	Yes <10%	Yes <10%	(Ishizaka et al., 1998) (Ushio-Fukai et al., 2001) (Leclerc et al., 2002) (Wyse et al., 2003)
Bradykinin B1	-	No	(Lamb et al., 2002)
Bradykinin B2	-	Yes	(de Weerd and Leeb-Lundberg, 1997) (Haasemann et al., 1998) (Ju et al., 2000) (Lamb et al., 2002)
Ca sensing	Yes	-	(Kifor et al., 1998) (Kifor et al., 2003)
mGluR	Variable result	-	(Becher et al., 2001) (Eroglu et al., 2003)
Cholecystokinin CCK	Yes	-	(Roettger et al., 1995)
Sphingosine EDG-1	-	Yes	(Igarashi and Michel, 2000)
Endothelins ETA$_A$	Yes	-	(Chun et al., 1994) (Okamoto et al., 1998a)
Endothelins ETA$_B$	Yes	Yes	(Teixeira et al., 1999) (Yamaguchi et al., 2003)
Metabotropic GABA$_B$	Yes	-	(Becher et al., 2001)
Gonadptropin	Yes	Yes	(Navratil et al., 2003)

releasing hormone GnRH			(Pawson et al., 2003)
Oxytocin OTR	Yes < 10%	Yes < 10%	(Gimpl and Fahrenholz, 2000) (Guzzi et al., 2002)
Somatostatin SST2	-	Yes	(Krisch et al., 1998) (Mentlein et al., 2001)
Serotonin 5HT2	-	Yes	(Dreja et al., 2002)
Thyrotrophin TRH	-	Yes	(Drmota et al., 1999)

Aim and outline of work

For years membrane proteins have been the most interesting and challenging field of work possessing enormous medical importance. G-protein coupled receptors (GPCRs) play a pivotal role in many physiological functions. The bottleneck lies especially in the structure determination and characterization of GPCRs. Owing to the lack of a robust system, structure determination of GPCRs still remain a dream.

The first part of the current study is focused upon employing molecular cloning strategies to over-express the metabotropic $GABA_B1b$ receptor (rat) in the recombinant baculovirus (RBV) and *E.coli* system. In this study attempts are made to optimize the expression and purification of the ligand binding extracellular domain of the metabotropic $GABA_B1b$ receptor (GBR1bNT) at molecular level by computational and experimental studies. This information aimed to be useful in designing vectors which contain fusion partners or signal peptides, which would improve the GBR1bNT expression and purification.

Two expression systems, RBV or *E.coli*, have been considered for the GBR1bNT expression purposes. Different biochemical strategies will be applied to optimize the expression and purification of GBR1bNT.

The second part of the study was aimed at understanding the regulation of Drosophila metabotropic glutamate receptor (DmGluRA). The study will be focused biochemically characterizing the putative role of cholesterol binding motif (pCBM) in DmGluRA regulation. Attempts will be made to obtain the minimal domain requirements of the DmGluRA that is capable of glutamate binding with the same affinity as observed in the full length protein.

II. Materials and methods

II.1 Materials

II.1.1 Chemicals

All chemicals were of analytical grade and were purchased from Sigma, Fluka or Merck laboratories if not stated otherwise.

II.1.2 Enzymes and other proteins

Restriction endonucleases, NEB buffers and T4-DNA ligase	New England Biolabs
High fidelity DNA polymerase system	Roche applied science
Complete® protease inhibitors cocktail	Roche applied science

II.1.3 Kits and chemicals

QIAquick Gel Extraction kit	Qiagen
QIAprep Spin Miniprep kit	Qiagen
TA cloning kit	Invitrogen
BaculoGold DNA kit	Pharmingen
Bicinchoninic acid assay kit	Sigma
L-[^{3}H]-Glutamate	Amersham Pharmacia
Silver staining kit	Sigma
Ethylene glycol monomethyl ether	Sigma
Triton X-100	Serva

II.1.4 Instruments and equipments

Automated DNA sequencing	MWG Biotech
Neubauer chamber	Hecht-Assistant
Beckmann liquid scintillation counter	Packard Instruments
ZetaSizer S1000 HAS	Malvern instruments
Model J-180 CD spectropolarimeter	Jasco
Electrophoretic system	BioRad
Ultra-clear^{TM} ultracentrifugation tubes	Beckmann Instruments
Hoefer vacuum filtration setup	Amersham Pharmacia
Nitrocellulose membranes	Schleicher and Schuell
Extruder	Avestin

II.1.5 Stock solutions

All stock solutions were prepared as described in (Sambrook 2001).

IPTG stock solution	100mM
Ampicillin stock solution	100 mg/mL
Kanamycin stock solution	50 mg/mL
Chloramphenicol stock solution	50 mg/mL in ethanol

II.1.6 DNA and Protein ladders

DNA ladder

DNA ladder 100 bp DNA ladder	New England Biolabs
1 kb Plus DNA ladder	Gene ruler^{TM}

Protein ladder

Rainbow marker	Amersham Pharmacia
Broad Range marker	BioRad

II.1.7 Competent cell strains of E.coli for cloning

Chemically competent NOVABlue cells and SOC medium	Novagen
Electrocompetent DH5α cells	prepared in-house

II.1.8 Antibodies

Primary antibodies

Anti penta-His antibody (Mouse) (1:1000 dilution)	Qiagen
Anti-DGR (Rabbit) (1:2500 dilution)	Produced in-house

Secondary antibodies

Anti-rabbit IgG, Horse radish peroxidase (HRP) linked whole antibody	Amersham Pharmacia
Anti-mouse IgG, Horse radish peroxidase linked whole antibody	Sigma

II.1.9 Plasmids

PCR2.1	Invitrogen
pVL1393	BD biosciences
pEVMOD	
pCDNA3.1-GPI	

II.1.10 DNA sample preparation buffers

6X Sample buffer for DNA (Fermentas)	0.25% Bromophenol blue, 40% sucrose, 60mM Tris-HCl, pH 7.4 and 6mM EDTA.

II.1.11 Media

Lauria-Bertani broth (LB)	Prepared as per the manufacturer's instructions. 1L contained 10g of NaCl, 10g of Bacto-Trypton and 5g of yeast extract. pH was adjusted to 7.4. For plates, 15 g/L agar was added to the preparation.

II.1.12 Buffers

10X Phosphate Buffered Saline (PBS)	1.36 M NaCl, 357mM Na_2HPO_4, 143mM KH_2PO_4 and 30mM KCl. PBS was adjusted to pH 7.4.
1X TBE buffer	11g Tris base, 5.5g of Boric acid and 4mL of 0.5M EDTA pH 8.0 in 1L MilliQ water.

II.1.13 Solution and reagents for Sodium Dodecyl Sulphate – Polyacrylamide Gel Electrophoresis (SDS-PAGE and western blotting

2X denaturing SDS-PAGE buffer	60mM Tris-HCl pH 6.8, 8M Urea, 5% Sodium dodecyl sulphate, 0.25% sodium deoxycholate, 10% ß-mercaptoethanol and Bromophenol blue.
10% APS	2g APS in 20mL water
10% TEMED	1mL in 10mL water
Resolving gel buffer	375mM Tris-HCl pH 8.8 and 0.1 % SDS
Stacking gel buffer	125mM Tris-HCl pH 6.8 and 0.1% SDS
Staining solution	100mL Methanol, 20mL glacial acetic acid, 0.8g Coomassie blue R-250 in 100mL MilliQ water
Destaining solution	50mL ethanol and 70% Acetic acid in 1L of MilliQ water
10X Transfer buffer	19g Tris base and 90g glycine, and adjusted to 1L solution with MilliQ water.
PBST buffer	300µL Tween 20 in 100mL of 1X PBS
Blocking buffer	3% skimmed milk powder in PBST buffer

II.1.14 Insect cell strains in the Recombinant BaculoVirus (RBV) system

II.1.14.1 Medium and Buffer

SF900-II and TNM-FH (Hinks media) Gibco	Was prepared according to the manufacturer's protocol and was supplemented with Penicillin (100 mg/mL and Streptomycin (100 mg/mL) antibiotic.
Transfection buffer	25mM Hepes, 140mM NaCl and 125mM CaCl$_2$ pH 7.1.

II.1.14.2 Insect cell lines

Insect species	Cell line
Spodoptera frugiperda	*Sf9*
Spodoptera frugiperda	*Sf9*
Spodoptera frugiperda	*SF+*
Trichoplusia ni	HighFive

II.2 Materials for the work involving molecular cloning strategies to improve the expression and purification of ligand binding extracellular domain of rat metabotropic GABA$_B$1b receptor in *E.coli* expression system

II.2.1 Vectors for GBR1bNT over-expression

Vector	Promoter	Selection	Tags		Fusion partners (N-term)
			N-term	**C-term**	
pETM 11	T7-lac	Kan	6-His	6-His	-
pETM 30	T7-lac	Kan	6-His	6-His	GST
pETM 50	T7-lac	Kan	6-His	6-His	DsbA
pETM 52	T7-lac	Kan	6-His	6-His	DsbA (leaderless)
pETM 60	T7-lac	Kan	6-His	6-His	NusA
pET 15b-GST	T7-lac	Amp	-	6-His	GST
Kan – Kanamycin			*Amp – Ampicillin*		

II.2.2 Host strains for GBR1bNT over-expression

BL21(DE3)
BL21(DE3) pLysS
C43(DE3)
Rosetta (DE3) pLysS
Tuner

II.2.3Buffers for column chromatography

Lysis buffer   50mM Tris pH 8.0, 300mM NaCl, 0.2 % Triton X-100, 1mM PMSF, 5 % Glycerol and Complete protease inhibitors.

II.2.4 Buffers for purification using Glutathione S-Transferase (GST) column

GST wash buffer 136mM NaCl, 35.7mM Na$_2$HPO$_4$, 14.3mM KH$_2$PO$_4$, 3mM KCl and protease inhibitors.

GST elution buffer 136mM NaCl, 35.7mM Na$_2$HPO$_4$, 14.3mM KH$_2$PO$_4$, 3mM KCl, 10mM Glutathione and protease inhibitors.

TEV buffer   50mM Tris pH 8.0, 500mM EDTA and 1mM DTT.

II.2.5 Buffers for the purification using Nickel column

Buffer A   50mM Tris, 300mM NaCl, 10 % Glycerol and 4mM MgCl$_2$. pH adjusted to 8.0

Buffer B   50mM Tris, 300mM NaCl, 10 % Glycerol, 4mM MgCl$_2$ and 500mM Imidazole. pH adjusted to 8.0

Dialysis buffer   50mM Tris, 300mM NaCl, 10 % Glycerol and 2mM $MgCl_2$.
                   pH adjusted to 8.0

II.2.6 Buffers for purification using ceramic hydroxyl apatite column (CHT)

Equilibration buffer   20mM potassium phosphate buffer pH 6.0
(Buffer Q)

Wash buffer   20mM potassium phosphate buffer pH 6.0 and 500mM NaCl.
(Buffer W)

Elution buffer   100mM Potassium phosphate buffer pH 8.0 and 300mM NaCl
(Buffer E)

II.3 Materials for the work involving biochemical characterization of the cholesterol binding motif and determination of the minimal construct required for maintaining the high affinity state for binding glutamate in DmGluRA

II.3.1 Buffer for homogenization of Sf9 cells

Homogenization buffer   50mM Sodium phosphate buffer pH 7.4, 300mM NaCl, 2mM $MgCl_2$, 1mM EGTA, 250mM Sucrose containing protease inhibitors.

II.3.2 Buffer for enrichment of plasma membranes

TNE buffer   50mM sodium phosphate buffer pH 7.4, 300mM NaCl, 2mM $MgCl_2$ and 1mM EGTA containing protease inhibitors.

II.3.3 Buffers for L-[^{3}H]-Glutamate binding assays

Binding buffer   50mM Tris HCl pH 7.4 and 0.2% BSA

Buffer for filter saturation   50mM Tris HCl pH 7.4 and 1%BSA

"No salt" buffer   50mM Tris-HCl pH 7.4

"Salt" buffer   50mM Tris-HCl pH 7.4 and 500mM NaCl

II.3.4 Buffer for raft isolation from insect cells

TXNE buffer   1% TritonX-100, 50mM sodium-phosphate buffer pH 7.4, 300mM NaCl, 2mM $MgCl_2$, 1mM EGTA and 2 tablets of protease inhibitors for 25mL buffer (to be added before use)

II.3.5 Buffer for Liposome floatation assay

Assay buffer   20mM phosphate buffer pH 7.5, 150mM NaCl, 2mM $MgCl_2$ and 240mM Sucrose

II.3.6 Synthetic peptides

The synthetic peptides for circular dichroism studies were synthesized from JPT peptide technologies GmbH.

Peptide Name	Peptide sequence
Pep$_{611-624}$	H-**SCYALDIQYMKWNS**-NH$_2$
Pep$_{602-624}$	H-**GLWPYADKLSCYALDIQYMKWNS**-NH$_2$

II.4 Methods

II.4.1 Polymerase Chain Reaction (PCR)

All primers were diluted in sterile MilliQ water to a stock of 100μM and stored at -20°C. The DNA concentration was determined using spectrophotometer reading at A_{260}.

The following reaction mixture was set up for all PCRs.

Template (10 ng/μL)	2 μL
100 μM forward primer	1.5 μL
100 μM reverse primer	1.5 μL
100mM dNTP mix	1 μL
Expand high fidelity (3 units/μL)	1 μL
10X Expand high fidelity buffer	5 μL
Sterile MilliQ water	volume made up to 50 μL

The samples were prepared in thin-walled PCR tubes and the reaction was carried out in a thermocycler PCR machine. The temperature cycle was setup as per the standard protocol.

Initial denaturation	92°-94°C	5 min	
Denaturing	92°-94°C	1 min	
Annealing	50°-54°C	30-35 sec	25-30 cycles
Elongation	72°C	90-120 sec	
Final Elongation	72°C	10 min	

50μL of the PCR product mixed with 6X tracking dye was observed on a 1% agarose gel containing ethidium bromide. 1 kb Plus DNA ladder was used to determine the molecular size of the PCR amplified product after electrophoresis in *1X TBE buffer* at 100 volts. The electrophoresed gel was visualized under a transilluminator and photographed.

II.4.2 Restriction enzyme digestion of the vector and the PCR product

The minipreps plasmid DNA was prepared by following the protocol and buffers provided by QIAprep spin miniprep kit. The cells were pelleted by centrifugation at 4000 rpm at 4°C for 10 min, and resuspended in 250 µL of *Buffer P1* containing RNase. The resuspended cells were lysed by the addition of 250 µL of *Buffer P2*, followed by careful mixing of the contents. The lysates were neutralized by the addition of 300 µL of *Buffer N3*. The supernatant was cleared from the cell lysate by centrifugation; the supernatants were loaded onto the binding column and spun down. The flowthrough was discarded, and the columns were washed with *Buffer PE*. In the last wash, centrifugation was performed for 1 min to remove the traces of ethanol. The plasmids were eluted with 30 µL sterile MilliQ water.

The PCR amplified product was extracted from the gel matrix using the QIAGEN Gel extraction kit, the purified PCR product was eluted in 30 µL sterile MilliQ water from the agarose resin.

The plasmid and the PCR products for ligation were digested using appropriate restriction enzymes. Typically, a restriction enzyme digestion setup consists of

Plasmid DNA/PCR product	1 µg
Restriction enzyme 10 units/µl	1 µL
Appropriate buffer 10X	2 µL
Sterile MilliQ water	volume made up to 20 µL

The microfuge tubes were incubated for 1 hr at 37°C. After incubation the digestion mixture was resolved on 1% agarose gel.

II.4.3 Ligation and transformation of the constructs into competent cells

The appropriate bands of the digested plasmid and the PCR products were gel purified and ligated using T4 DNA ligase enzyme. The ligation reaction was set up as follows at 18°C for 12-16 hrs.

Digested Plasmid DNA: PCR product ratio 1:15 and 1:30 (by volume)

T4 DNA ligase enzyme 400 units/µL   1 µL

10X Ligase buffer   2 µL

Sterile MilliQ water   volume made up to 20 µL

For a bacterial transformation, about 2*µL* of ligation mixture was mixed with 100*µL* of competent cells and incubated on ice for at least 30 min. The mixture was heat shocked at 42°C for 30 secs, followed by incubation on ice for 2 min. A volume of 250 µL pre-warmed SOC medium was added to the transformation mixture followed by incubation at 37°C for 30min on a shaker. The cells were plated on LB agar plates containing appropriate antibiotic as selection marker and incubated at 37°C for 12-16 hrs. About 10-15 colonies were randomly picked to check for any recombinant clones and inoculated into 4mL of LB media containing antibiotic in 15mL falcon tubes. The cultures were incubated at 37°C for 12-16 hr on a shaker.

The minipreps of the clones were prepared and all recombinant plasmids were identified and verified by restriction digestion with appropriate enzymes. The constructs were sequenced to check for mutations using following primers designed for verifying constructs cloned in the multiple cloning site of the pVL1393 vector.

Primers	Sequence
Pvl_for	*5'*-TAA AAT GAT AAC CAT CTC GC-*3'*
Pvl_rev	*5'*-TGA AGA GAG TGA GTT TTT GG-*3'*

II.5 Cell culture: Recombinant baculovirus system

Baculovirus are a diverse group of viruses that are found mostly in insects which represent their natural host and they are not known to have any non-anthropod hosts (O'Reilly et al., 1992). The baculovirus DNA is of 80-200 kilobase pairs (kbp) double-stranded, covalently closed, and circular. The most commonly used baculovirus is *Autographa californica* multiple nuclear polyhedrosis virus (AcMNPV), which belongs to the family baculoviridae. The properties of insect cell lines for baculovirus propagation include growth rate, ability to support virus replication and plaque formation, ability to grow in both monolayer and suspension cultures. Most commonly used cell line is the *Sf9* cell line, derived from *Spodoptera frugiperda* pupal ovarian tissue. The insect baculovirus expression system provides a eukaryotic environment that is favourable for the proper folding, disulphide bond formation, oligomerisation and posttranslational modification of the protein essential for the biological functionality of a large number of foreign proteins.

The general procedure used was adapted from Baculovirus and cloning techniques described by (O'Reilly, 1994). All cell counts were carried out under a light microscope using a Neubauer chamber.

II.5.1 Maintenance and adaptation of *Sf9, HighFive (Hi5) and SF+* cells

The *Sf9, Hi5 and SF+* cells double every 18 to 24 hr and were maintained in erlenmeyer flasks as suspensions in Sf900-II medium with 10% fetal calf serum (FCS) or 75 cm^2 tissue culture flasks as monolayer culture (in TNM-FH medium). The monolayers were grown to 80 to 90% confluency and finally diluted to 30% confluency. The suspension cultures were routinely grown to a cell density of 4 to 4.2x10^6 cells permL and diluted to a final density of 0.3 to 0.4 x10^6 cells per mL. All cell lines were incubated at 27 °C on a flat surface incase of monlayers or stirred at 80 rpm incase of suspension cultures. The maintenance of the culture is summarize as follows:

Cell line	Culture type	Growth medium
Sf9	Monolayer	TNM-FH with 10% FCS
Sf9	Suspension	*Sf*900-II (serum free medium)
SF+	Suspension	*Sf*900-II (serum free medium)
HighFive	Monolayer	TNM-FH with 10% FCS

II.5.2 Production of recombinant baculovirus by co-transfection

The linearized AcNPV genome and pVL1393 constructs were co-transfected into *Sf9* cells (monolayers) by calcium phosphate co-precipitation as described (O'Reilly, 1994).

A 6 cm diameter tissue culture dish was seeded with 1 x 10^6 *Sf9* cells/ml in 3mL of TNM-FH medium containing 10 % (v/v) fetal calf serum (FCS) and incubated at 27°C for 2 hr to let the cells attach.

The *transfection mix* was prepared in a microfuge tube by mixing 0.5 µg Baculo Gold DNA and 2 µg transfer plasmid in 750µL of transfection buffer. The medium was carefully removed from the dish containing *Sf9* cells and 750µL of fresh medium was added. The *transfection mix* was transferred drop-wise onto the cells with gentle rocking. The culture dish was sealed with parafilm and was incubated at 27°C. Following 4 hr of incubation, the *transfection mix* was removed from the culture dish and 4mL of fresh TNM-FH medium supplemented with 10 % (v/v) FCS was added. Cells were incubated for 3 to 4 days until cytopathic effects (lack of cell growth, floating cells, nuclear enlargement, cell lysis) were apparent. Cell culture supernatant were collected in 2mL sterile amber colored microfuge tubes and maintained as primary viral stock (1°VS) and stored at 4°C. The cell pellet was washed twice with PBS. Samples of total cells were prepared for SDS-PAGE electrophoresis followed by western blot analysis to check the protein expression of the recombinant truncation constructs.

II.5.2.1 Sample preparation for SDS-PAGE

The total cells or plasma membrane obtained from expression of DmGluRA truncation constructs were prepared for SDS-PAGE by addition of 2X denaturing SDS-PAGE buffer followed by incubation for 30 min at 40°C or left overnight at room temperature. For soluble proteins, samples were boiled with 2X SDS-PAGE denaturing buffer at 98°C for 3 min.

Gels for SDS-PAGE were prepared according to the guidelines of Molecular cloning (Sambrook 2001). 8% and 10% separation gels were used in this experimental work. The electrophoresed gels were either silver stained or Coomassie blue dye stained or used for western blot analysis.

II.5.2.2 SDS-PAGE for electrophoretic separation of proteins

Resolving gel	8%	10%		Stacking gel	
Resolving gel buffer pH 8.8	2500µL	2500µL		Stacking gel buffer pH 6.8	1250µL
30% Acrylamide	1330µL	1670µL		30% Acrylamide	310µL
Water	1050µL	714µL		Water	840µL
10% APS	75µL	75µL		APS	75µL
10% TEMED	45µL	45µL		TEMED	30µL

II.5.2.3 Coomassie blue staining

Proteins resolved on polyacrylamide gels were fixed and stained in staining solution (Sambrook 2001). After rinsing the gel briefly in water, the gel was destained in the destaining solution, which eliminates the blue background while the proteins retain the blue dye. Gels were either dried on Whatmann filter paper or on gelatin sheets.

II.5.2.4 Silver staining

Silver staining was carried out on electrophoresed SDS-PAGE gels following the protocol given by the manufacturer.

II.5.2.5 Western Blot analysis

The proteins resolved on polyacrylamide gels were electro-transferred to PVDF membranes 0.45 µm pore size membranes (Immobilon-P) with the aid of electroblotting apparatus. The PVDF membrane was activated by briefly rinsing with methanol prior to transfer. The "sandwich" was prepared as described in Molecular cloning (Sambrook 2001). Protein transfer from the gel to the membrane was carried out at 130 mA at constant current for 70 min.

The membrane was blocked with blocking buffer for 1 hr. The membrane was washed once with PBST and then incubated with primary antibody (1:2500 dilution of anti-DGR or 1:1000 of anti penta-His in blocking buffer) for 10-16 hr in the cold room. The membrane was washed thrice with PBST and incubated with HRP-linked secondary antibody (1:1000 dilution of anti-rabbit IgG, whole molecule in blocking buffer) for 1 hr at room temperature. The membrane was washed again thrice and developed using ECL western blotting detection system.

II.5.3 Purification of Recombinant Virus – End point dilution cloning

The required recombinant virus obtained from the 1°VS by calcium phosphate co-precipitation was selected and purified by the end-point dilution cloning technique as described (O'Reilly, 1994).

The dilution of the primary viral stock was prepared as follows:

Firstly, the virus was diluted in series in 10 sterile microfuge tubes as shown in *Scheme 1* to obtain a final virus dilution of 10^{-5}, 10^{-6}, 3×10^{-7}, 10^{-7}, 3×10^{-8}, 10^{-8}, 3×10^{-9} and 10^{-9}. Then prepared about 30mL of a *Sf9* cell suspension in TNM-FH medium at a density of 10^4 *Sf9* cells/mL and distributed 2250 µL it into 8 sterile 15mL Falcon tubes. One falcon tube containing TNM-FH medium was kept as "control". To the 8 Falcon-tubes (microfuge tubes 3-10) added $250\mu L$ from the respective dilution (with the diluted virus). The total content (2500µL) was mix thoroughly.

A 96-well plate was labeled as per the scheme shown below; distributed about $100\mu L$ in to 22 wells for a given dilution. To the "Control" tube, $250\mu L$ medium (instead of virus) was added and distributed it as a control into the column in the 96-well plate shown as shaded part in the scheme. The plates were then sealed with parafilm.

Scheme 1: Dilution of primary viral stock

Medium (µL)	900 ⌐	900 ⌐	900 ⌐	900 ⌐	700 ⌐	600 ⌐	700 ⌐	600 ⌐	700 ⌐	600
Virus (µL)	10 ⌐→	100 ⌐→	100 ⌐→	100 ⌐→	300 ⌐→	300 ⌐→	300 ⌐→	300 ⌐→	300 ⌐→	300
Label	**1**	**2**	**3**	**4**	**5**	**6**	**7**	**8**	**9**	**10**
Virus-solution (µL)			250	250	250	250	250	250	250	250
Cell-suspension (µL)			2250	2250	2250	2250	2250	2250	2250	2250
final virus dilution			10^{-5}	10^{-6}	3×10^{-7}	10^{-7}	3×10^{-8}	10^{-8}	3×10^{-9}	10^{-9}

96-well plate for selection of the recombinant clone

		1	2	3	4	5	6	7	8	9	10	11	12
3 10^{-5}	A	100µL	…	…									▓
	B	..	..										▓
4 10^{-6}	C	..											▓
	D												▓
5 3×10^{-7}	E												▓
	F												▓
6 10^{-7}	G												▓
	H												▓

		1	2	3	4	5	6	7	8	9	10	11	12
7 3×10^{-8}	A												▓
	B												▓
8 10^{-8}	C												▓
	D												▓
9 3×10^{-9}	E												▓
	F												▓
10 10^{-9}	G												▓
	H												▓

96-plates were left for approximately 7 days at 27°C for sufficient infection. The contents in the well were observed under a light microscope and the number of wells that contained infected cells of each dilution was counted and the percentage was calculated.

According to the Poisson distribution, the proportion (p) of wells receiving either 0 or 1 infectious unit at a mean concentration of virus (**μ**) of 1 is given by the equation

$$P = \mu e^{-\mu} = e^{-1} = 0.367$$

Thus, at an Multiplicity of Infection (MOI) of 1, 36% was assumed to have been infected with a single particle of virus. About 5 clones were chosen and seeded in a 6-well microtiter plate containing 2×10^6 *Sf9*-cells/mL. The 96 well plates were left in the incubator for 1h at 27°C. Added 2mL fresh medium, sealed with parafilm and incubated for 5-7 days at 27°C.

The contents were centrifuged and the supernatant was labeled as primary pure virus stock **(1°pVS)** along with the clone number. A sample of the cell pellet was prepared for Western blotting to check the protein expression of the recombinant truncation constructs.

II.5.4 Preparation of high titre working stocks – secondary and tertiary stocks

The secondary virus stocks were prepared by mixing 500μL of the 1°pVS with 100mL of 2×10^6 *Sf9* cells/mL in a 500mL spinner flask. The infection was carried out for 5-7 days at 27°C until all the cells were infected and lysed to ensure maximal virus yield. The contents were centrifuged; supernatant was collected in an amber colored glass-bottle, labeled as "**2°pVS**" (secondary pure virus stock) and stored at 4°C.

The tertiary virus stocks "**3°pVS**" were similarly prepared by infecting 500mL of 2×10^6 *Sf9* cells/mL in a spinner flask with 1mL of the 2°pVS. The 3°pVS was maintained as the working stock after the determination of the titer values.

II.5.5 Determination of viral titre – End point dilution assay

To start a protein expression in the baculovirus system it is mandatory to determine the titre value or plaque forming units/mL (pfu/mL) of the working stock to be reproducible from stock to stock in the infection kinetics and stoichiometry. This value is achieved by a method called **End point dilution assay (EPD assay)** as described in O'Reilly. In the EPD assay, Hi5 cells were used in monolayers instead of *Sf9* monolayers. Since Hi5 cells are fibroblasts and enable easy of identification of infected cells. The dilution scheme for the endpoint dilution is as follows.

Medium (µL)	900	900	900	900	900	900	900	900	900	900
virus (µL)	100 →	100 →	100 →	100 →	100 →	100 →	100 →	100 →	100 →	100

virus-solution (µL)	250	250	250	250	250	250	250	250
Cell-suspension (µL)	2250	2250	2250	2250	2250	2250	2250	2250
final virus dilution	10^{-4}	10^{-5}	10^{-6}	10^{-7}	10^{-8}	10^{-9}	10^{-10}	10^{-11}

		1	2	3	4	5	6	7	8	9	10	11	12
10^{-4}	A	100µL	…	…									
	B	…	…										
10^{-5}	C	…											
	D												
10^{-6}	E												
	F												
10^{-7}	G												
	H												

		1	2	3	4	5	6	7	8	9	10	11	12
10^{-8}	A												
	B												
10^{-9}	C												
	D												
10^{-10}	E												
	F												
10^{-11}	G												
	H												

The cells were observed under a light microscope from third day post-infection until a clear discrimination of infected and uninfected cells was achieved. The infected wells for each dilution were counted and the percentage was calculated. The following formula was applied to determine the pfu/mL of the working stocks. The dilution is calculated by linear interpolation between the infection rates observed at the given dilutions.

First the proportionate distance (PD) of 50% response from the response above 50% is calculated using the formula:

$$TCID_{50} = P - (A - 50) / (A - B)$$
$$TCID_{50} \times 0{,}69 = pfu/ml$$

$TCID_{50}$ = 50% tissue culture infectious dose

P is log of the dilution causing an infection greater than 50% wells (A)

A = percentage of infected wells above 50% threshold

B = percentage of infected wells below 50% threhold

II.5.6 Growth and expression studies

In the Baculovirus system, the optimal protein expression is dependent on the following parameters.

- Cell-type (*Sf9/SF+* in monolayer/suspension)
- Multiplicity of infection (MOI)
- Duration of infection

Multiplicity of infection (MOI) is defined as the average number of viruses that infects a single *Sf9/SF+* cell. It is determined using the following formula:

$$\textbf{MOI (pfu/cell)} = \frac{\textbf{Vol of viral inoculum required (mL) x titre of the virus (per mL)}}{\textbf{Number of cells}}$$

$$\textbf{(OR)}$$

$$\textbf{Vol of viral inoculum required (mL)} = \frac{\textbf{MOI (pfu/cell) x Number of cells}}{\textbf{titre of the virus (per mL)}}$$

After determination of the titre values of the viral stocks, test expressions were setup to determine the conditions for optimal recombinant protein expression. The expressions were performed in 100mL *SF+* suspension cultures at a cell density of 2 x 10^6 *SF+* cells/mL. The cells were infected with recombinant virus at a MOI of 1,2,3,5 and 10 at 27°C. The infected cells were counted after 24, 36, 48, 60, 72 and 96 hr post infection. Samples of cells and supernatants at mentioned time points were prepared for analyzing expression in western blots. After the determination of optimal conditions, large scale protein expression was setup.

II.5.7 Purification of proteins expressed and secreted by *SF+* cells to the insect cell medium

The protein expression by *SF+* cells posed difficulties in purification of proteins expressed and secreted to the *Sf*900-II medium owing to the media ingredients (such as aminoacids and salts) which inhibit the chelation of the His-tag to the Nickel ion and also the high loading volumes (500 ml-1 L) of the medium containing the secreted protein.

Hence the purification of secreted protein in the medium was conducted in 2 stages. The first stage involved a Ceramic hydroxy apatite (CHT) column, where the *Sf*900-II

medium was replaced with *Buffer E*. The CHT column served the purpose of concentrating the protein to a lower loading volume into the Nickel-sepharose bed and as a buffer exchanger compatible with the Ni-sepharose column. The eluate from the CHT column was loaded on to the Ni-sepharose column.
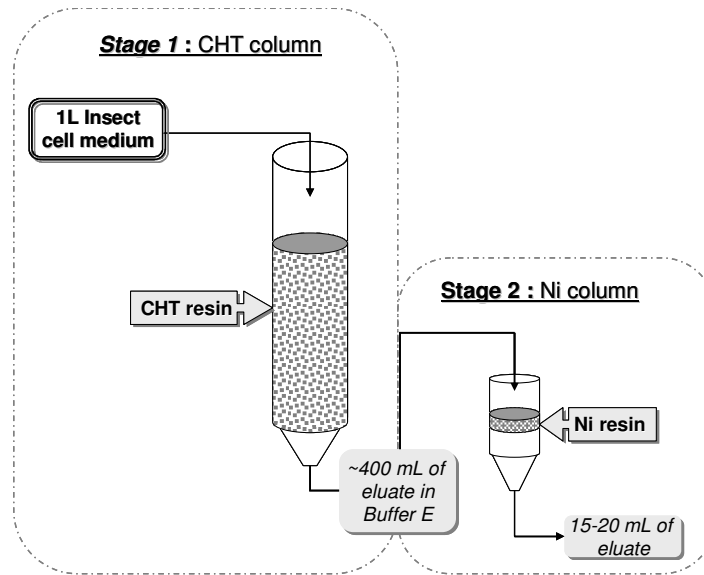
Fig. 13. **Stages of purification of proteins secreted to the insect cell medium.**
Stage 1.Concentration and exchange of secreted proteins in insect cell medium to Buffer E on a ceramic hydroxyl apatite column (CHT).
Stage 2. Purification of secreted proteins on a Ni-sepharose column.

The experimental setup for the purification was carried out as shown in the *fig.13*. 1L of $2x10^6$ *SF+* cells/mL in suspension were infected with virus stock expressing DGX at MOI of 3 for 72-96 hr (until 70% cells were observed infected and lysed under light microscope). Culture supernatant was clarified by centrifugation and the supernatant was collected and filtered through a steritop vacuum filtration setup (0.22 μm poresize).

II.5.7.1 Ceramic hydroxy apatite purification (CHT purification)
All purification procedures were carried out in the cold room. The CHT column was prepared and equilibrated with 200mL of *Buffer Q*. The filtered supernatant was loaded into the equilibrated CHT column after addition of protease inhibitors and buffered with potassium phosphate buffer pH 6.0 to a final concentration of 20mM. The loaded column was washed until baseline (approx. 300 mL) with *Buffer W* and eluted with *Buffer E*.

II.5.7.2 Nickel column purification

The eluate from the CHT column was prepared for loading into the Ni-sepharose column after addition of *Buffer B* to a final Imidazole concentration of 10mM.

The loaded column was washed with buffer containing 10mM Imidazole until baseline. The Nickel bound protein was eluted from the column by a gradual increase in the Imidazole concentration (50, 75, 100, 150, 200, 250 and 500mM) and collected in 2mL fractions. Western blot was preformed on all the elution fractions where the peak was observed in the chromatogram. The fractions containing the required protein were pooled, concentrated on an membrane filter and dialyzed in 2L of *dialysis buffer* overnight in the cold room.

The amount of protein obtained was determined by the absorbance of the sample at wavelength 280 nm. The extinction coefficients were theoretically calculated. 50 μL aliquots were prepared, flash frozen in liquid nitrogen and stored at -80°C.

II.6 Methods for molecular cloning strategies to improve the expression and purification of extracellular domain of GBR1bNT (rat) in RBV and *E. coli* system

II.6.1 Expression of extracellular domain of GABA 1b receptor (GBR1bNT) in the insect cells

II.6.1.1 Molecular constructs

The GABA 1b receptor (GABA$_B$R) cDNA cloned in pVL1392-Mel vector was used as a template for obtaining the GABA$_B$R construct containing only the extracellular ligand binding domain lacking the native signal peptide. The GABA$_B$R was terminated at 1332 bp to obtain the GBR1bNT construct (the GBR1bNT spans from 88-1332 bp containing a C-terminal 8-His tag). All constructs for expression of GBR1bNT were cloned into the transfer vector, pVL1393. Recombinant Baculovirus production and protein expression in the RBV system were conducted as previously described (*see Materials and methods, Section II.5*).
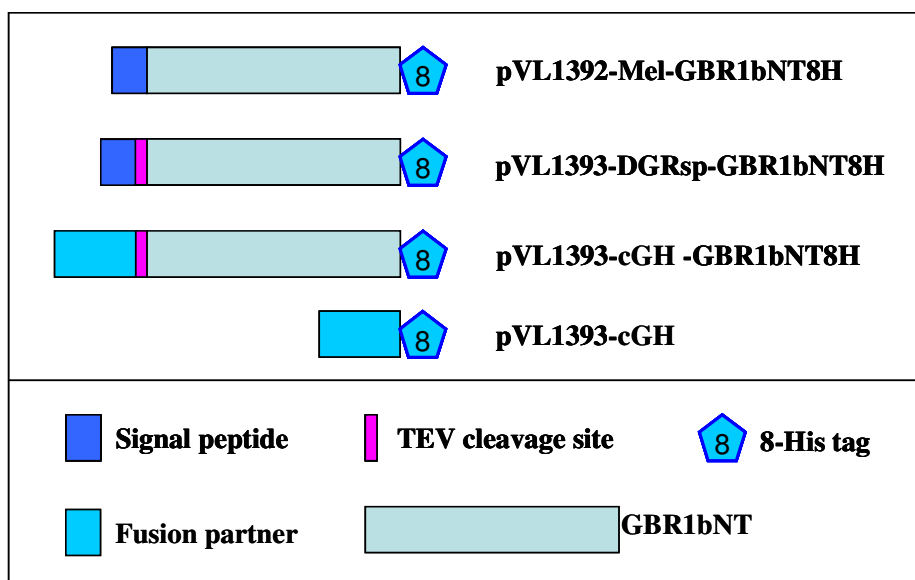
Fig. 14. Molecular constructs considered for the study of expression and purification of GBR1bNT in the RBV system.

II.6.1.1a Preparations of pVL1392-Mel-GBR1bNT construct

The pVL1392-Mel-GBR1bNT construct was previously prepared in the lab by cloning the PCR amplified GBR1bNT into the *PstI/EcoRI* MCS region of pVL1392-Mel vector preceeded by the Mellitin signal sequence.

II.6.1.1b Preparations of pVL1393-DGRsp-GBR1bNT construct

For the pVL1393-DGRsp-GBR1bNT construct, the native signal peptide of GBR1bNT was replaced with DmGluRA signal peptide (DGRsp, 29 residues). The DGRsp complementary oligonucleotides were designed such that the forward primer (DGR_sp_rev) contained the *BamHI* overhang at the 5' end and *XbaI* cleaved sequence at the 3' end. The reverse primer (DGR_sp_for) contained *BamHI* cleaved sequence at 3' end and overhang of *XbaI* cleavage sequence at the 5' end.

Primers	Sequence
DGR_sp_for	5'-**GATCC** A CCA TGA AAC AGA AAA ATA ATA ACG GAA CAA TTT TAG TCG TCG TGA TGG TTT TAT CCT GGA GTC GAG TAG TAG ACT TAA AAA GT **T**-3'
DGR_sp_rev	5'- **CTAGA** A CTT TTT AAG TCT ACT ACT CGA CTC CAG GAT AAA ACC ATC ACG ACG ACT AAA ATT GTT CCG TTA TTA TTT TTC TGT TTC ATG GT **G**-3'

The primers were annealed prior to ligation by mixing 900 µmol of each primer and cycling it 5 times between temperature 92 °C (2 min) and 72 °C (5 min); and finally let the reaction proceed at 72 °C for 10 min. The 90 bp DGRsp insert was ligated into *BamHI/XbaI* digested pVL1393 vector to obtain the ***pVL1393-DGRsp plasmid***.

To obtain the pVL1393-DGRsp-GBR1bNT construct, the PCR product (TEV-GBR1bNT) containing a TEV protease cleaveage site was amplified using Xba1_tev_gbr1b_for and cgh_corr_rev primers, using pETM11-GBR1bNT as template. TEV-GBR1bNT PCR product was digested with *XbaI/NotI* and ligated into *XbaI/NotI* digested pVL1393-DGRsp plasmid. The plasmid constructs were transformed into competent cells, plated on LB agar plates and the minipreps of colonies were verified by restriction enzyme digestion and sequencing for the recombinant clone (**pVL1393-DGRsp-GBR1bNT**).

Primers	Sequence
Xba1_tev_gbr1b_for	*5'-ATT CAG TT<u>T CTA GA</u>G GCG GCA TGA GCG ATT ACG ACA TCC -3'*
cgh_corr_rev	*5'-AAG CGA A<u>GC GGC CGC</u>* **TCA** *GTG ATG GTG ATG GTG ATG TCT AGA GAT GGT GCA GTT GCT CTC -3'*

II.6.1.1c Preparation of pVL1393-cGH and pVL1393-cGH-GBR1bNT constructs

The pEVmod vector containing the coding sequence of cGH was a kind gift from laboratories of D.N.Foster (University of Minnesota, USA). The coding sequence of cGH was amplified from pEVmod vector using cgh_for and cgh_rev primers. The primers were designed in such a way that the PCR product of cGH at the 5'-end contained *SmaI* restriction site followed by *Kozak* translation initiation sequence (both included by cgh_for primer) and the 3'-end contained *XbaI*-8His-Stop-*NotI* (included by cgh_rev). The PCR product of cGH was cloned into *SmaI/NotI* MCS region of pVL1393 transfer vector. The resulting plasmid construct served as ***pVL1393-cGH*** construct. The TEV-GBR1bNT PCR product (*see Materials and methods, section II.6.1.1b*) was digested with *XbaI/NotI* and ligated into *XbaI/NotI* digested pVL1393-cGH plasmid to obtain the ***pVL1393-cGH-GBR1bNT*** construct.

II.6.2 Methods for the work involving molecular cloning strategies to improve the expression and purification of ligand binding extracellular domain of rat metabotropic GABA$_B$1b receptor in *E.coli* expression system

II.6.2.1 Expression of the extracellular domain (ECD) of GABA 1b receptor (GBR1bNT) in the *E.coli* system

II.6.2.1a Plasmids for protein expression in *E.coli*

All plasmids were of pBR322 vector origin and contained a TEV protease cleavage sequence proceeded by the His tag / fusion partner at the N-terminus of GBR1bNT construct or the His-tag is fused to the C-terminus of GBR1bNT construct.

II.6.2.1b Molecular cloning of GBR1bNT constructs in *E.coli*

All molecular cloning strategies were conducted as previously described in the *Materials and methods, Section II.4*. The PCR was carried out by using pVL1392-Mel-GBR1bNT (GABA 1b receptor truncated at 1332 bp and lacks the native signal peptide) as the template using the primers, 5'-ATTCATCT*CCATGG*GGTCTCACTCCCCTCATCTC-3' (gbr1bnt_for, forward primer) and 5'-AAGCGAA*GCGGCCGC*TCAGTGATGTGATGGTG-3' (gbr1bnt_rev, reverse primer). All GBR1bNT PCR products were cloned into the *NcoI/NotI* multiple cloning site (MCS) of the pETM series (pETM11, pETM30, pETM50, pETM52 and pETM60 plasmids) for over-expression in *E.coli*. For pET15b-GST-GBR1bNT construct, pETM30-GBR1bNT was digested with *XbaI/XhoI* to obtain the GST-GBR1bNT insert and re-ligated in to the *XbaI/XhoI* digested pET15b vector.

II.6.2.1c Expression of GBR1bNT in the total cells of *E.coli*

In all test expression setups were carried out in 3mL LB medium (containing appropriate antibiotic) inoculated with a single bacterial colony transformed with the plasmid containing GBR1bNT. The bacterial culture was incubated at 37 °C on a circular rotor until the OD$_{600}$ reached range of 0.6 - 0.8. About 1.5mL was transferred to a fresh falcon tube followed by induction with IPTG at a final concentration of 1mM. The cultures were let to induce with IPTG for 6 hr at 30 °C. The cells were harvested by centrifugation. Samples of total cells under IPTG uninduced and induced

were prepared for SDS-PAGE analysis. The SDS-PAGE resolved total cells were stained with Coomassie blue contained in the staining solution to see the levels of protein expression.

II.6.2.1d Large scale over-expression and purification of GBR1bNT in *E.coli*

After optimisation of expression parameters such as expression vector, expression host, concentration of IPTG for induction, induction time and temperature, a large scale production (1 L) of GBR1bNT from *E.coli* was carried out under the optimised conditions.

50mL LB medium containing appropriate antibiotic were inoculated with a single bacterial colony and incubated overnight at 37°C with shaking (280 rpm) in a 100mL flask. 10mL of the overnight culture was washed with PBS and resuspended in fresh LB medium. This served as a preinoculum to inoculate 1L of medium for a large scale over expression of GBR1bNT incubated at 37°C with shaking until the OD_{600} reached 0.6-0.8 value. The cells were then induced with IPTG to a final concentration of 0.1mM for 3 hr at 30°C or for 16 hr at 18°C. The IPTG induced cells were harvested and lysed by sonication in the *Lysis buffer* on ice for 5 min followed by 5 passes through the Emulsiflex (Microfluidiser was used in the later part of the work for cell lysis). The cell lysate was centrifuged on a high-speed vacuum centrifuge at 108, 000 xg for 15 min on a T647.5 rotor. The supernatant containing the soluble form of GBR1bNT was applied to a pre-equilibrated Ni-sepharose column or a GST column depending on the tag fused to the construct.

The loaded Ni-sepharose column was washed with buffer containing predetermined minimal concentration of Imidazole sufficient to remove the nonspecifically bound proteins to the column. In a Ni-sepharose column, the proteins were eluted from the bound column by a gradual step increase in the Imidazole concentration achieved by proportional mixing of *Buffer A* and *Buffer B* (containing 500mM Imidazole). In case of a GST column, the GST-tagged protein bound to the resin was resuspended in 2mL of TEV buffer. The cleavage reaction was carried out by incubating the GST-GBR1bNT protein bound resin with 20 µg of TEV protease for 12-16 hrs at 4 °C. Samples at different stages of purification and after TEV cleavage were resolved on a SDS-PAGE and stained with Coomassie Blue dye.

II.7 Biochemical characterization of the cholesterol binding motif and determination of the minimal construct required for maintaining the high affinity state for binding glutamate in DmGluRA

II.7.1 Molecular constructs

DmGluRA cDNA cloned in the pRK7 vector (Parmentier et al., 1996) was used as the template for all PCR amplifications of truncation constructs. For all truncation constructs of DmGluRA, the same forward primer (DGR_for_1, table 1) was used. Apart from the 18-25 complimentary base pair region, both forward and reverse primer contained the following features. The forward primer comprised of a *BamHI* restriction enzyme cleavage site followed by 5' *Kozak* translation initiation sequence (*5'*-CCACC-*3'*), (Parmentier et al., 1996). The reverse primers (table 1) comprised of an *EcoRI* restriction enzyme cleavage site followed by a 5'-TTA-3' (stop codon) and coding sequence for *flag* tag. The reverse primers coding for the DmGluRA truncated constructs were prepared by introducing a 5'-TTA-3' (stop codon) after 1989 bp (DGRTM1), 2214 bp (DGRTM3) and 2451 bp (DGRTM5) of DmGluRA cDNA. The PCR products were ligated into the PCR2.1 vector then subcloned into the *BamHI/EcoRI* multiple cloning region of the pVL1393 transfer vector.
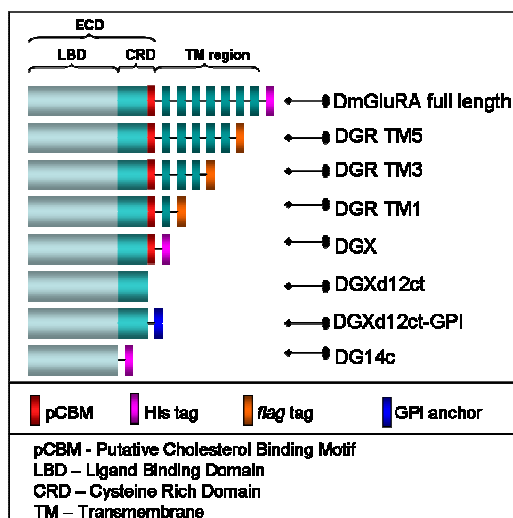
Fig. 15. Schematic representation of the truncation constructs of DmGluRA cDNA cloned into the pVL1393 vector.

Table 1. Amplification of the truncation constructs – Polymerase Chain reaction

Construct	Primers
DGRTM1	**DGR_for_1** : 5'-CTA GA*G GAT CC*A CCA TGA AAC AG-3' **DGR_TM1_rev** : 5'-CCG *GAA TTC* **TTA** CTG ATC GTC ATC GTC CTT GTA ATC CTC TCG TCC TGA TGC TCT TAC C-3'
DGRTM3	**DGR_for_1** : 5'-CTA GA*G GAT CC*A CCA TGA AAC AG-3' **DGR_TM3_rev** : 5'-CCG *GAA TTC* **TTA** CTG ATC GTC ATC GTC CTT GTA ATC TTG TGA TTG TGG ACT AAT ATA CTT AAG-3'
DGRTM5	**DGR_for_1** : 5'-CTA GA*G GAT CC*A CCA TGA AAC AG-3' **DGR_TM5_rev** : 5'-CCG *GAA TTC* **TTA** CTG ATC GTC ATC GTC CTT GTA ATC TTC GAC TCA TTA AAG TTT CAG G-3'
DGXd12ct	**DGR_for_1** : 5'-CTA GA*G GAT CC*A CCA TGA AAC AG-3' **DGXd12ct_rev** : 5'-AAG CGA A*GC GGC CGC TCT AGA* **TTA** *GAA TTC* GCA GGA GAG CTT GTC AGC-3'
DGXd12ct-GPI	**DGR_for_1** : 5'-CTA GA*G GAT CC*A CCA TGA AAC AG-3' **DGXd12ct_rev** : 5'-AAG CGA A*GC GGC CGC TCT AGA* **TTA** *GAA TTC* GCA GGA GAG CTT GTC AGC-3'

Incase of DGXd12ct and DGXd12ct-GPI constructs, the PCR products were directly cloned into the pVL1393 vector as follows. The PCR amplified DGXd12ct construct contained the restriction sites *EcoRI-stop-XbaI-NotI* in the 3'-end as included by the reverse primer (*as shown in the table*). The DGXd12ct PCR product construct was cloned into the *BamHI/NotI* MCS of pVL1393 transfer vector. The resulting plasmid (pVL1393-DGXd12ct) was digested with *EcoRI/XbaI* restriction endonuclease enzymes and ligated at the 3' end with a GPI anchor isolated from *EcoRI/XbaI* restriction site of pCDNA3.1-GPI vector containing the GPI coding sequence. The GPI coding sequence was a kind gift from Costagliola (Cornelius et al., 2001). It is a 170 bp fragment encoding the motif required for GPI addition at the C-terminus of mouse Thy-1 and contained in the plasmid pCDNA3.1-GPI. The constructs were prepared as shown in the *fig. 16*.
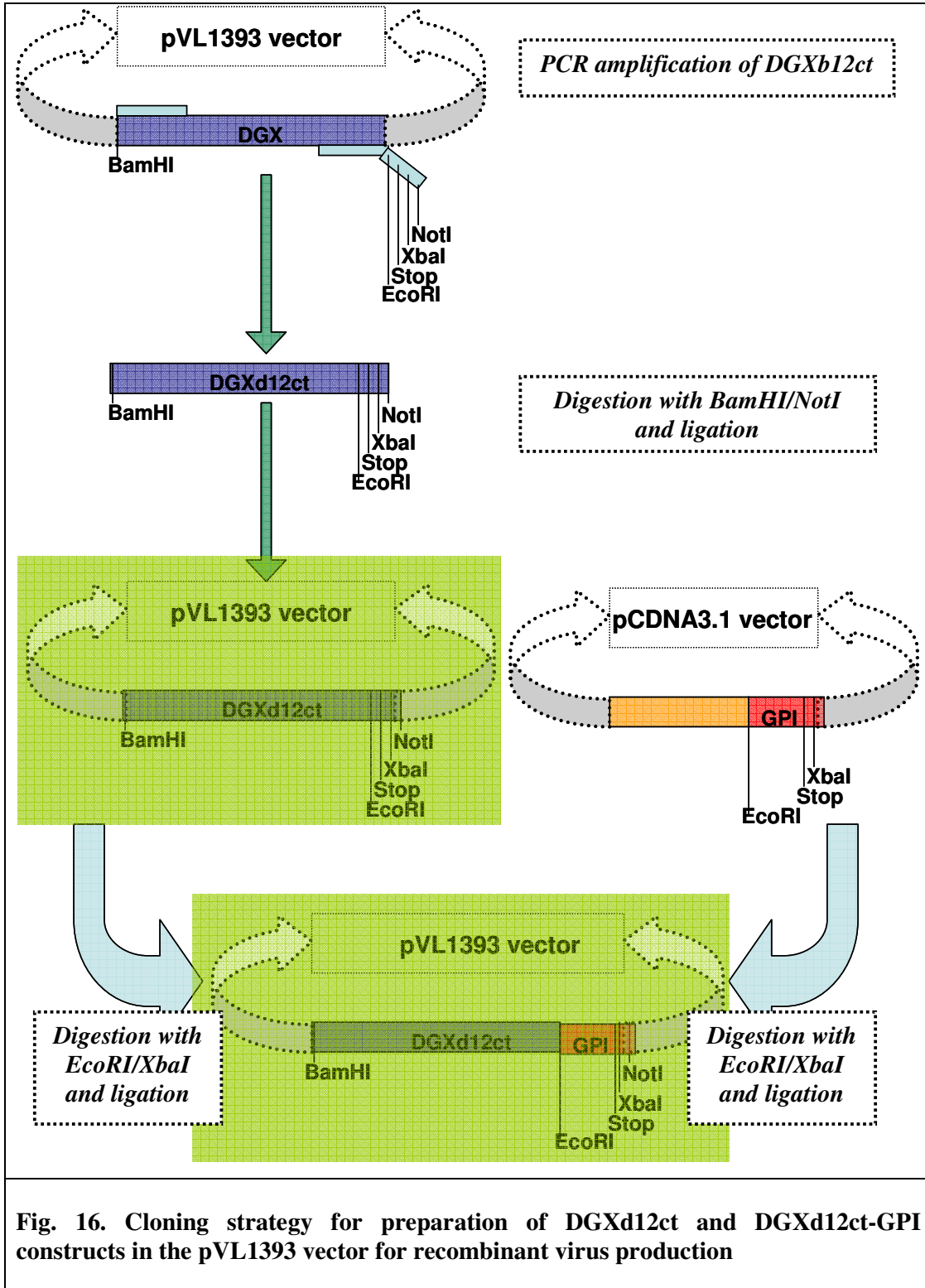
Fig. 16. Cloning strategy for preparation of DGXd12ct and DGXd12ct-GPI constructs in the pVL1393 vector for recombinant virus production

II.7. 2 Preparation and enrichment of plasma membranes from *Sf9* cells

The *Sf9* cells were harvested by centrifugation. The cell pellet was washed twice with PBS and resuspended in equal volume of ice cold *homogenization buffer* containing protease inhibitors. The resuspended cells were homogenized in a pre-cooled Dounce glass homogenizer (20 strokes) on ice. The homogenate was centrifuged at 300xg for 10 min at 4°C, to remove the nuclei or any unbroken cells.

The plasma membranes were pelleted by ultracentrifugation of the postnuclear supernatant at 40,000xg for 30min at 4°C. The membranes were washed with *homogenization buffer*. The crude membranes were further purified and enriched by density gradient ultracentrifugation using an Optiprep^{TM} step gradient.

II.7.3 Purification and enrichment of plasma membranes by density gradient ultracentrifugation

The crude membranes were resuspended in minimum volume of *TNE buffer*. The buffers for setting up the gradient were prepared as follows:

30% Optibuffer   5mL Optiprep^{TM} (60%) + 5mL TNE buffer

5% Optibuffer   160μL Optiprep^{TM} (60%) + 1.76mL TNE buffer

The stepwise gradient was laid carefully in the following order (as shown in the *fig. 17*) into 11x60 mm Ultra-clear^{TM} ultracentrifugation tubes

40% layer   Mixed 350μL membranes with 700μL of Optiprep^{TM} solution (60%)

30% layer   1.9mL of 30% Optibuffer

5% layer   0.4mL of 5% Optibuffer
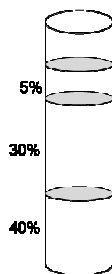
fig. 17. Density gradients in ultracentrifugation tube for enrichment of plasma membranes.

Plasma membrane enriched fraction formed a dense band at the 30-5% interface after 3 hr of centrifugation at 105,000xg at 4°C in a Beckmann SW60 rotor. The enriched fractions were washed twice with ice cold *homogenization buffer*.

$50\mu L$ aliquots of plasma membranes were distributed in microfuge tubes, flash frozen under liquid nitrogen and stored at -80°C. The membranes were detected for protein of interest by western blotting; quantified for total membrane protein content by BCA assay. The frozen aliquots of membranes were used for other experimental work such as ligand binding trials and isolation of detergent resistant membranes (DRMs) by 1% Triton X-100 detergent.

II.7.4 Total membrane protein content determination by Bicinchoninic acid Assay (BCA)

The total membrane protein content was determined using the BCA kit for protein determination. The BCA working reagent was prepared by mixing 50 parts of Reagent A (Bicinchoninic Acid Solution) with 1 part of Reagent B (4% (w/v) $CuSO_4 . 5H_2O$ Solution). A standard curve with BSA (1 mg/mL) was prepared to determine the protein concentration in the unknown samples.

The standard assay was setup as shown in the following table

Tube no	Water (µL)	BSA (1mg/mL) (µL)	BCA working reagent (mL)
1	100	0	2
2	80	20	2
3	60	40	2
4	40	60	2
5	20	80	2
6	0	100	2
7	100 µl (q.s.)	Unknown 1	2
8	100 µl (q.s.)	Unknown 2	2

Standard curve with BSA for BCA assay

OD 562	0	0,192	0,359	0,527	0,685	0,848
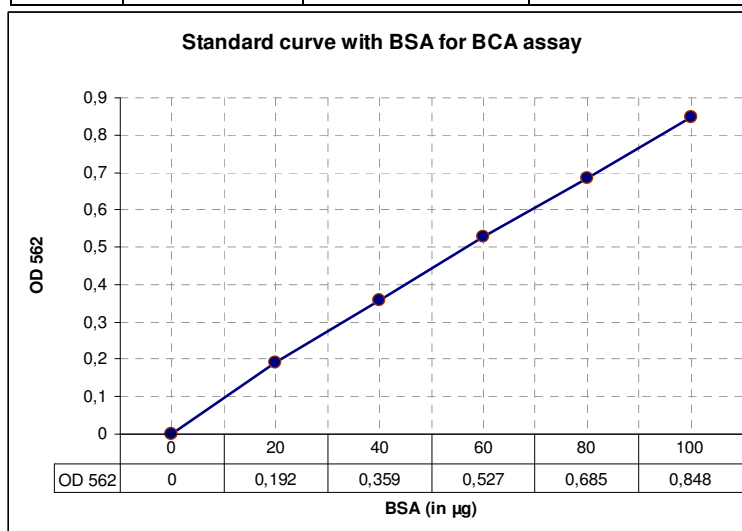
Fig 18

Blank was prepared by mixing 2mL BCA working reagent with $100 \mu L$ buffer or water. The contents were vortexed for thorough mixing and incubated at 37 °C for 30 min. The absorbance of the solution was measured at 562 nm. The protein concentration was determined by comparison of the absorbance of the unknown samples to the standard curve prepared using the BSA protein standards.

II.7.5 Radiolabeled ligand Binding Assay – Homologous competition experiment

Saturation binding experiment is a method applied to determine the receptor number and its affinity. In one of the methods, the radioligand concentration is constant, and competes for binding with the same unlabeled ligand. Since the radiolabeled and unlabeled ligands are chemically identical, the method is called a **homologous competition experiment**.

In a homologous competition experiment, the graph is plotted for the % specific binding obtained versus the logarithm of concentration of the unlabeled ligand. The curve obtained is a sigmoid curve wherein the top of the curve is a plateau at a value equal to radioligand binding in the absence of the competing unlabeled drug. The concentration of unlabeled drug that produces radioligand binding half way between the upper and lower plateaus is called the IC50 (inhibitory concentration 50%) or EC50 (effective concentration 50%).

The dissociation constant for the unlabeled ligand for the receptor is often referred to as the K_i rather than K_d because it is obtained from inhibition experiments rather than saturation experiments. The K_i value for the unlabeled ligand can be obtained from the IC_{50} value using the Cheng-Prusoff equation, whereL is the concentration of radioactive ligand used and K_d is the affinity of the radioactive ligand for the receptor.

$$K_i = \frac{IC_{50}}{1 + \dfrac{L}{K_d}}$$

The bottom of the curve is a plateau equal to nonspecific binding. In addition to binding to receptors of interest, radioligands also bind to other sites. Binding of the receptor of interest is called *specific binding,* while binding to other sites is regarded as *nonspecific binding*.

Nonspecific binding represents:

- Interaction of the ligand with the biological membranes. The nonspecific binding depends on the charge and hydrophobicity of the ligand.
- Binding to receptors, transporters or other proteins not of interest for the study.
- Binding to the filters used to separate bound from free ligand.

Non-specific binding is detected by measuring radiolabeled ligand binding in the presence of a saturating concentration of an unlabeled ligand bound to the receptor. Under those conditions, virtually all the receptors are occupied by the unlabeled drug so the radioligand can only bind to the nonspecific sites. This forms the plateau at the bottom of the curve; subtract the nonspecific binding from the total binding at that concentration to calculate the specific radioligand binding to receptors.

Binding studies were performed with L-[^{3}H] Glutamate on all truncation constructs in triplicate setups and each setup too made in triplicates. The experimental setup for L-[^{3}H]-Glutamate binding studies was carried out as shown in the table 2. About 20 μg of *Sf9* membranes were incubated with 3.4 μM of L-[^{3}H]-Glutamate in a volume of 50 μL of *binding buffer* to which increasing concentrations of unlabeled L-Glutamate (10^{-3} to 10^{-8} M) were added as shown in the table below. The contents were briefly mixed by vortexing and incubated at 25 °C for 60 min on a shaker.

Table 2 : Experimental setup for radioligand binding assay

Sno	Binding buffer (μL)	Unlabeled L-Glutamate	[^{3}H] L-Glutamate	Membranes 2mg/mL	Tubes Label		
1	32.6 μL	0	3.4 μM	10 μL	*1*	*13*	*25*
2	30.6 μL	1×10^{-8} M	3.4 μM	10 μL	*2*	*14*	*26*
3	31.6 μL	5×10^{-8} M	3.4 μM	10 μL	*3*	*15*	*27*
4	30.6 μL	1×10^{-7} M	3.4 μM	10 μL	*4*	*16*	*28*
5	31.6 μL	5×10^{-7} M	3.4 μM	10 μL	*5*	*17*	*29*
6	30.6 μL	1×10^{-6} M	3.4 μM	10 μL	*6*	*18*	*30*
7	31.6 μL	5×10^{-6} M	3.4 μM	10 μL	*7*	*19*	*31*
8	30.6 μL	1×10^{-5} M	3.4 μM	10 μL	*8*	*20*	*32*
9	31.6 μL	5×10^{-5} M	3.4 μM	10 μL	*9*	*21*	*33*
10	30.6 μL	1×10^{-4} M	3.4 μM	10 μL	*10*	*22*	*34*
11	31.6 μL	5×10^{-4} M	3.4 μM	10 μL	*11*	*23*	*35*
12	30.6 μL	1×10^{-3} M	3.4 μM	10 μL	*12*	*24*	*36*

Salt and *No salt* buffers were prepared for harvesting the filters and were maintained ice cold. The assay was terminated by dilution with 1mL of ice cold *No salt* buffer. The bound ligand was separated from the free ligand by rapid filtration over nitrocellulose membrane filter (NC45, poresize 45 μm, 25 mm diameter) presoaked with *Buffer for filter saturation* using a vacuum filtration setup. The filters were

washed once with 2mL of ice cold *No salt buffer* and 2mL of ice cold *Salt buffer*. The filters were placed in scintillation vials and dried at room temperature. The filters were dissolved in 600 µL ethylene glycol monomethyl ether solvent with thorough vortexing and after 10 min about 10mL of Scintillation cocktail was added. The radioactivity in the filters was measured for 1 min on a liquid scintillation counter. Data analysis of the binding experiments was performed using the GraphPad program.

All DPM values were converted into % specific binding using the following formula:

$$\% \text{ Specific binding} = \frac{(\text{DPM} - \text{Nonspecific binding})}{(\text{Total binding} - \text{Nonspecific binding})} \times 100$$

The IC50 values and Standard Error of Mean (SEM) were determined, analyzed and plotted.

II.7.6 Isolation of light density detergent resistant membranes (ld-DRMs) – by 1% Triton X-100 detergent treatment

About 800 µg of enriched plasma membranes prepared from *Sf9* cells expressing the protein of interest were extracted with 250 µL ice-cold *TXNE* buffer on ice for 15 min. The extraction was carried out under ice cold conditions (pipettes, tips, Pasteur pipettes, etc used for the experiments were maintained cold).

The gradient buffers were prepared using Optiprep^{TM} as follows:

 30% Optibuffer   7mL Optiprep^{TM} (60%) + 7mL TXNE buffer
 5% Optibuffer   160μL Optiprep^{TM} (60%) + 1.76mL TXNE buffer

The extraction mixture was taken in 11x 60mm ultracentrifugation tubes and the gradient was prepared as follows

 40% layer   Extraction mixture with 500μL of Optiprep^{TM} solution (60%)
 30% layer   1.2mL of 30% Optibuffer solution
 5% layer   0.4mL of 5% Optibuffer solution
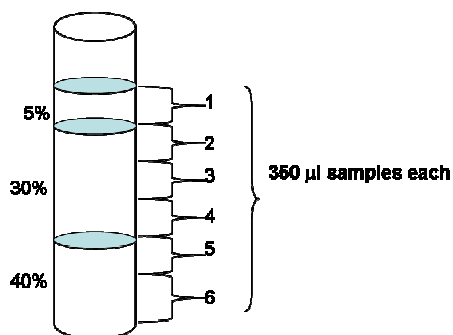
Fig. 19. the Gradient setup in an ultracentrifugation tube and sample fractions.

The gradients were centrifuged for 2 hr at 4°C at 259,182xg on a Beckmann TLS55 rotor. 350 µL fractions were collected from the top and analyzed on a western blot.

II.7.7 Preparation of liposomes for floatation assay `

Lipid	Mol wt (Da)	Ratios (mol %)	
		Raft liposomes	**Non-raft liposomes**
DOPC	786.15	30	60
DPPC	734	30	-
Cholesterol	386.6	40	40

DOPC   Dioleoyl phosphatidyl choline
DPPC   Dipalmitoyl phosphatidyl choline

Liposomes of raft and non-raft composition were prepared by dehydration-rehydration process in glass tubes previously rinsed with chloroform. Briefly, the lipids dissolved in chloroform were transferred to the glass tube. The solvent was removed under mild nitrogen stream to a thin film before being finally resuspended in the *Assay buffer* (250 μL). The mixture was vortexed for 30 sec and was subjected to 10 cycles of freezing (liquid nitrogen, -196.4°C) and thawing (50°C in a water bath).

The liposome suspension was sized by extrusion through two stacked polycarbonate membranes (pore size 100 nm) by 21 passes using an extruder. The liposomes were verified for homogeneity using dynamic light scattering and were used for protein interaction study by floatation assay with DGX or Circular dichroism.

II.7.8 Liposome size determination by dynamic light scattering

The mean diameter and particle size distribution of the liposomes were determined using a Dynamic Light Scattering (DLS). The measurements were made at 10 mW maximum, output He Ne; 633 nm. This technique measures the particle diffusion due to Brownian motion and relates this to the size of the particle. The parameter calculated is defined as the translational diffusion coefficient (D).

The particle size is then calculated from D using the Stoke-Einstein equation;

$$d(H)=(kT)/(3\pi\eta D)$$

Where

d(H) is the hydrodynamic diameter   **k** is the Boltzman's constant
D is the translational diffusion coeffiecient   **T** is the absolute temperature
η is the viscosity

The DLS equipment produces a correlation of the particle position decay based on its movement. Since a large particle diffuses slower than a smaller one, the decays are different and a mathematical model correlates its decay to the size of the particle.

Measurements were performed at a constant temperature (25°C) because the viscosity of a liquid is related to its temperature. Samples were diluted in the *Assay buffer* and 6 measurements of 10 seconds each were performed. The mode chosen was continuous and the detection angle at 90°. The detection modes available were based on intensity, volume and number of the liposomes. 6 recordings were made for each of the liposome samples.

II.7.9 Liposome floatation assay

10 μg of purified protein was incubated with Raft and Non-raft liposomes (500 μg) for 10 min at 37°C in an ultracentrifugation tube. Floatation assay was carried out by subjecting the proteoliposome mixture in a gradient ultracentrifugation. The gradient buffers were prepared using Optiprep^{TM} as follows:

50% Optibuffer	2mL of Optiprep^{TM} solution (60%) + 480 μL *Assay buffer (1X)*
30% Optibuffer	2mL of Optiprep^{TM} solution (60%) + 1mL *Assay buffer (5X)* + 1.5mL MilliQ water

The step gradients were prepared in the following order in an ultracentrifugation tube as shown in the table

50% layer	Proteoliposome with $360\mu L$ of Optibuffer solution (50%)
30% layer	$1160\mu L$ of 30% Optibuffer solution
0% layer	$450\mu L$ of *Assay Buffer 1x*

The gradients were ultracentrifuged on a TLS55 rotor at 166,000xg for 3 hrs. The samples were collected carefully in four fractions (600, 400, 400 and 600 μL) from the top.

II.7.9.1 Protein precipitation by 10% Trichloro acetic acid (TCA)

For Western blot analysis the fractions needed to be concentrated. The fractions collected were diluted to 900 μL with water and 100 μg of Bovine serum albumin (BSA) was added to aid mass precipitation. 110 μL Trichloro acetic acid (TCA, 90%) was added to the samples and left on ice for 5 min to precipitate. The contents were

centrifuged at 13,000 rpm for 10 min. The pellet was washed twice with 500 μL of 70% ethanol in PBS to remove any residual TCA and vacuum dried. Samples for western blot was prepared by the addition of 1X *denaturing SDS loading buffer*.

II.7.10 Conformational changes of peptides with liposomes – Circular Dichroism spectra analysis

The interactions of $Pep_{602-624}$ and $Pep_{611-624}$ with liposomes prepared of "raft" composition were determined by circular dichroism. The peptide samples were solubilised in MilliQ water to a concentration of 2 mg/mL. The samples contained 50 μM peptides with or without "raft" liposomes (10mM) in 50mM phosphate buffer pH 7.4. Samples comprising buffer or raft "liposomes" without peptide were used for background correction. CD spectra were obtained at room temperature (25°C) in a 1mm circular quartz cell and a spectropolarimeter. Each spectrum was recorded from 190 to 250 nm with step resolution of 1 nm. For each determination, data were smoothed, back-ground subtracted and converted into mean residue molar ellipticity [θ] (deg.cm^2/dmol).

III. Results

III.1 Expression and purification of extracellular domain (ECD) of the Rat metabotropic $GABA_B1b$ receptor (GBR1bNT) in the Recombinant Baculovirus system (RBV) and *E.coli*

Metabotropic $GABA_B$ receptors ($GABA_BR$) are heterodimeric receptor and composed of $GABA_B1b$ and $GABA_B2$ subunits involved in the inhibitory effects at the neural synapses. It was shown that the N-terminal extracellular domain (ECD) of the $GABA_B1$ subunit alone is sufficient of bind GABA with the same affinity like the heterodimeric receptor complex, whereas the N-terminal ECD of the $GABA_B2$ subunit cannot bind GABA.

The ligand binding ECD of both metabotropic glutamate receptors (mGluR), $GABA_B1b$ share common structure features, being in the same class of GPCRs and are homologous to the leucine, isoleucine and valine binding protein (LIVbp). Among the three, the ECD of mGluR and LIVbp are expressible as soluble proteins and the X-ray crystal structure of both resembled the *venus fly trap structure* (Kunishima et al., 2000). But incase of the ECD of $GABA_B1b$, there were not many successes in the overexpression and purification of this domain.

The current study was focussed upon developing strategies and tools to over-express and purify the rat ECD of $GABA_B1b$ (GBR1bNT) in the recombinant baculovirus (RBV) system and *E.coli* expression systems. Both experimental and computational approaches were applied to design strategies for over-expression and purification of GBR1bNT in these expression systems.

III.1.1 Expression and purification of GBR1bNT in the RBV system

III.1.1.1 Expression and purification of pVL1392-Mel-GBR1bNT expressed in SF+ cells using a Ni-sepharose column

The expression of the ECD of GBR1bNT was first attempted under the control of Mellitin secretion signal peptide. In this construct, the native signal peptide of $GABA_B1bR$ was replaced with that of Mellitin secretion signal peptide for expression and secretion of GBR1bNT to the medium since the melltin signal peptide is native to the insect cells.

From the kinetics study, the protein expression to the medium was determined to be optimal at a MOI of 3 for 72-96 hrs. A large scale expression (in 1L) of the culture was setup to purify the GBR1bNT expressed and secreted to the medium. The expression and purification protocol was followed as described in the material and methods. About 1L of $2x10^6$ SF+ cells/mL in suspension culture was infected with pVL1392-Mel-GBR1bNT virus for 72-96 hrs at a MOI of 3. Culture supernatant was clarified by centrifugation; the supernatant was loaded on a CHT column followed by a Nickel-sepharose column.

A purification setup was carried out on the Ni-bound GBR1bNT to establish the purification strategy. The column was washed with different concentration of Imidazole (20mM, 50mM, 75mM and 250mM) in 20mL fractions. About 1.7mL of the elution fractions were precipitated by 10% TCA and washed with 70% ethanol in PBS. The samples were prepared by treating the pellet with 100µL of *2X denaturing SDS loading buffer*.

From the silver stained gel of the samples prepared from different Imidazole concentration (20mM, 50mM, 75mM and 250mM) a faint band for GBR1bNT was observed around 50kDa as indicated by the red arrow (*as shown in the fig. 20*).
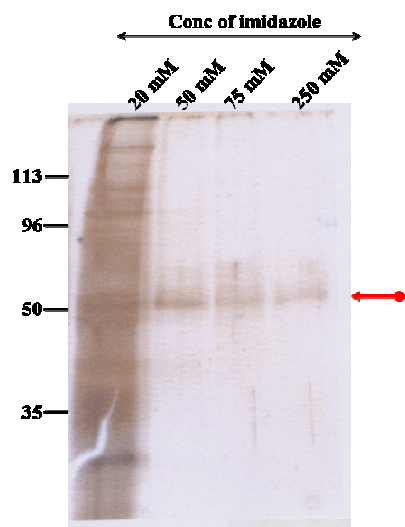
Fig.20. Silver stained SDS-PAGE of GBR1bNT purified on a Ni-column
Fractions obtained from wash steps of the Ni-column with 20mM, 50mM, 75mM and 250mM Imidazole were collected. About 10 µL of the sample was electrophoresed on a 10% SDS-PAGE and silver stained (using the silver staining kit). A faint brown single band was observed at the expected molecular size (50kDa) of GBR1bNT (as indicated by red arrow).

From the first attempt of GBR1bNT expression under the control of mellitin signal only low amounts of GBR1bNT could be purified. The possible reasons are that either the mellitin signal peptide suitable for the secretion of GBR1bNT or that the GBR1bNT was poorly expressed and retained within the cell.

Inspite, GBR1bNT construct lacking the RXXR-endoplasmic reticulum retention motif at the C-terminus of the GABA$_B$1b subunit and the native signal peptide replace by a mellitin signal peptide still failed to express good amounts of the proteins.

GBR1bNT is homologous to the ECD of mGluR that belongs to the same receptor class for which the X-ray crystal structure is solved. The next attempts are to study the GBR1bNT at a sequence level and derive a relationship between the ECD of mGluR and GBR1bNT

III.1.1.2 Sequence analysis and molecular modelling studies on GBR1bNT – a computational approach
Inorder to compare the primary sequence of ECD of mGluR and GBR1bNT, PERL scripts were written to fasten the purpose. The primary protein sequence of the ECD of mGluR for which the crystal structure was solved (from residue 36 to 505) was aligned with GBR1bNT (from residue 30 to 445).
The amino acid composition of aligned ECD of mGluR and GBR1bNT was clustered depending upon the physicochemical parameters. The clusters were carefully

examined and compared with each other, the residues that were present more in number are shaded in grey (*as shown in the Fig. 21*).

```
                              P=19  <=======SMALL              C=5            P=24  <=======SMALL
        C=6                                                          A=28  G=27      <=========TINY
        A=35  G=25  G=25  <=========TINY                             G=27
        G=25                                                   C=5   T=27
        C=6   T=23                                                   S=33
              S=39                                                              N=16
                    N=23
   I   V                                           I   V
   22  31                    D= 27                 23  24             D= 19
   L=35                                             L=33
                                                                    E=29
              E=23          <-----------CHARGED                           <===========CHARGED
   M=3        K=22                                  M=9         K=23
        Y=14        H             Q=18                    Y=17        H      Q=14
        F     W=5   9   <=================POSITIVE        F     W=9   11          <=======POSITIVE
        16              <======POLAR                      19              R      <======POLAR
              R                                                          24
              18
   AROMATIC        Ligand binding domain of mGluR   AROMATIC    Ligand binding domain of GABA_B1bR
   ALIPHATIC                                        ALIPHATIC              (GBR1bNT)
   NON-POLAR                                        NON-POLAR
```

Fig. 21. A cluster depiction of amino acids composition of the ECD of mGluR *(left panel)* **and GBR1bNT** *(right panel)* **based on physiochemical properties of the amino acids. The residues that are found to be more in number are shaded in grey boxes.**

Incase of composition analysis of mGluR ECD, residues alanine, serine, asparagine, aspartate, valine and glutamine were found more in number (7, 6, 7, 8, 4 and respectively) in comparison to the GBR1bNT. This indicates that mGluR contained more of small and polar residues in comparison to the ECD of GBR1bNT.

Incase of composition of GBR1bNT, residues proline, threonine, glutamate, methionine, phenyl alanine, tyrosine, tryptophan and arginine were found more in number (5, 4, 6, 6, 3, 3, 4 and 6 respectively) in comparison to the ECD of mGluR.

Inspite of comparing 469 residues of ECD of mGluR aligned with 415 residues of ECD of GBR1bNT, still GBR1bNT contained more of bulky and branched hydrophobic residues rendering GBR1bNT hydrophobic.

This interesting difference between the physicochemical compositions of amino acids further raised the interest to study the receptor at structure level. Homology modelling was performed on the aligned sequences of the ECD of mGluR and GBR1bNT. PERL scripts were self writtern and compiled on the LINUX workstation to carry out the

modelling process. The GBR1bNT model was obtained by transferring the atomic coordinates of ECD of mGluR (PDB code: 1EWK) to the corresponding aligned residue of GBR1bNT using the PERL script. Energy minimizations were carried out using generate.inp, model_minimize.inp and model_anneal.inp modules of the CNS package (Rice and Brunger, 1994) and the script was modified to obtain 15 best energy minimised structure. The root mean square deviation (RMSD) between the mGluR structures template (1EWK) and the 15 GBR1bNT models were found to be 1.85±0.05. the structure were further verified using ProCheck (Laskowski et al., 1993).

The representative structure of the GBR1bNT model was superposed on the mGluR structure template (*see middle panel of Fig. 22*). Upon careful examination of the superposed structures it was observed that there was a significant difference in the secondary structure at the N-terminus of GBR1bNT. The first 45 residues of mGluR structure template contained a well ordered secondary structure of Sheet-Helix-Helix (*see right panel of Fig. 22*) inspite having 4 proline residues. Incase of correspondingly aligned GBR1bNT (*see top panel of Fig. 22*), the 45 residue stretch contained a very disordered structure with random coils and formed a helix structure after 30 residues (*see left panel of Fig. 22*). This unstructured region was found immediately after the signal peptide cleavage site and contained 7 proline residues at position 33, 36, 38, 40, 43, 44 and 46 postions.

From the computational modelling studies it was inferred that GBR1bNT apart from being hydrophobic contained proline-rich disordered region just after the signal peptide cleavage site that might hinder the expression and secretion of GBR1bNT. Therefore, new constructs were considered that can surpass these observed hindrances and express the protein in good amounts.

Top

mGluR   : 45-LESVHHQ**PPA**EKV**P**ERKCGEIREQYGIQRVEAMFHTLDKINAD**P**VLL

GBR1bNT : 30-SHSP̲HL̲P̲RP̲HP̲RV**PP**H**P**SSERRAVY----IGALF̲PMSGGWPGGQACQ

Right

Middle

Left

Fig. 22 Computational modelling studies on GBR1bNT

Top : Aligned N-terminal 41 residues of GBR1bNT from the 30th residue of the mature chain after the signal peptide cleavage site to the 45 residues of mGluR from 45th residue for which the structure data is available.
Middle panel : The GBR1bNT model superposed on the ECD mGluR structure template (PDB code : 1EWK) with an RMSD of 1.85±0.05, the N-terminal 45 residues aligned in the _top panel_ are highlighted as ribbons (green-ECD mGluR and red-GBR1bNT model). _Left Panel_ : Closer view of the N-terminal 41 residues as modelled forming a disorder structure with random coil followed by a helix. _Right Panel_ : Closer view of the N-terminal 45 residues as seen in the crystal structure of ECD of mGluR (PDB : 1EWK) forming a ordered secondary structure. The pictures were prepared using PyMOL.
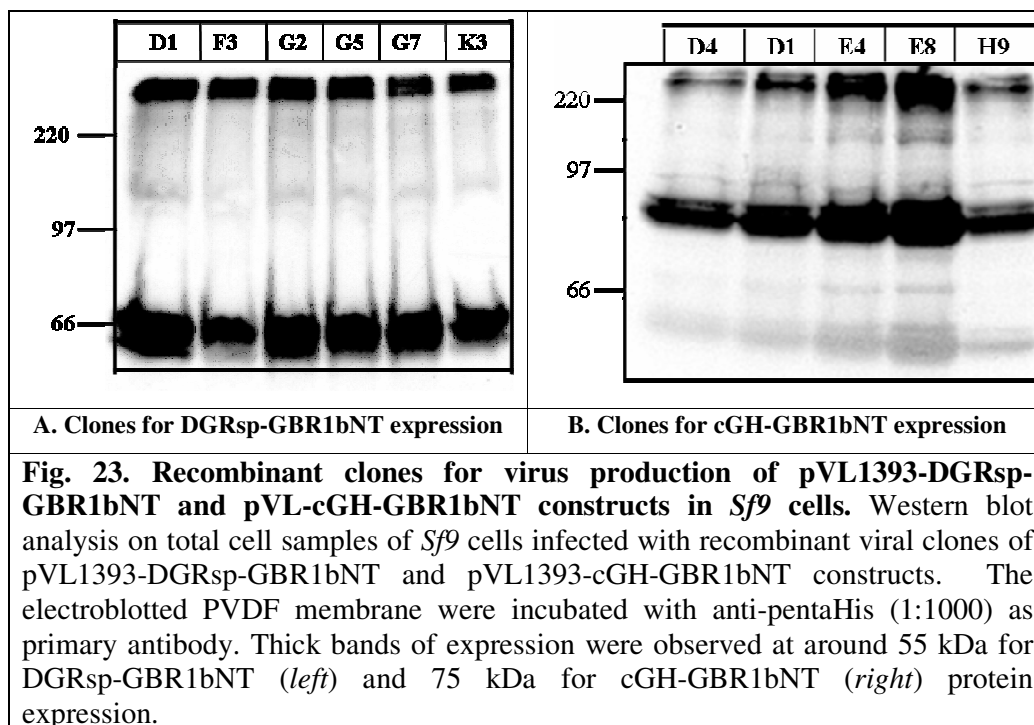
III.1.1.3 Recombinant virus production for constructs pVL1393-DGRsp-GBR1bNT, pVL1393-cGH and pVL1393-cGH-GBR1bNT in the RBV system

In the previous attempt, only low yields of GBR1bNT was obtained (*see fig. 20*), inspite of expression driven under the control of native mellitin signal peptide. Therefore, the pVL1393-DGRsp-GBR1bNT construct was prepared. In the pVL1393-DGRsp-GBR1bNT construct, the native signal peptide of $GABA_B1bR$ was replaced with the *Drosophila* metabotropic glutamate receptor A (DmGluRA) signal peptide, in place of the mellitin signal peptide as studied before. The rationale behind considering the DmGluRA signal peptide is that, the signal peptide is native to the insect cells; moreover in the studies by Eroglu it was reported that the ligand binding domain (DG14c construct in pVL1393, Cagla Eroglu, PhD thesis, 2002) of DmGluRA was well-expressed in the insect cells yielding quantities for crystallization trials.

From the inferences made from the computational modelling studies, the pVL1393-cGH-GBR1bNT construct was prepared. In the pVL1393-cGH-GBR1bNT construct, the expression and secretion of GBR1bNT was attempted by tagging chicken growth hormone (cGH) at the N-terminus of GBR1bNT. The rationale behind preparing the construct is proline-rich region observed unstructured at the N-terminus when modelled on mGluR template and energy minimised (*see Fig. 22*). Further at the N-terminus apart from being proline-rich it contained several bulky and hydrophobic residues that might interfere with the expression of GBR1bNT when expressed alone. It was reported that the human growth hormone (hGH) was used as a fusion partner for over expression, purification and 3D-structure determination of cysteine rich domain (CRD) of secreted Frizzled related protein 3 (sFRP-3) in chinese hamster ovary cells (CHO cells) (Dann et al., 2001). In another work it was reported that cGH was well expressed in the RBV system (Foster et al., 1997). So the cGH that was well-expressed in the RBV system was considered as the fusion partner for the expression and secretion of GBR1bNT. The pVL1393-cGH construct was prepared as a control to compare the expression levels of cGH, when expressed alone or when tagged with GBR1bNT.

Recombinant viruses for pVL1393-DGRsp-GBR1bNT, pVL1393-cGH and pVL-cGH-GBR1bNT were produced following the procedure as described in the materials and methods. The recombinant clones were tested for protein expression by western blot analysis (*see fig. 23*).

A. Clones for DGRsp-GBR1bNT expression   **B. Clones for cGH-GBR1bNT expression**

Fig. 23. Recombinant clones for virus production of pVL1393-DGRsp-GBR1bNT and pVL-cGH-GBR1bNT constructs in *Sf9* cells. Western blot analysis on total cell samples of *Sf9* cells infected with recombinant viral clones of pVL1393-DGRsp-GBR1bNT and pVL1393-cGH-GBR1bNT constructs. The electroblotted PVDF membrane were incubated with anti-pentaHis (1:1000) as primary antibody. Thick bands of expression were observed at around 55 kDa for DGRsp-GBR1bNT (*left*) and 75 kDa for cGH-GBR1bNT (*right*) protein expression.

From the Western blot, *Fig. 23A,* a thick band was observed at around 60 kDa that corresponded to the molecular weight of the expressed DGRsp-GBR1bNT in all the clones. Clone D1 expressed cGH-GBR1bNT was selected for further production of baculovirus stocks. Similarly, in *Fig. 23B*, a thick band was observed at around 80kDa that corresponded to the expressed cGH-GBR1bNT in the all the clones. Clone E8 was selected for futher production of baculovirus stocks.

The titre values were determined for the viral stocks of the constructs by End point dilution and they are as follows:

Construct Name	Titer value (Pfu/ml)	Theoretical mol wt
DGRsp-GBR1bNT	1.5×10^8	~55 kDa
cGH-GBR1bNT	1.33×10^8	~75 kDa

III.1.1.4 Optimization of expression and purification of pVL1393-DGRsp-GBR1bNT expressed in *SF+* cells using Ni-sepharose column

The DGRsp-GBR1bNT (GBR1bNT with the DmGluRA signal peptide) expression was carried out in 1L of 2×10^6 *SF+* cells/mL suspension culture infected with pVL1393-DGRsp-GBR1bNT virus at MOI of 3 for 72-96 hrs. The purification protocol was carried out as described in the *Materials and methods, section II.2.5.7.1* for CHT column purification.

The Ni-bound DGRsp-GBR1bNT was eluted from the column by a gradual increase in the Imidazole concentration (10, 20, 30, 50, 75, 100, 150, 200, 250 and 500mM) and collected in 2mL fractions. A chromatogram was obtained plotting the protein concentration under UV 280nm (Blue line) against the % Imidazole concentration of Buffer B (purple line) (*as shown in the fig. 24, left*). A single peak was obtained in the elution profile at 10% Imidazole concentration of Buffer B (50mM Imidazole). Western blot analysis on the fractions collected at the peak (fractions labelled 1-10) were incubated with anti-pentaHis antibody (1:1000). Bands were observed at molecular weights around 60 kDa (corresponding to the molecular weight of purified DGRsp-GBR1bNT (as indicated by an arrow in the *fig. 24, right*) and a contaminant bound to the Ni-sepharose column around 100 kDa (as indicated by a dashed line in *fig. 24, right*). The fractions from 6-10 containing Dsp-GBR1bNT protein were pooled, concentrated on an Amicon filter (30 kDa) and dialyzed in 2L of dialysis buffer overnight in the cold room.

The total protein content of purified DGRsp-GBR1bNT was determined by the absorbance of the sample at 280 nm. Extinction coefficients were theoretically calculated (73210 M^{-1} cm^{-1}) and it was found that about 1.3 mg of purified DGRsp-GBR1bNT was obtained from 1L of expression volume. 50 μL aliquots were prepared, flash frozen in liquid nitrogen and stored at -80 °C.

From this experimental setup it was observed that good amount of purified DGRsp-GBR1bNT were obtained that can be used for ligand binding trials with [^{3}H]-GABA and [^{3}H]-CGP54626A.
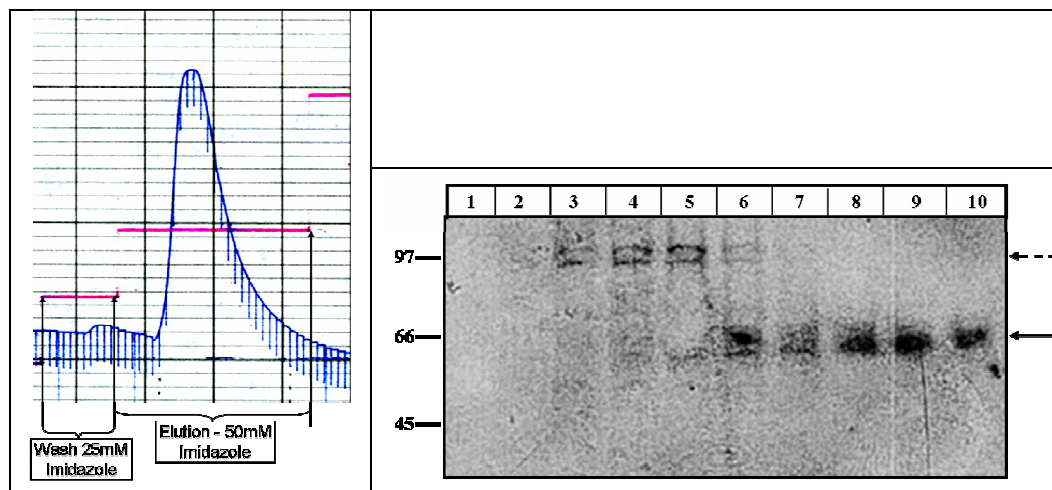
Fig. 24. Purification of DGRsp-GBR1bNT expressed in *SF+* cells using Ni-sepharose column. *Left*, Elution profile of DGRsp-GBR1bNT monitored at UV 280 (blue line) and *%* Imidazole concentration (purple line) are shown. *Right,* Western blot on the elution fractions from the Ni column. 10 µl of each fraction was electroblotted in PVDF membrane and incubated with anti-mouse antibody. DGRsp-GBR1bNT was observed at around 60kDa as pointed by the arrow in fractions 6,7,8,9 and 10. there was another band of higher molecular weight observed at 100 kDa indicated by dashed arrow.

III.2 Over-expression and purification of GBR1bNT in the _E.coli_ system

III.2.1 Molecular constructs

The expression vectors considered in the study were of pBR322 vector origin and tagged at the N-terminus with fusion proteins (_see table, below_) for better soluble over-expression in the cytoplasm. The vector contained 6-His tag at the C-terminus for the ease of purification using a Ni-sepharose column or to detect it on western blots using an anti-pentaHis antibody. The host strains used for the study were selected based on the features possessed by the strain in handling over-expression of GBR1bNT in more soluble form.

	Tags and fusion partners	
Vector	**N-term**	**C-term**
pETM 11	-	6-His
pETM 30	GST	6-His
pETM 50	DsbA	6-His
pETM 52	DsbA (leaderless)	6-His
pETM 60	NusA	6-His
pET15b-GST	GST	6-His

The constructs considered for the study and the molecular weight of the expressed GBR1bNT with its fusion partner is summarized in the _table, below_ :

Table no. 3 : GBR1bNT cloned into different vectors and their molecular weights		
Vector	**Name of the expressed protein**	**Theoretical Mol wt***
pETM 11+GBR1bNT	GBR1bNT	~ 50 kDa
pETM 30+GBR1bNT	GST-GBR1bNT	~ 76 kDa
pETM 50+GBR1bNT	DsbA-GBR1bNT	~ 72 kDa
pETM 52+GBR1bNT	DsbA2-GBR1bNT	~ 72 kDa
pETM 60+GBR1bNT	NusA-GBR1bNT	~ 105 Da
pET 15b-GST+GBR1bNT	GST-GBR1bNT	~ 76 kDa
* Molecular weight of fusion partner and GBR1Bnt		

The GBR1bNT over-expression in _E.coli_ and optimization of purification was carried out in following stages:

1. Selection of the expression vector.
2. Selection of the expression host.
3. Efficiency of the purification column.

    4. Improvement of the soluble expression and efficient purification.

III.2.2 Expression of GBR1bNT cloned in different vectors and transformed into BL21(DE3) strain – to select appropriate expression vector

The intial screen was carried out for the selection of a suitable vector capable of overexpressing GBR1bNT in *E.coli*. The PCR amplified GBR1bNT was ligated into the pETM series (pETM11, pETM30, pETM50, pETM52 and pETM60 plasmids) as mentioned in the *table no. 3* and transformed into BL21(DE3) strain. The Expression was carried out as described in the materials in the methods using 1mM IPTG. About 10 µL of samples from total cells of BL21(DE3) were analyzed on a SDS-PAGE (10%) after staining with Coomassie blue. The stained gel was photographed on a BioRad gel documentation system.

No expression was observed in the total cells under uninduced conditions containing the plasmid. In case of 1mM IPTG induced conditions, bands of over-expression were observed corresponding to the expected molecular weights (*see fig. 25*). Under IPTG induced conditions of pETM11+GBR1bNT construct, a thick band was observed at around 50 kDa (for GBR1bNT); for pETM30+GBR1bNT at around 76 kDa (for GST-GBR1bNT); for pETM50+GBR1bNT, no bands were observed for DsbA-GBR1bNT as the IPTG induction resulted to be toxic as there was no growth observed in the cells; for pETM52+GBR1bNT, band was observed at around 72 kDa (for DsbA2-GBR1bNT), a triplet samples were loaded as a counter check over the loading volumes and incase of pETM60+GBR1bNT, the band was observed at around 105 kDa (for NusA-GBR1bNT).

From the test expression, it was observed that there was a good expression of GBR1bNT in the total cells. The next step is to verify whether the expression observed in total cells are present in soluble form in the cytoplasm of *E.coli* or not and whether it was purified using the Ni-sepharose column.
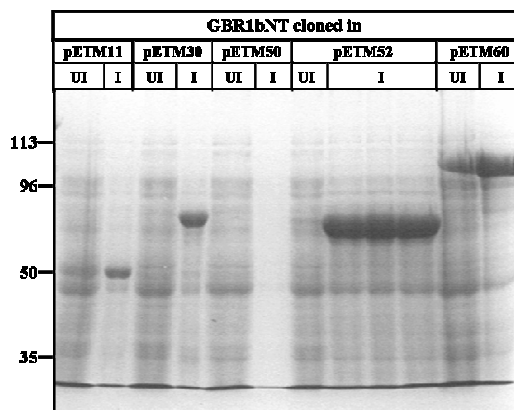
Fig 25. Expression of GBR1bNT cloned in pETM series in BL21(DE3) strain of *E.coli* and induced with 1mM IPTG. UI – Uninduced; I – Induced
10μL of total cells loaded in 10% SDS-PAGE stained with Coomassie blue and photographed on BioRad gel documentation system. Bands of over-expression under 1mM IPTG induced (I) condition was observed for GBR1bNT cloned into pETM11, pETM30, pETM52 and pETM60 vectors. No bands of over-expression were observed in the any of the plasmids under IPTG uninduced (UI) conditions and in induced conditions for GBR1bNT cloned in pETM50 vector.

III.2.3 Optimization of purification of GBR1bNT cloned in pETM60 (containing NusA fusion partner) vector and expressed in BL21(DE3) strain– to verify soluble expression of GBR1bNT

An efficient over-expression of GBR1bNT was observed in total cells transformed with the plasmids pETM11, pETM30 and pETM60 containing the GBR1bNT construct. pETM60+GBR1bNT plasmid was chosen to optimise the purification of NusA-GBR1bNT.

Expression was carried out in 1L and was induced with 0.1mM IPTG at 30 °C for 3 hrs. Cell pellet was lysed in the lysis buffer by sonication and passing through Emulsiflex. Cell lysate was centrifuged and supernatant was loaded in a Ni-sepharose column. The column was washed with 30mM Imidazole and eluted with 125mM Imidazole collected in 1.5mL fractions. Samples were prepared and resolved on a SDS-PAGE.

About 10μL of TCA precipitated sample was resolved on a 10% SDS-PAGE gel. Bands were observed corresponding to the expected size of the purified NusA-GBR1bNT (approx 105 kDa) as indicated by a black arrow in the *fig.26*. There was other protein bands at lower molecular weight as indicated by a dashed arrow in the

fig. 26 which could be contaminants bound to the Ni-sepharose column during purification.
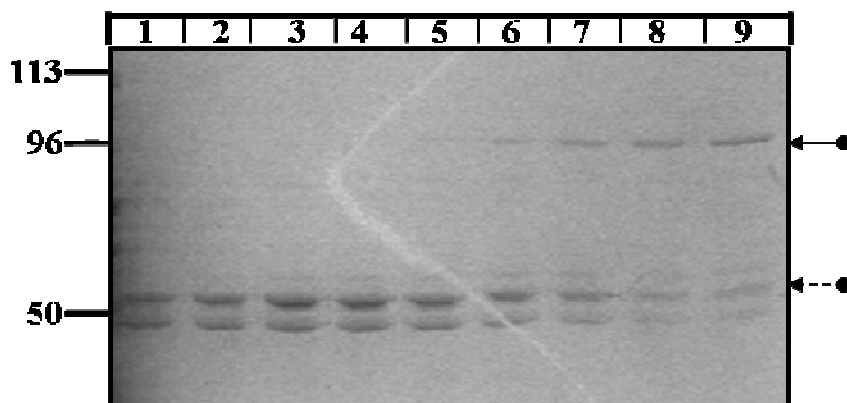

Fig. 26. Purification of NusA-GBR1bNT (pETM60+GBR1bNT expressed in BL21(DE3)) on a Ni-sepharose column.
L – Load; W – Wash.
$10\mu L$ of TCA precipitated elution fraction loaded in 10% SDS-PAGE wells, Coomassie blue stained and documented in a BioRad Gel documentation system. The eluted NusA-GBR1bNT (~105 kDa) as indicated by an arrow and its degradation products (as indicated by dashed arrow) were observed upon Coomassie blue staining.

A considerable amount of NusA-GBR1bNT was found in the soluble form in the 0.1mM IPTG induced pETM60+GBR1bNT plasmid transformed BL21(DE3) cells. The supernatant containing the soluble expression of NusA-GBR1bNT thus obtained was purified in a Ni-sepharose column but it yielded low quantities.

III.2.4 Expression of GBR1bNT cloned in pETM11 and pETM60 vector (containing NusA as fusion partner) and transformed into different strains of *E. coli* – to select appropriate expression host to improve the over-expression

In order to improve the soluble expression of GBR1bNT, pETM11+GBR1bNT and pETM60+GBR1bNT plasmids were transformed into BL21(DE3)pLysS, C43(DE3) and Rosetta(DE3)pLysS strains. There are several factors involved for not obtaining a good amount of soluble expression. To name a few the reasons could be

1. The *E.coli* has a thick cell wall that so *the induced cells would have remained unbroken* inspite of treatment with lysis buffer, passage through emulsiflex and sonification. This problem can be *overcome by overexpressing GBR1bNT in*
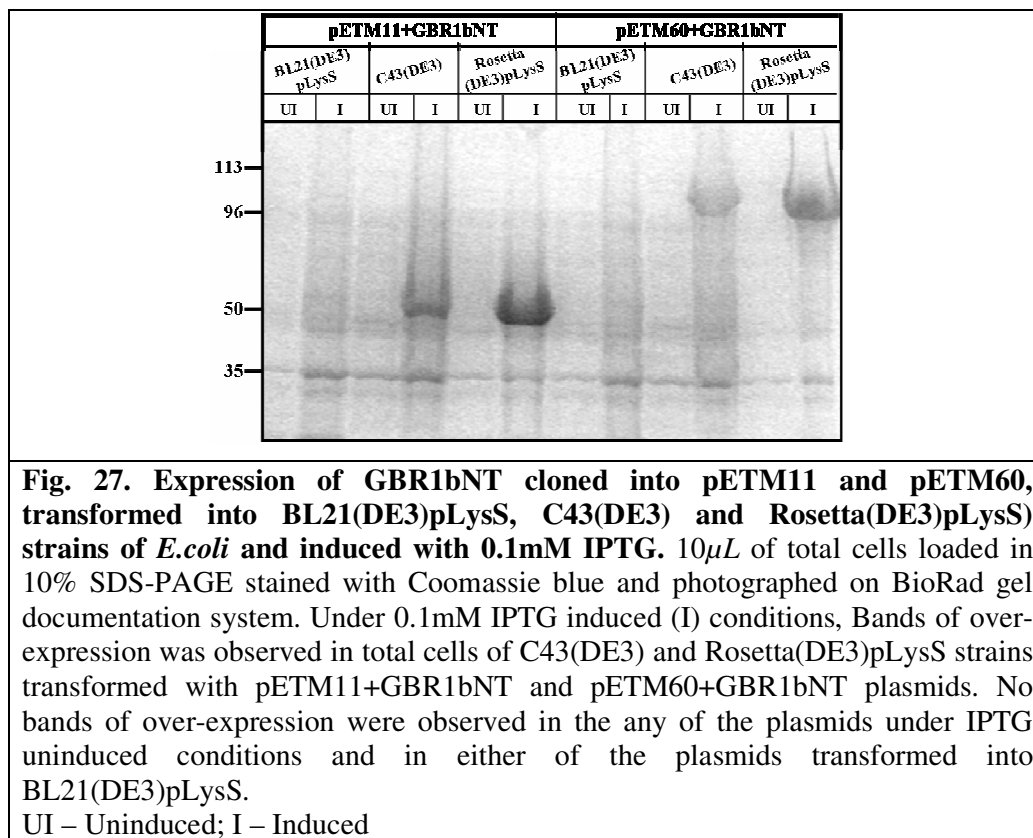
BL21(DE3)pLysS strain. This strain carries an extra plasmid pACYC184 encoding T7 lysozome gene that can disrupt the inner membrane enabling rapid lysis of cells.

2. The GBR1bNT being hydrophobic (*see fig. 21*) *would have adhered to the inner walls of the membrane* and resistant to 500mM NaCl in the lysis buffer. This problem could be *overcome by overexpressing GBR1bNT in C43(DE3) strain* as C43(DE3) cells.

3. Finally, GBR1bNT being an eukaryotic protein contains codons that are rarely used by *E.coli,* this leads to a poor transcription of the mRNA. This problem could be overcome by overexpressing GBR1bNT in Rosetta(DE3)pLysS strain that contains tRNA genes for AGG, AGA, AUA, CUA, CCC, GGA on a Col-E1 compatible chloramphenicol-resistant plasmid.

A Expression was carried out on these strains upon IPTG induction. 10µL of total cell samples were loaded on a 10% SDS-PAGE, Coomassie stained and documented on a gel documentation system.

Except in the case of plasmids pETM11+GBR1bNT and pETM60+GBR1bNT transformed into BL21(DE3)pLysS strain, bands of over-expression upon IPTG induction were observed in other cases. In pETM11+GBR1bNT transformed into C43(DE3) and Rosetta(DE3)pLysS, a band around 50 kDa (GBR1bNT) was observed and in pETM60-GBR1bNT constructs transformed in to Rosetta(DE3)pLysS and C43(DE3), the band was observed around 105 kDa (NusA-GBR1bNT) at 0.1mM IPTG induced conditions *as shown in the fig 27*.

Fig. 27. Expression of GBR1bNT cloned into pETM11 and pETM60, transformed into BL21(DE3)pLysS, C43(DE3) and Rosetta(DE3)pLysS) strains of *E.coli* and induced with 0.1mM IPTG. 10μL of total cells loaded in 10% SDS-PAGE stained with Coomassie blue and photographed on BioRad gel documentation system. Under 0.1mM IPTG induced (I) conditions, Bands of over-expression was observed in total cells of C43(DE3) and Rosetta(DE3)pLysS strains transformed with pETM11+GBR1bNT and pETM60+GBR1bNT plasmids. No bands of over-expression were observed in the any of the plasmids under IPTG uninduced conditions and in either of the plasmids transformed into BL21(DE3)pLysS.
UI – Uninduced; I – Induced

III.2.5 Purification of GBR1bNT cloned in pETM60 (containing NusA as fusion partner) vector and expressed in C43(DE3) strain

C43(DE3) strain of *E.coli* is used exclusively for expressing recombinant proteins toxic for other strains of *E.coli* and has proven to be efficient in expressing membrane proteins or highly hydrophobic proteins. Hence, the pETM60+GBR1bNT plasmid transformed into C43(DE3) strain was selected for optimising the purification.

About 1L culture was induced with 0.1mM IPTG at an OD_{600} of 0.8 – 1.0 and harvested after 16 hrs at 18 °C post-induction. The cells were lysed in the lysis buffer by sonication and passing through Emulsiflex. The cell lysate was centrifuged and the supernatant was loaded on a Ni-sepharose column. The column was washed with 20mL of buffer containing different concentration of Imidazole (30mM, 50mM, 70mM, 100mM, 150mM, 200mM and 250mM). Samples were prepared for every fraction and 10 μl of each sample was electrophoresed on a 10% SDS-PAGE and stained with Coomassie blue dye.
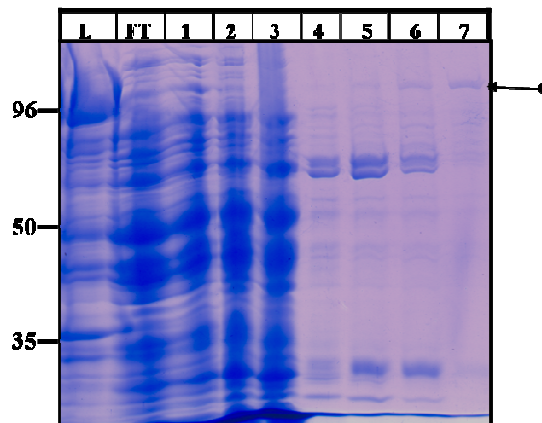
Fig. 28. Purification of GBR1bNT cloned into pETM60 vector and expressed in C43(DE3) strain.
L = Load; FT = Flow through; 1-7 = Elution fractions with Imidazole concentration at 30, 50, 70, 100, 150, 200, 250mM respectively. The arrow indicates the band that corresponds to the NusA-GBR1bNT protein (105 kDa).

From the fig. 28 it was observed that Ni-bound NusA-GBR1bNT contained non-specific proteins and was difficult to purify as a single component at wash steps containing high concentration of Imidazole (see Lanes marked 4,5,6 and 7 *in the fig. 28*). Moreover, only a faint band was observed for NusA-GBR1bNT (at around 105 kDa indicated by an arrow *in the fig. 28*). After trials of purification optimization with NusA-GBR1bNT expressed in C43(DE3) and BL21(DE3), it was observed that Ni-sepharose column was not effective for NusA-GBR1bNT purification.

III.2.6 Expression of GBR1bNT cloned in pETM30 vector (containing GST as fusion partner) and expressed in different strains– to select appropriate expression host

The Ni-sepharose column was not efficient in the purification of GBR1bNT containing 8-His tag. Hence the pETM30+GBR1bNT plasmid tagged with GST fusion protein N-terminally was selected and GST-GBR1bNT protein was purified using a GST column.

The pETM30+GBR1bNT plasmid was checked for over-expression of GST-GBR1bNT protein in the total cells upon induction with 0.1mM IPTG in BL21(DE3), C43(DE3) and Rosetta(DE3)pLysS strains. $10\mu L$ of the total cell samples were electrophoresed on a 10% SDS-PAGE gel.

In the Coomassie blue stained SDS-PAGE of the total cell samples, a 77 kDa band corresponding to GST-GBR1bNT protein (as indicated by arrow *in the fig*. 29) was found for the 0.1mM IPTG induced BL21(DE3) and Rosetta (DE3)pLysS strains, whereas no bands for GST-GBR1bNT bands were seen upon 0.1mM IPTG induction in C43(DE3) strain. This data suggests that BL21(DE3) is suitable for overexpression.
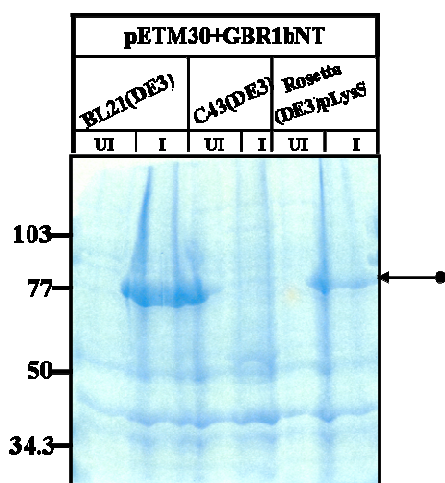

Fig. 29. Expression of GBR1bNT cloned in pETM30 vector (containing GST as fusion protein) and transformed into different strains of *E. coli*.
UI- Uninduced
I-Induced

A 76kDa band was observed under the induced condition of BL21(DE3) and Rosetta(DE3)pLysS.

III.2.7 Purification of GST-GBR1bNT (pETM30-GBR1bNT vector) in BL21(DE3) strain of *E.coli*

From the expression test carried out on pETM30+GBR1bNT plasmid transformed in BL21(DE3) and Rosetta(DE3) pLysS strains, the plasmid in BL21(DE3) was chosen for expression in 1L culture and purification.

About 1L culture of BL21(DE3) containing pETM30+GBR1bNT plasmid was grown to a OD_{600} of 0.8-1.0 and induced with 0.05mM IPTG at 18 °C for 12-16 hrs. The culture was harvested post-induction by centrifugation. The cell pellet was lysed using a Microfluidiser®. The supernatant obtained by ultracentrifugation of the cell lysate was loaded into the GST-sepharose column, pre-equilibrated with lysis buffer. The column was washed thrice with GST wash buffer.

The GST-GBR1bNT protein bound to the resin was resuspended in 2mL of TEV buffer. The cleavage reaction was carried out by incubating the GST-GBR1bNT protein bound resin with 20 µg of TEV protease for 12-16 hrs at 4 °C. Samples at

different stages of purification and TEV cleavage were resolved on a SDS-PAGE and stained with Coomassie Blue dye.

From the Coomassie blue stained gel, it was observed that major proportion of GST-GBR1bNT protein expression remained insoluble in the cell pellet. But, the soluble portion obtained in from the supernatant of the cell lysate was well-purified using a GST-sepharose column. On a Coomassie blue stained gel, a 77 kDa band was observed as indicated by an arrow in the *fig.30, left*. The GST-GBR1bNT protein contained a TEV protease cleavage site. So, the band observed in the SDS-PAGE was verified for GST-GBR1bNT by digestion with TEV protease. The samples were resolved on a SDS-PAGE. From the digestion pattern showed 3 bands *(fig 30, right)* with band 1 corresponding to TEV undigested GST-GBR1bNT (around 77 kDa); band 2 corresponding to cleaved GBR1bNT (around 50 kDa) and band 3 corresponding to the TEV protease (around 29 kDa), cleaved GST and the contaminant observed during elution (*see fig* 30, *right*). Together, this data suggests that GST-GBR1bNT can be effieciently purified using GST column.
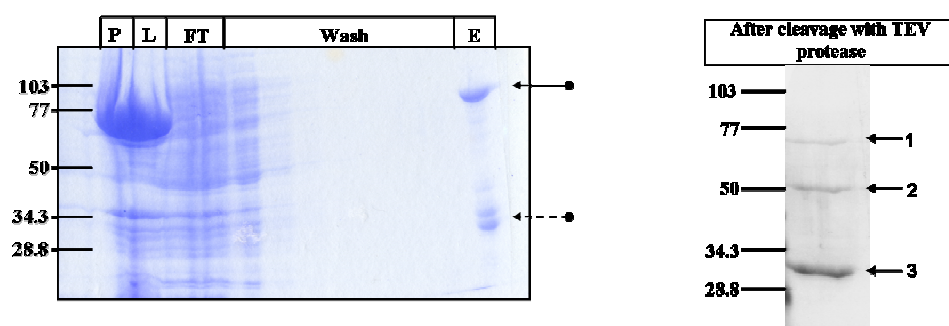
Fig. 30. Expression and purification of GST-GBR1bNT (pETM30-GBR1bNT vector) in BL21(DE3) strain of *E.coli*
P – Pellet;L – Load; FT – Flow through; W – Wash
Left, A fat band corresponding to the overexpression of GBR1bNT was observed in the pellet(P) and load (L). A good amount of GST-GBR1bNT was observed at the expected 79 kDa (indicated by an arrow) and another band bound unspecfically to the columncat 30 kDa.
Right, The TEV cleavage pattern show *Band 1-* at 76 kDa indicates the uncleaved GST-GBR1bNT. *Band 2* – at 50 kDa indicates the cleaved GBR1bNT. *Band 3* – at 30 kDa indicates the TEV protease, GST (cleaved) and the contaminant found in the elution, See fig. 30, left.

III.2.8 Expression and purification of GST-GBR1bNT (pET15b-GST-GBR1bNT vector) in Tuner strain of *E.coli* – to improve the soluble expression

From the previous trial it was observed that the GST-sepharose column was effective for GST-GBR1bNT protein purification but the limiting factor was obtaining sufficient expression of GST-GBR1bNT protein in the soluble fraction. Though the induction was carried out at minimal parameters such as 0.05mM IPTG for 12-16 hrs at 18°C still most of the over-expression was observed in the pellet due to unregulated IPTG induction. A regulated low level expression might enhance the solubility of the expressed proteins. So, the expression of GST-GBR1bNT protein in Tuner strain that contains such a characteristic was studied.

Tuner strains contain a lac permease (lacY) mutation that allows uniform entry of IPTG into the cells and produces a concentration-dependent, homogeneous level of induction. The expression levels can be regulated to a wide range by adjusting the concentration of IPTG. The Tuner cells contained kanamycin marker to enable its selection, so the GST-GBR1bNT construct was recloned into pET15b vector containing an ampicillin selection marker.

The expression was carried out in a 1L culture and incubated at 37 °C to an OD_{600} of 0.8-1.0. The culture was induced with 0.1mM IPTG for 12-16 hrs at 15 °C. The induced cell culture was lysed in the lysis buffer using a Microfluidiser®. The rest of the GST-sepharose purification protocols were carried out as described before. Samples were prepared for SDS-PAGE electrophoresis and stained with Coomassie Blue dye. A single band was observed at around 77 kDa corresponding to GST-GBR1bNT protein (as indicated by arrow in the *fig 31*). The elution fractions were pooled, concentrated and dialysed. There was good improvement in the amounts of GST-GBR1bNT protein expressed as a soluble protein. The soluble GST-GBR1bNT protein was purified effectively using the GST-sepharose column. The amount of GST-GBR1bNT purified was estimated by BCA assay and was found to be about 1mg/L of culture volume.
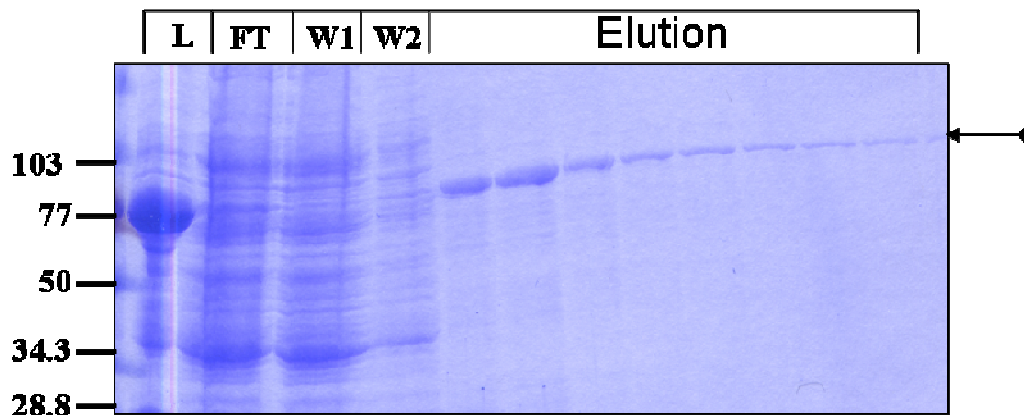
Fig. 31. Expression and purification of GST-GBR1bNT (pET15b-GST-GBR1bNT vector) in Tuner strain of *E.coli*
A band was observed at 77kDa (as indicated by arrow) that corresponds to the molecular weight of GST-GBR1bNT. The Load (L) still considerable amount of soluble GBR1bNT. The Elution fraction shows bands for well-purified GBR1bNT.

From this experiment, it was concluded that a good amount of purified GBR1bNT can be obtained upon expressing the GBR1bNT in pET15b-GST vector and transforming the plasmids in Tuner cells. The expressed protein can be purified using a GST column.

After several trials of optimizations, with the vector, host strain and column used for purification good expression of GBR1bNT was obtained. The complete optimisation process has been described in the following scheme. The vectors or host strains that are used are in blue boxes, the strain that failed to give expression in yellow boxes. And the final strategy that gave a good result is given below.
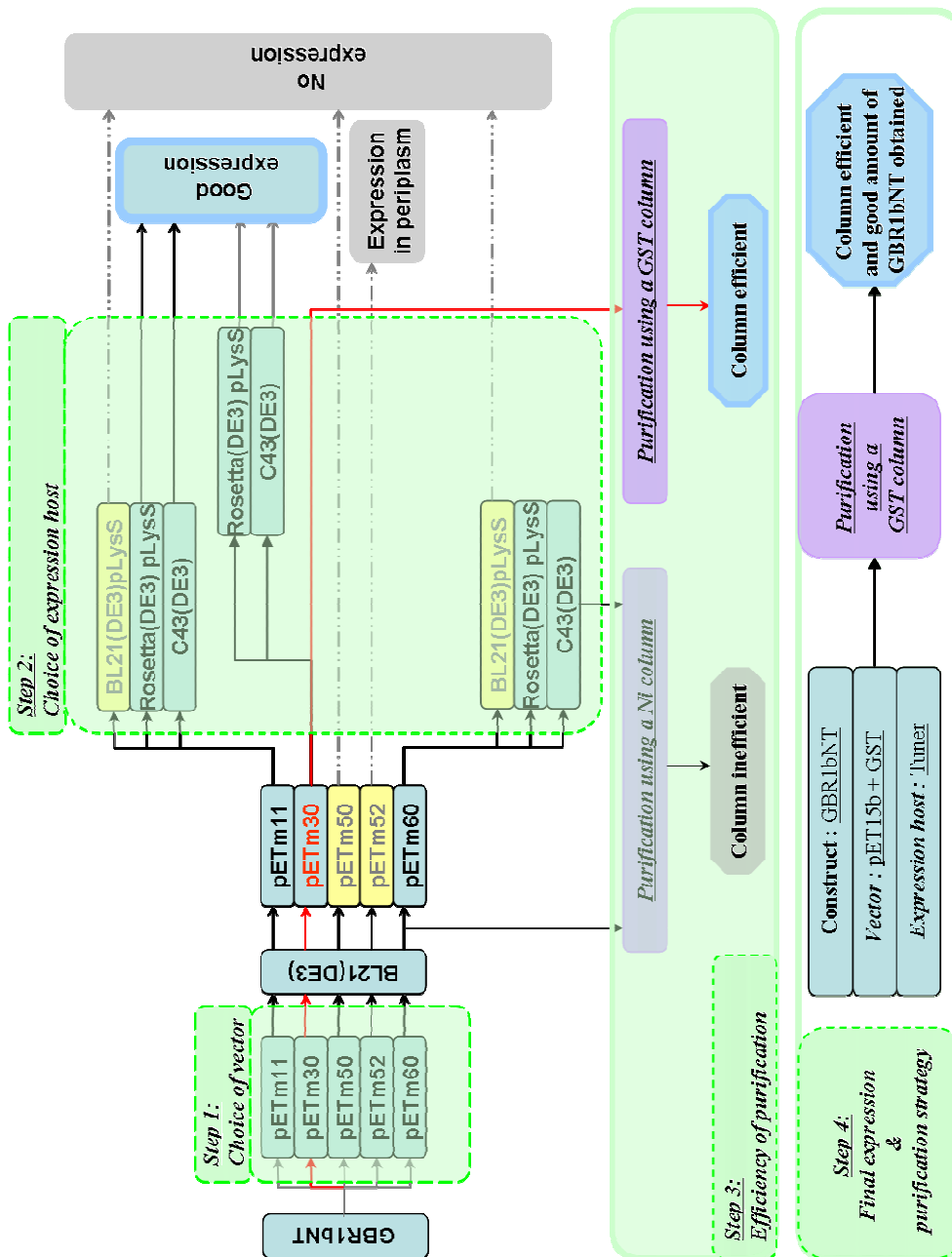
Scheme 2. A diagramatic representation of the expression and purification
optimisation of GBR1bNT in *E.coli*

III.3 Results for the biochemical characterization of the cholesterol binding motif and determination of the minimal construct required for maintaining the high affinity state for binding glutamate in Drosophila metabotropic glutamate receptor (DmGluRA)

Previously it was reported by (Eroglu et al., 2003) that the high-affinity glutamate binding to DmGluRA was regulated by its association with lipid rafts. The DmGluRA expressed in the membranes of *Sf9* cells had much higher affinity when compared to the DmGluRA expressed in the photoreceptor cells (PRC) of the fly eye (Eroglu et al., 2002). Mass spectrometric analysis on the lipid composition of DmGluRA virus infected *Sf9* membranes and DmGluRA expressed PRC shows that there is a significant difference in the sterol content. The *Sf9* membranes were enriched in cholesterol, forming lipid microdomains (or rafts), which are insoluble and extractable by treatment with Triton X-100 detergent, whereas the PRC contained ergosterol, which is unfavourable for raft formation. The high affinity state of the DmGluRA expressed in the PRC of fly eye was recovered by reconstituting the solubilised receptor in liposomes of raft composition.

(Li and Papadopoulos, 1998) reported a low consensus putative cholesterol binding motif (**L/V-[X]$_{1-5}$-Y-[X]$_{1-5}$-R/K**) in the transmembrane region of the peripheral benzodiazepine receptor. By site-directed mutagenesis and truncated constructs of the receptor showed that this motif was essential for regulation of binding of benzodiazepine to the receptor. Such motifs were observed in other proteins such as the mammalian cytochrome P450s, apolipoprotein A-I (mouse), caveolin (mouse), human hedgehog, Annexin II (rat), cholesterol oxidase (streptpcoccus), cholesterol 7α-monooxygenase (Mouse), cholesterol dehydrogenase (Nocardia), bile salt activated lipase (Human) and acyl-CoA cholesterol acyltransferase (Rabbit) but not much functional data is available to understand the role of the putative cholesterol binding motif (pCBM) in these proteins.

The role of the pCBM was further supported by the work carried out to study cholesterol binding at the cholesterol recognition amino acid consensus (CRAC) of the peripheral-type benzodiazepine receptor and inhibition of steroidogenesis by an

HIV TAT-CRAC peptide (Li et al., 2001). In another biophysical and   on-ionic studies, on the interaction of pneumolysin (a toxin and major virulence factor of the bacterium *Streptococcus pneumoniae* containing 4 of these motifs) with cholesterol showed that pneumolysin lyses cells whose walls contain cholesterol (Nollmann et al., 2004).

It is understood that the high affinity status of DmGluRA to glutamate is strictly regulated by membrane cholesterol and that the putative cholesterol-binding motif observed in different transmembrane helices could play a pivotal role in the selectivity of cholesterol.

The current study would be focused on the biochemical characterize the putative cholesterol binding motif observed in the DmGluRA and to obtain the minimal construct that is sufficient to maintain the receptor in high affinity state.

III.3.1 Molecular constructs

4 hits for putative cholesterol-binding motif (L/V-[X]$_{1-5}$-Y-[X]$_{1-5}$-R/K) were observed upon scanning through the primary sequence of DmGluRA. The following considerations were made in designing the constructs:

- The topology of the receptor on the membrane,
- Orientation of cholesterol in the bilayer and
- The accessibility of the residues in the motif to cholesterol.

Three of the pCBM motifs were present in the transmembrane ™ helices (TM3, TM5 and TM7) of the receptor and one was present in the linker region between ECD and TM1 (as *shown in the fig 32*).

Table 3 :	Details of the DmGluRA truncation constructs				
Construct Name	Truncation point	Construct size* (bp)	C-term Tag	No. of TMs[#]	No. of pCBM
DmGluRA[$]	Full length	2974	6-His	7	4
DGRTM5	Lys 817	2451	*flag*	5	3
DGRTM3	Gln 738	2214	*flag*	3	2
DGRTM1	Glu 663	1989	*flag*	1	1

* includes tag and stop codon   pCBM – Putative cholesterol binding motif
TM – Transmembrane   [$] Construct already prepared by (Eroglu et al., 2003)
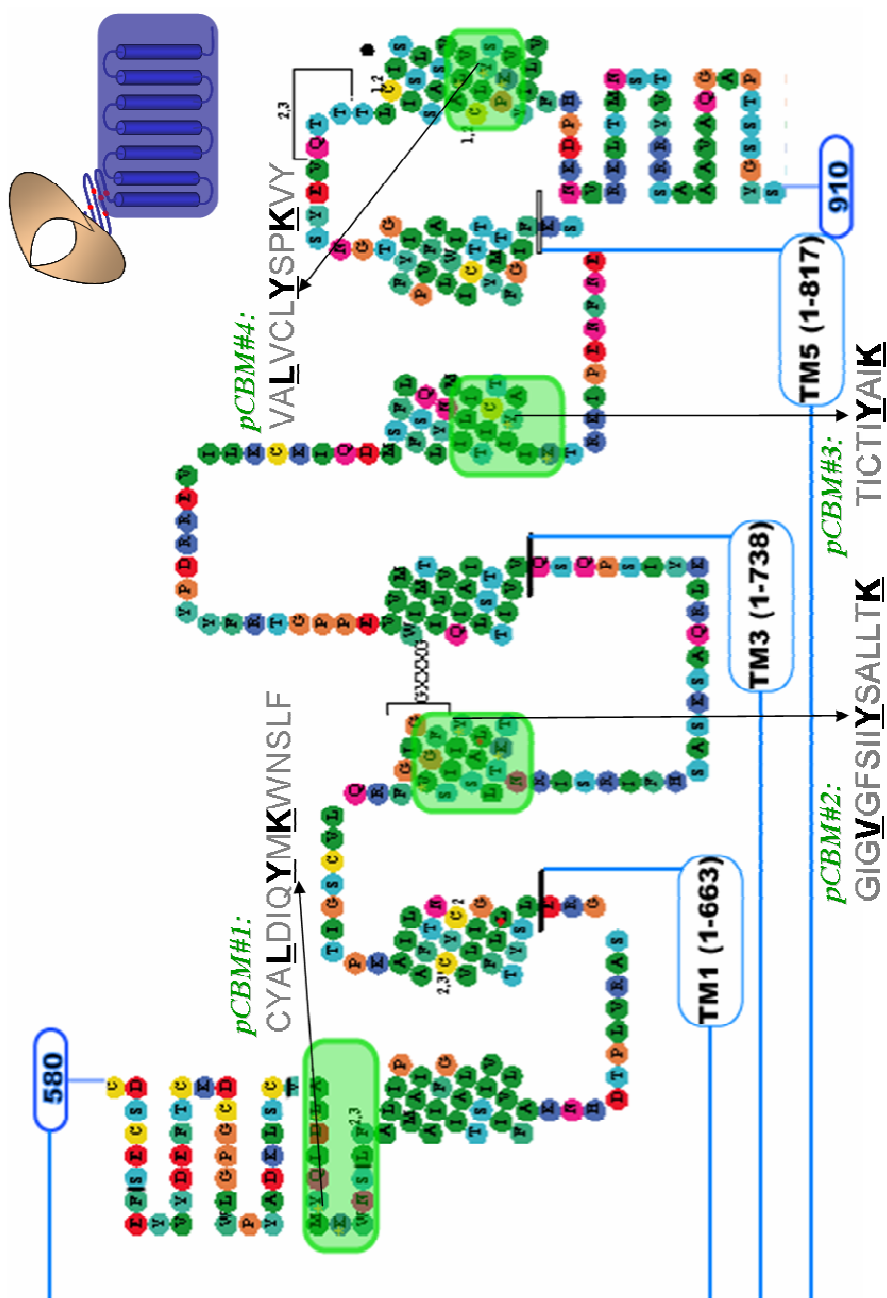[#] includes the extracellular domain (ECD)

Fig. 32 : The topology of the transmembrane region containing the 4 putative Cholesterol-binding motif in DmGluRA are highlighted in green boxes and denoted as *pCBM#* (topology diagram adapted from GPCR database, http://www.gpcr.org).

III.3.2 Virus production for the truncation constructs of DmGluRA in the Recombinant BaculoVirus (RBV) system

The viral stocks of DmGluRA construct were readily available as the construct was prepared for the previous study by Eroglu, PhD thesis 2002. The constructs (DGRTM1, DGRTM3 and DGRTM5) were cloned into pVL1393 transfer vector and co-transfected in to *Sf9* cells for recombinant virus production. A series of recombinant baculovirus production protocols such as clonal selection, primary recombinant viral stock, secondary viral stock and tertiary viral stock production were carried out as described in detail in the *Materials and methods section II.5*. The viral titre values of the tertiary stock determined by end point dilution method are as follows in *Table 5*:

Table 5	Titre values for constructs
Construct	Titre value (Pfu/ml)
DmGluRA$^{\$}$	3.4×10^8
DGRTM5	4.7×10^8
DGRTM3	1.9×10^8
DGRTM1	2.2×10^9
$^{\$}$ - (Eroglu et al., 2003)	

The protein expressions in the total Sf9 cells were analyzed by performing a Western blot using anti-DGR (1:2500) as primary antibody (anti-DGR is polyclonal antibodies raised against the extracellular domain of DmGluRA in rabbit). It was determined that the *Sf9* cells infected by the recombinant viruses at a MOI of 3 for 2-3 days at 27°C yielded a good expression level in all constructs. Therefore, these parameters were maintained throughout the study involving expression of truncation constructs of DmGluRA in Sf9 plasma membranes.

III.3.3 Preparation and purification of constructs expressed in plasma membranes of *Sf9* cells

The Sf900 medium was supplemented with 10% Fetal calf serum (FCS) in all expression setups for *Sf9* membrane preparation to enrich the cholesterol content in the plasma membrane. Plasma membranes of *Sf9* cells infected by the recombinant virus expressing different constructs were prepared as per the method described in the *Materials and methods, section II.7.2*. The post-nuclear supernatant was purified on a density gradient centrifugation to enrich the plasma membrane fraction. It should be noted that the membranes thus obtained by homogenization and gradient centrifugation still contain a small proportion of membrane from the ER.

About 5 µg of total membrane protein (estimated by BCA assay) was resolved on a 8% SDS-PAGE and electroblotted on a PVDF membrane. Western blot analysis was performed on the electroblotted PVDF membrane using anti-DGR (rabbit, 1:2500 dilutions) as primary antibody and HRP-linked whole antibody, anti-rabbit IgG as secondary antibody (1:1000). The results showed that all the constructs were well expressed in the plasma membrane fraction as shown in the figure 3.

In the samples prepared for membranes containing DGRTM5 and DmGluRA, most of it aggregated in the wells owing to the greater hydrophobicity and resistance to the reducing agents leading to very faint signal at their corresponding molecular weight. Several trials of different loading volumes, different concentrations of ß-mercaptoethanol in the loading buffer and denaturation temperature did not make a significant difference in the intensity of signal (data not shown).

Construct name	Theoretical Mol wt
DGRTM1	~ 74 kDa
DGRTM3	~ 82 kDa
DGRTM5	~ 92 kDa
DmGluRA	~ 109 kDa
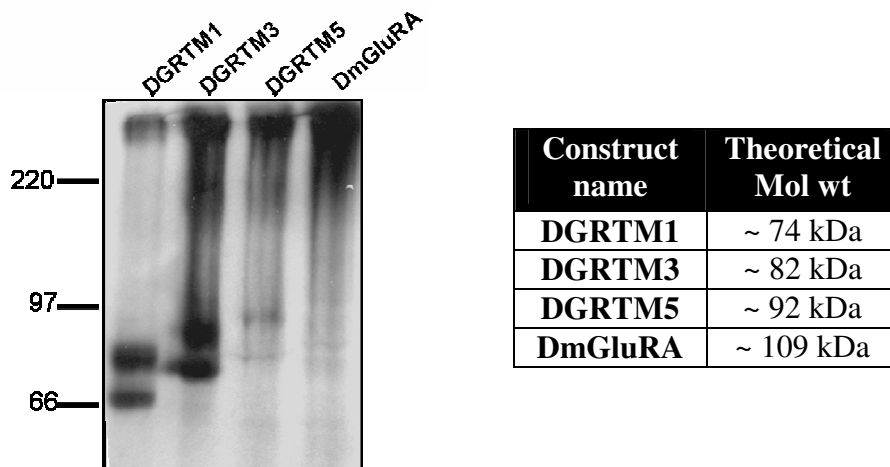
Fig. 33: Western blot on membranes of DGRTM1, DGRTM3, DGRTM5 and DmGluRA constructs expressed in RBV system (*Sf9* cells).
5 μg of total membrane protein (estimated by BCA assay) was loaded in a SDS-PAGE (8% gel) for each construct and electroblotted on a PVDF membrane using anti-DGR (rabbit, 1:2500 dilutions) as primary antibody and HRP-linked whole antibody, anti-rabbit IgG as secondary antibody (1:1000).

In the Western blots, two bands running at different molecular weights were observed in all constructs which could be a contamination of the pre-matured protein in the ER membranes generally obtained during plasma membrane preparation from cells.

III.3.4 The affinity of truncation constructs DGRTM5, DGRTM3 and DGRTM1 for glutamate is similar to the full length DmGluRA

Glutamate binding studies were performed on DGRTM5, DGRTM3 and DGRTM1 using Radioligand Binding assay. All L-[^{3}H]-Glutamate binding trials were conducted on the plasma membrane preparations of DGRTM5, DGRTM3 and DGRTM1. Every trial had triplicate setups and three such trials were conducted on the membrane preparation of the constructs. Homologous competition binding was performed by incubating the membranes with [^{3}H]-glutamate along with increasing concentration of unlabeled glutamate. The percentage standard error of mean (SEM) was determined for the triplicate sample in each of the trials. The IC_{50} values were determined by applying nonlinear regression analysis of the GraphPad Prism software prescribed for kinetics model analysis. The reliability of the curve fit was tested by considering the values of statistical parameters such as 95% confidence interval and R^2 values.

The full length **DmGluRa** has a K_d value of **3.4 ± 1 µM**, this is a very low value to conduct a binding trial and to obtain a concurrent value for every setup. The mean IC_{50} value for glutamate binding studies on DmGluRA was found to be **4.9 ± 1.2 µM** (Panneels et al., 2003).

From the glutamate binding trials on **DGRTM5** expressed membranes (containing 3 pCBMs and 5 TM helices) the mean IC_{50} values was determined to be **2.8 ± 1.2 µM** (*fig. 34*). In **DGRTM3** expressed membranes (containing 2 pCBMs and 3 TM helices) the mean IC_{50} values was determined to be **3.1 ± 1.5 µM** (*fig. 35*) and in **DGRTM1** expressed membranes (containing only one pCBM and 1 TM helix) the mean IC_{50} values was determined to be **2.4 ± 0.35 µM** (*fig. 36*).

[^{3}H]-Glutamate binding studies on DGRTM5 expressed membranes

Fig. 34. Homologous competitive binding of L-Glutamate on DGRTM5 expressed in *Sf9* **membranes**. Competitive binding assay on DGRTM5 membranes showed similar affinity as observed in the wild-type DmGluRA membranes (IC$_{50}$=4.9±.2 μM) (Panneels et al., 2003). Total binding in DGRTM5 expressed *Sf9* membrane is 8160±1237 DPM and unspecific binding is 1660±148.2 DPM. The curves represent the mean of independent experiments (n = 3) with 3 triplicates in each experiment.

Best-fit values	Trial 1	Trial 2	Trial 3
BOTTOM	0	0	0
TOP	100	100	100
IC$_{50}$	4.29×10^{-6}	1.9×10^{-6}	2.59×10^{-6}
Log IC$_{50}$	-5.36	-5.72	-5.58
95% Confidence Intervals			
IC$_{50}$	1.9×10^{-6} to 9.29×10^{-6}	9.29×10^{-7} to 3.69×10^{-6}	1.29×10^{-6} to 5.49×10^{-6}
Log IC$_{50}$	-5.72 to -5.04	-6.04 to -5.44	-5.92 to -5.27
Goodness of Fit			
R²	0.8458	0.9068	0.9078
Mean IC$_{50}$ values of 3 trials with SEM			2.8 ± 1.2 μM

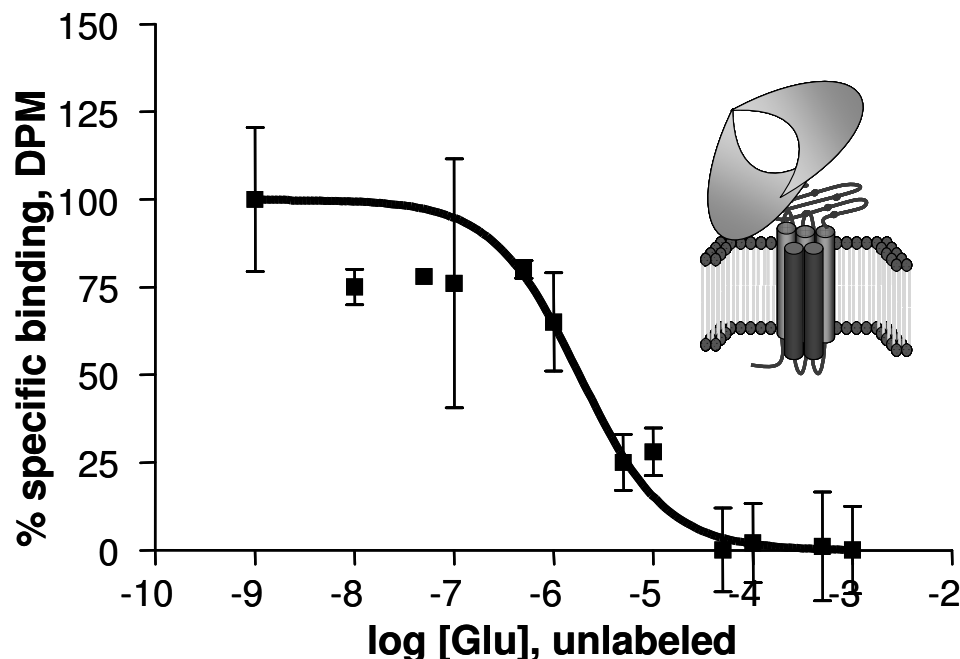# [³H]-Glutamate binding studies on DGRTM3 expressed membranes

Fig.35. Homologous competitive binding of L-Glutamate on DGRTM3 expressed in *Sf9* membranes. Competitive binding assay on DGRTM3 membranes showed similar affinity as observed in the DGRTM5 and wild-type DmGluRA membranes. Total binding in DGRTM3 expressed *Sf9* membrane is 17128±2529 DPM and unspecific binding is 1662±672 DPM. Curves represent the mean of independent experiments (n = 3) with 3 triplicates in each experiment.

Best-fit values	Trial 1	Trial 2	Trial 3
BOTTOM	0	0	0
TOP	100	100	100
IC_{50}	3.5×10^{-6}	4.3×10^{-6}	1.3×10^{-6}
Log IC_{50}	-5.46	-5.37	-5.89
95% Confidence Intervals			
IC_{50}	2.6×10^{-6} to 4.6×10^{-6}	2.6×10^{-6} to 7.04×10^{-6}	6.1×10^{-7} to 3.0×10^{-6}
Log IC_{50}	-5.57 to -5.33	-5.57 to -5.15	-6.21 to -5.52
Goodness of Fit			
R²	0.9865	0.9545	0.8458
Mean IC_{50} values of 3 trials with SEM			$3.1 \pm 1.5 \ \mu M$

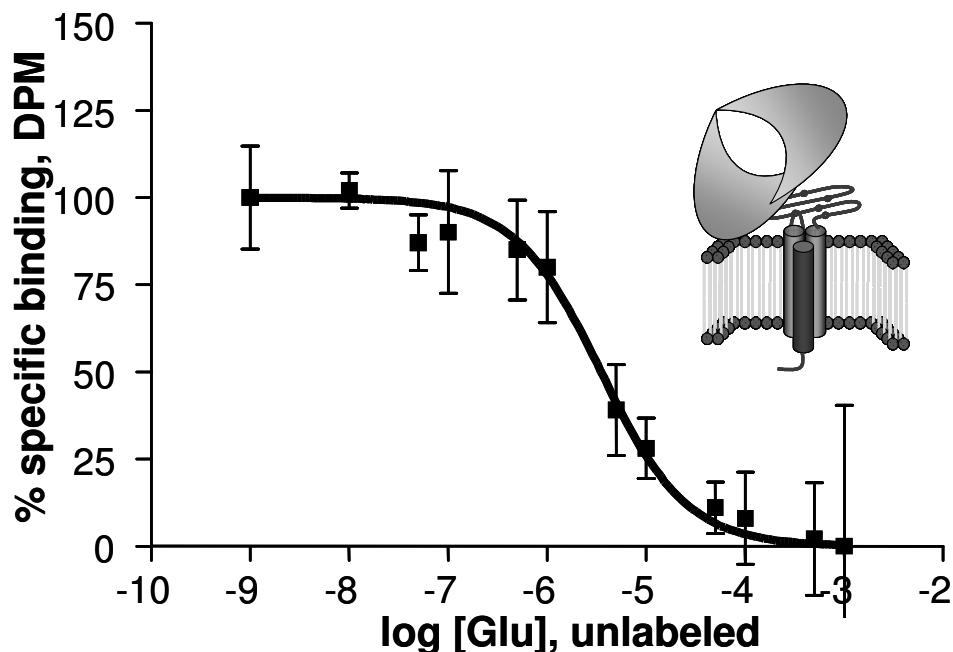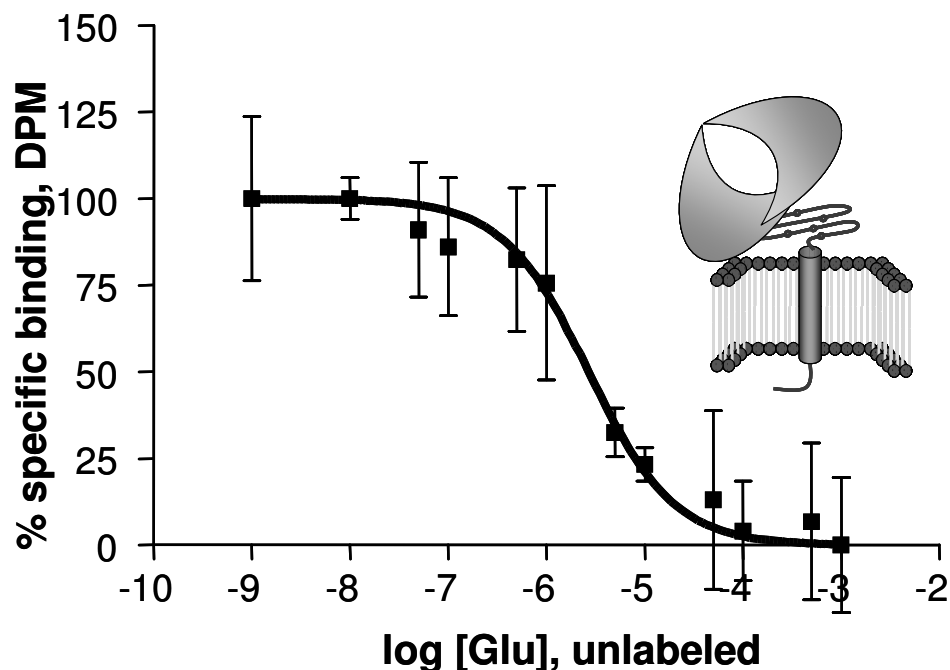# [³H]-Glutamate binding studies on DGRTM1 expressed membranes

Fig. 36. Homologous competitive binding of L-Glutamate on DGRTM1 expressed in *Sf9* membranes. Competitive binding assay on DGRTM1 membranes showed similar affinity as observed in the DGRTM3, DGRTM5 and wild-type DmGluRA membranes. Total binding in DGRTM1 expressed *Sf9* membrane is 14019±420.8 DPM and unspecific binding is 2166±331.7 DPM. Curves represent the mean of independent experiments (n = 3) with 3 triplicates in each experiment.

Best-fit values	Trial 1	Trial 2	Trial 3
BOTTOM	0	0	0
TOP	100	100	100
IC_{50}	2.01×10^{-6}	2.70×10^{-6}	2.46×10^{-6}
Log IC_{50}	-5.70	-5.57	-5.61
95% Confidence Intervals			
IC_{50}	9.1×10^{-7} to 4.47×10^{-6}	2.01×10^{-6} to 3.64×10^{-6}	1.39×10^{-6} to 4.35×10^{-6}
Log IC_{50}	-6.04 to -5.35	-5.70 to -5.44	-5.86 to -5.36
Goodness of Fit			
R^2	0.8670	0.9847	0.9463
Mean IC_{50} values of 3 trials with SEM			2.4 ± 0.35 μM

III.3.4.1 Construct Vs Comparison of IC$_{50}$ values

From [^{3}H]-Glutamate binding studies on all of the constructs expressed in *Sf9* membranes, it was observed from the mean IC$_{50}$ values that DGRTM1 (2.4 ± 0.35 μM), DGRTM3 (3.1 ± 1.5 μM) and DGRTM5 (2.8 ± 1.2 μM) maintained similar affinity for glutamate as that of DmGluRA (4.9 ± 1.2) (*fig. 37*) (Panneels et al., 2003).
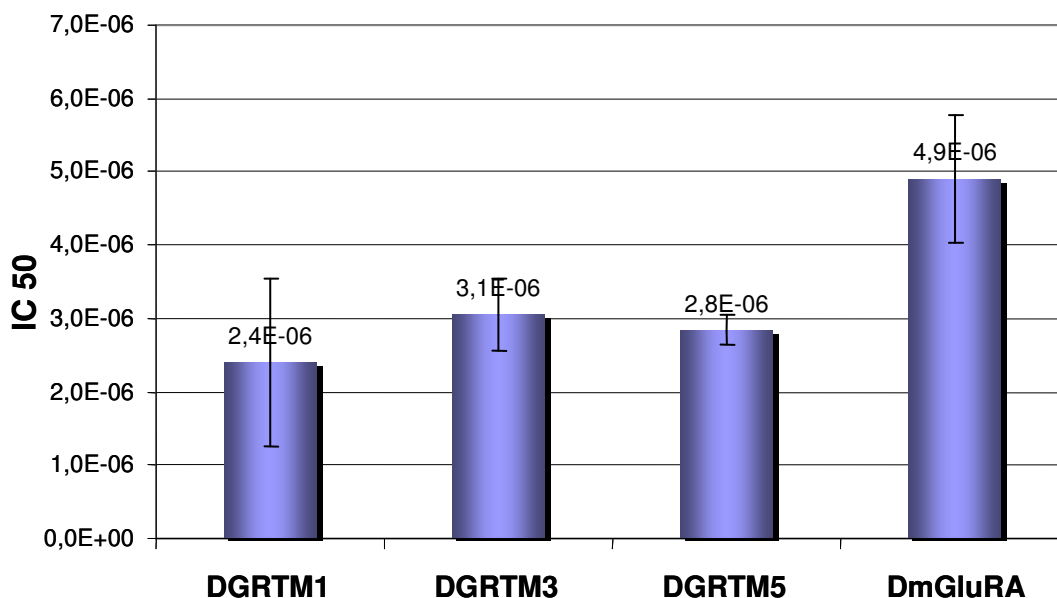

Fig. 37. Histogram of DmGluRA construct on X-axis and IC$_{50}$ values on the Y-axis. The histogram exhibits similar binding affinity of the receptor for glutamate in DGRTM1 (2.4 ± 0.35 μM), DGRTM3 (3.1 ± 1.5 μM) and DGRTM5 (2.8 ± 1.2 μM) constructs when compared to that of DmGluRa (4.9 ± 1.2 μM).

Among DGRTM5, DGRTM3 and DGRTM1 constructs, DGRTM1 construct was the minimal construct that contained one pCBM and one TM helix, and was still capable of maintaining the high affinity state to glutamate binding. Hence, the next attempts are to see which part of the plasma membrane DGRTM1 is localized to or associated with to maintain the high affinity state.

III.3.5 Analysis of association of DGRTM1 with detergent resistant membranes (DRMs) from *Sf9* cells – DGRTM1 was associated with DRMs

The plasma membrane contains subdomains that contain high concentrations of cholesterol and glycosphingolipids. These subdomains are tightly packed are often referred to as Lipid rafts. Several proteins involved in cell signalling, have been shown to be recruited and regulated in lipid rafts (Shenoy-Scaria et al., 1994). The lipid rafts are very often referred to as detergent resistant membranes (DRMs) as they exist in liquid-ordered phase in the membrane at low temperatures and are resistant to extraction with weak on-ionic detergents such as TritonX-100 (Simons and Ikonen, 1997).

In the studies on DmGluRA it was shown that the receptor was in low affinity state to glutamate binding when associated with non-rafts or non-DRMs favoured by membrane ergosterol found in the Drosophila fly eye whereas, it was found in the high affinity state when associated with rafts or DRMs favoured by cholesterol found in the *Sf9* membrane (Eroglu et al., 2003).

The DGRTM1 membrane extracted on ice using 1% Triton X-100 detergent was isolated from the detergent soluble components by a density gradient ultracentrifugation. The membranes that are resistant to 1% Triton X-100 treatment at 4 °C remained buoyant and floated to the 5-30% interface were regarded as light density DRMs; those resistant that floated to the 30-40% interface were regarded the heavy density membranes and the membrane proteins devoid of lipid members due to detergent solubilisation were pelleted.

Western blot analysis on the six samples collected from the top layers showed signals for DGRTM1 in the 1st fraction (5-30% interface, *Lane1* in the *fig. 38*) and in 3rd and 4th fractions (30-40% interface, *Lanes3 and 4* in *fig. 38*).
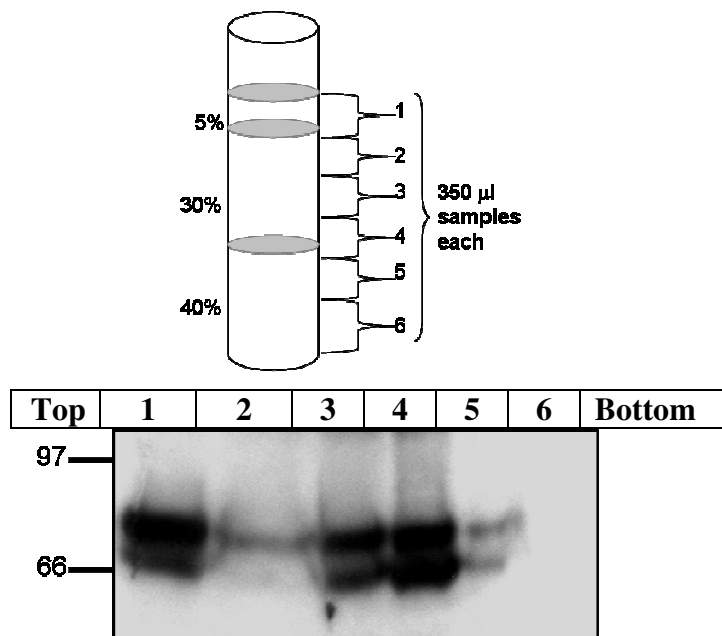
Fig. 38. Association of DGRTM1 in Triton X-100 extracted membranes (DRM)
10 µL of each sample was loaded in a SDS-PAGE (10% gel) and electroblotted on a
PVDF membrane using anti-DGR (rabbit, 1:2500 dilutions) as primary antibody and
HRP-linked whole antibody, anti-rabbit IgG as secondary antibody (1:1000).

From the [³H]-Glutamate binding studies and DRM association studies it was concluded
that DGRTM1 maintains its high affinity state to L-Glutamate due to its association with
DRMs. The next attempts are to find out whether the high affinity state for glutamate and
DRM association is due to the pCBM or TM helix in DGRTM1.

III.3.6 Studies on DGX and DG14c constructs in the RBV system

III.3.6.1 Description of DGX and DG14c constructs

Viral stocks of DGX and DG14c were previously produced (PhD thesis by Cagla Eroglu), for expression of the extracellular domain (ECD) in the RBV system, as an attempt to over-express the ECD for structural studies. DmGluRA was terminated at residue Ser 624 to obtain the DGX construct which lacked the transmembrane domain. The DGX construct thus obtained contained the complete ECD with one cholesterol binding consensus at the C-terminus. The DG14c construct was terminated at Ser 586 residue and lacked the cholesterol binding motif including the cysteine rich domain (CRD) in comparison with the DGX construct (as shown in the *fig. 39*). The

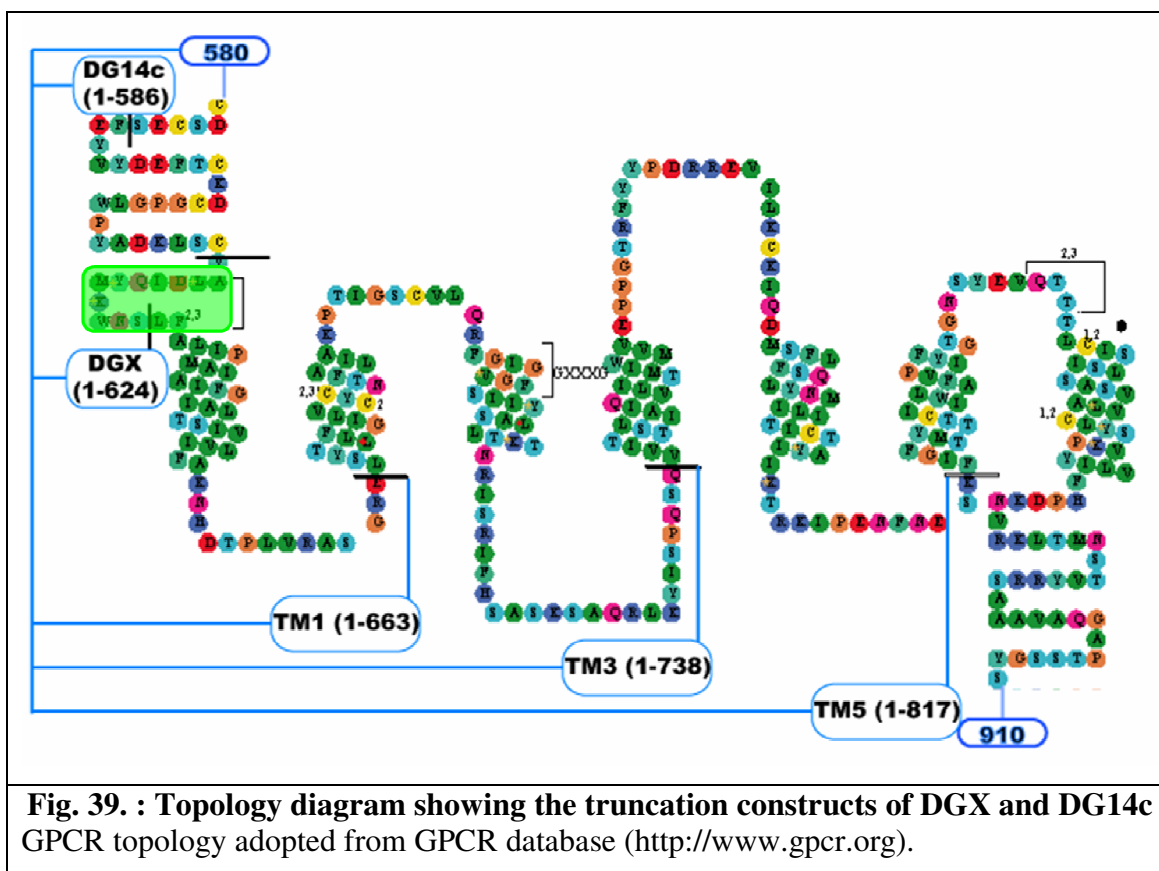| Construct Name	Truncation point	No. of pCBM
DG14c	Ser 586	-
DGX	Ser 624	1

Fig. 39. : Topology diagram showing the truncation constructs of DGX and DG14c
GPCR topology adopted from GPCR database (http://www.gpcr.org).

III.3.6.2 DGX and DG14c secretion to the insect cell medium – DGX was poorly secreted to the medium

In order to check the levels of secretion, *Sf9* cells were infected with the recombinant virus of DGX and DG14c constructs at a MOI of 3 for 3-4 days until the total cells were lysed. Western blot analyzed for protein expression and secretion in the medium showed that DGX was found secreted in lower amounts, when compared to the DG14c secretion to the Sf900-II medium.

Construct	Theoretical mol wt
DGX	~ 67 kDa
DG14c	~62 kDa
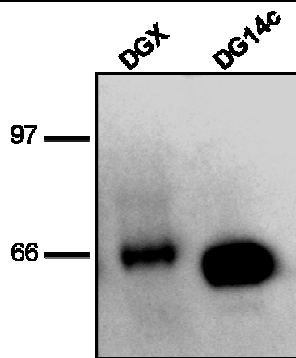
Fig. 40. Western blot of expression and secretion of DGX and DG14c to the medium.
DGX and DG14c secreted to the Sf900-II medium (10µL) were detected by incubating the electroblotted PVDF membrane with anti-DGR primary antibody.

Both DGX and DG14c constructs contained the complete or part of DmGluRa ECD and still there was a comparable difference in the amounts secreted to the medium. The possible reasons for such low expression of DGX to the medium could be that either the total expression of DGX in the *Sf9* cells itself were poor or it is localized/retained in the cellular compartments (such as the plasma membranes, endoplasmic reticulum or other cellular compartments).

III.3.6.3 Comparison of DGX and DG14c expression on *Sf9* membranes – DGX was well-expressed in the plasma membranes

DGX and DG14c were expressed in *Sf9* cells at a MOI of 3 for 2-3 days until 70% of the cells were observed infected. Plasma membranes containing DG14c and DGX were prepared and Western blot on the samples showed double bands running at different molecular weights as before *shown in fig 41*. Upon comparison with the western blot for DGX and DG14c secreted to the medium, only single bands were observed *(see fig. 40)*, where only the completely processed proteins are secreted to the medium. This observation further strengthens the assumption that the plasma membrane preparation might be contaminated with proteins from the ER membranes (containing some proportions of immature/unprocessed protein).

Further, it was surprising to note that DGX construct without any TM was observed associated in the plasma membrane fraction in high quantities relative to that of DG14c membrane fraction. This also clearly explains the lower expression levels of DGX in medium. The next attempt was to verify whether the DGX and DG14c observed in the membrane fractions were capable of binding L-Glutamate.
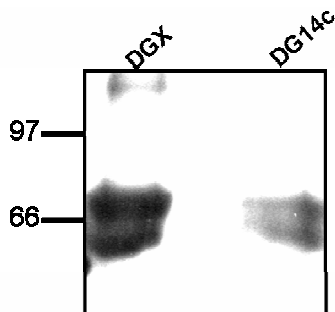

Fig. 41. Membrane expression of DGX and DG14c. 5 μg of total membrane protein estimated by BCA assay was loaded in a SDS-PAGE (8% gel) for each construct and electroblotted on a PVDF membrane using anti-DGR (rabbit, 1:2500 dilutions) as primary antibody and HRP-linked whole antibody, anti-rabbit IgG as secondary antibody (1:1000). Western blot shows high expression of DGX.

III.3.6.4 [³H]-Glutamate binding trials on DGX and DG14c expressed *Sf9* membranes

[³H]-Glutamate binding was carried out on DGX and DG14c expressed and prepared *Sf9* membranes. The values were plotted with increasing concentration of unlabeled glutamate against the total counts measured from the bound [³H]-Glutamate. Statistical parameters were analyzed for the model curve. The model curve was a good fit and furher it was inferred that the DGX membranes had the similar affinity (2.3±0.85 μM) as that of the DmGluRA and its other truncated constructs as shown before (fig 42). In the case of DG14c expressing membranes no binding was observed which justifies that the signals observed particularly in the western blots for plasma membrane preparations were due to contamination from the ER where proteins are immature, unfolded and inactive.

[³H]-Glutamate binding studies on DGX and DG14c constructs
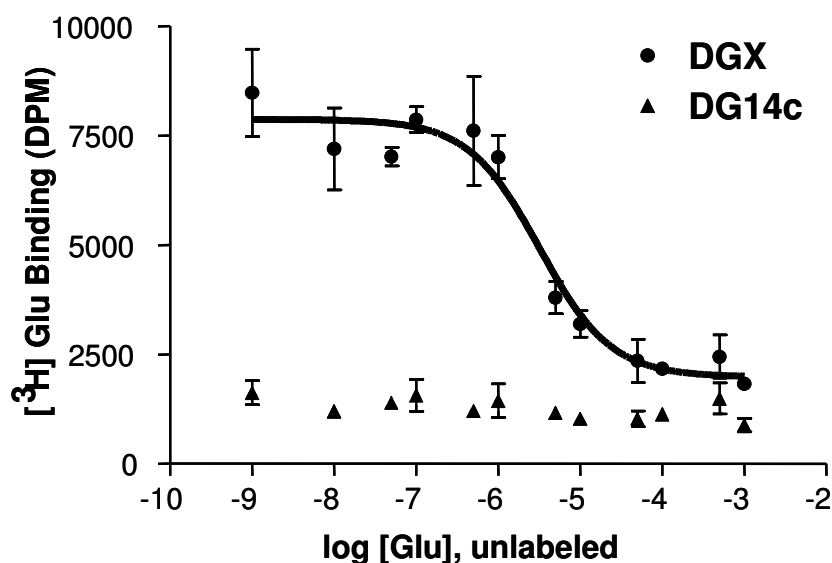
Fig. 42. Homologous competitive binding curve on DGX and DG14c expressed-*Sf9* membranes.
Competitive binding assay on 20-30 μg of BCA assay estimated DGX and DG14c DGX membranes showed similar affinity (IC$_{50}$=2.3±0.85 μM) to that of DmGluRA and binding trials of DGRTM1, DGRTM3 and DGRTM5 membranes. Total binding in DGX expressed *Sf9* membrane is 12960.3±1237 DPM and unspecific binding is 1286±127.4. DPM. No binding observed in case of membranes prepared from *Sf9* cells infected with DG14c virus was found to be 1623.279±279 DPM and unspecific binding is 881.7±154.2. DPM. Curves represent the mean of independent experiments (n = 3 for DGX and n=1 for DG14c).

From the binding studies and western blot of membrane preparations, it was evident that the DGX construct with pCBM was associated with the plasma membrane and still capable of binding L-glutamate.

Experiments were designed simultaneously to see the role of pCBM. The set of experiments designed were to purify the DGX secreted to the supernatant and conducting a floatation assay on the purified protein to see if it has any affinity for liposomes and to conduct CD spectral studies on peptides containing pCBM incubated with liposomes to observe any conformational change.

III.3.6.5 Purification of DGX secreted in the culture medium

1L of 2 x 10^6 *SF+* cells/mL was infected with recombinant DGX virus at a MOI of 3. Three-four days post-infection the culture was cleared from cells by centrifugation and filtered through 0.22 µm filter. The clarified supernatant was buffered to pH 6.0 using 1M Potassium phosphate buffer pH 6.0 and loaded into the CHT column equilibrated with *Buffer Q*. The protein bound column was washed with *Buffer W* until baseline and eluted with 400mL of *Buffer E* (pH 8.0). The concentrated and buffer replaced elute was loaded on to the Ni-sepharose column at a flow rate of 1mL/min and monitored under UV 280 nm.

A chromatogram was prepared plotting the protein concentration under UV 280 nm (Blue line) against the *% Imidazole concentration in Buffer B* (500mM) (purple line). The elution profile showed a single peak at 15% Imidazole concentration in *Buffer B* (75mM Imidazole). Western blot analysis on the DGX fractions collected at the peak showed a band around 50 kDa corresponding to purified DGX (indicated by a red arrow in the *fig 43b*) following CHT and Ni column. There were bands observed at around 100 kDa and 35 kDa (indicated by black arrows in the *fig. 43b*), detected by the anti-DGR antibody used as primary antibody in the western blot analysis. The bands running at 100 kDa were assumed to be oligomers of DGX resistant to reduction of disulpide bridges by β-mercaptoethanol and the 35 kDa band was to be degradation products of DGX, as there was a proportional change of these signals with respect to DGX signals detected by the

anti-DGR antibody. The elution fractions were pooled, concentrated and dialysed in the dialysis buffer. The DGX thus purified was obtained in amounts sufficient for liposome floatation studies.
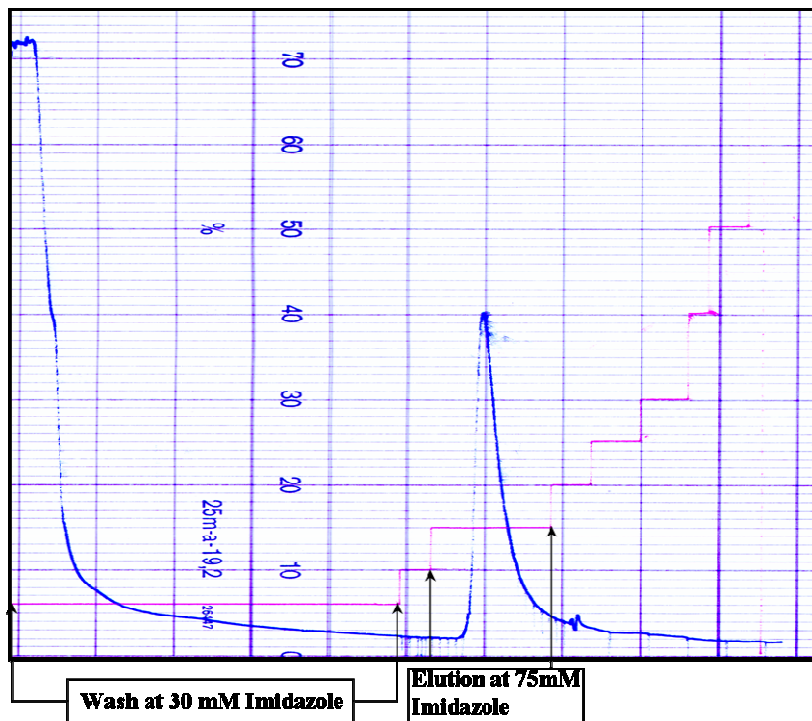
Fig. 43a : Chromatogram showing the elution profile of DGX from the Ni column Elution profile of DGX monitored at UV 280 (blue line) and % Imidazole concentration (purple line) are shown.
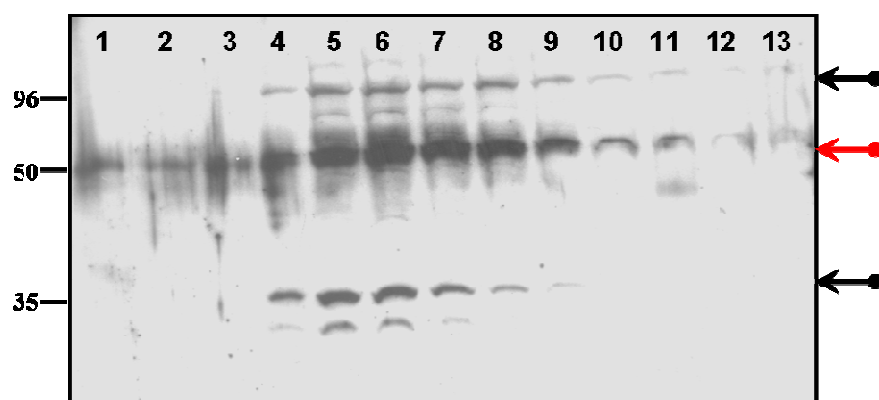

Fig. 43b : Western blot of DGX fractions eluted at 75mM Imidazole
Western blot on the elution fractions from the Ni column. 10 µl of each fraction was electroblotted in PVDF membrane and incubated with anti-DGR antibody. DGX band as pointed by the arrow.

III.3.6.6 Dynamic Light Scattering (DLS) studies for validation of liposomes

The liposomes of raft composition (DOPC:DPPC:Cholesterol, 30:30:40 mol%) and Non-Raft composition (DOPC:Cholesterol, 60:40 mol%) were analyzed on a DLS for its particle size distribution under different parameters such as the intensity, volume and number. The liposomes prepared were of good quality under the parameters discussed ealier. The size distribution (by percent number) was determined by plotting the logarithm of liposome diameter on the X-axis versus the percent number of liposome for the given liposome diameter on the Y-axis. The system was monodisperse in both preparations with a polydispersity index of less than 0.7. Single peaks were obtained in both compositions, about 30% of liposome mixture contained liposomes of about 100 nm diameter and 32% of 125nm diameter in raft and non-raft compositions respectively. The liposome diameter ranged between 75-250 nm for raft composition. For the non-raft liposomes the range was from 100-350nm. 4-6 measurements of 10 min were carried out for each of the liposome compositions and particle size distribution were found to be reproducible in all measurements.
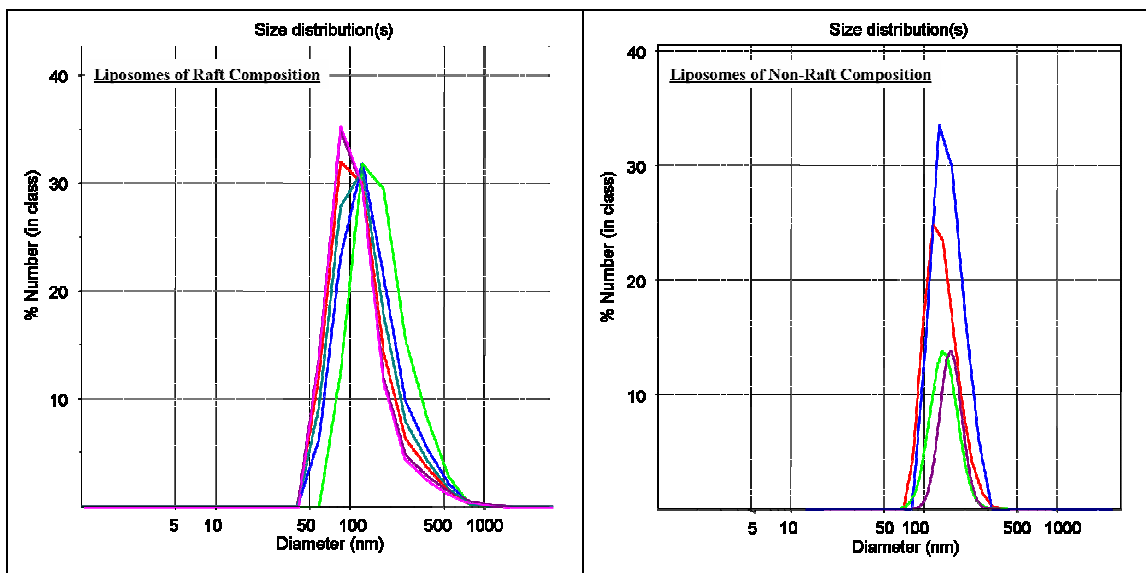

Fig. 44. Determination of size distribution of raft and non-raft liposome preparation using DLS.

The raft and non-raft liposomes thus prepared and analyzed were used for liposome floatation studies or CD spectra studies.

III.3.6.7 Liposomes floatation studies on the purified DGX

Raft and non-raft liposomes were prepared using extruder (of 100nm pore size polycarbonate membranes) were of good quality when analyzed in DLS. The secreted and purified DGX was incubated with liposomes of non-raft and raft compositions. The setup containing the DGX alone without any liposome severed as "control". The proteoliposome mixture were centrifuged and floated in a density gradient. The samples were collected as four fractions (600, 400, 400 and 600 μL) from the top to bottom and labeled from 1-4 respectively.
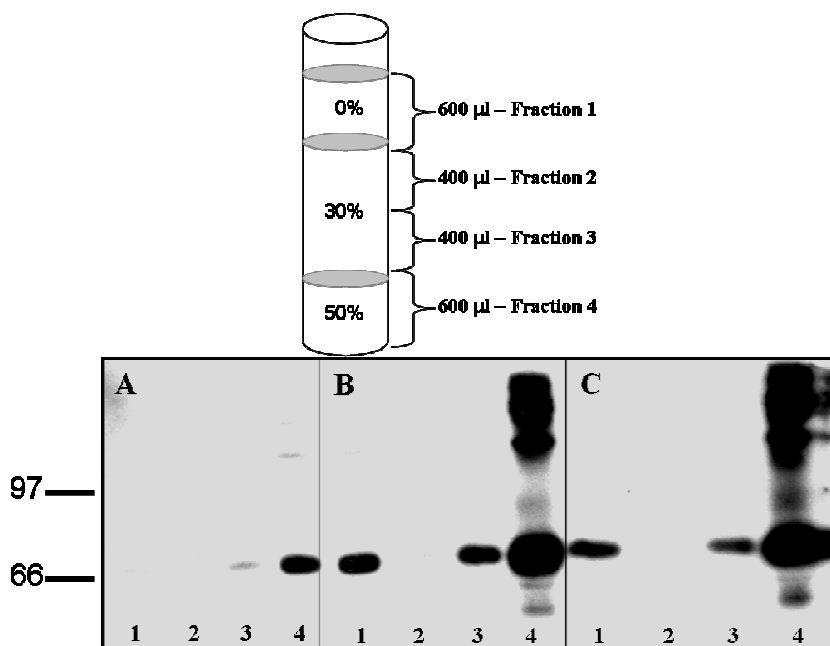
Fig. 45. Western blot on samples of liposome floatation assay with secreted DGX
The electroblotted PVDF membrane was incubated with anti-DGR (1:2500) and analysed. Bands were observed in the 1st lane of in (B) and (C) corresponding to the molecular weight of DGX which represents the DGX that floated to the first fraction. Bands in lane 3 and 4 in all (A), (B) and (C) represent the DGX that stayed at the bottom of the ultracentrifugation tube.
(**A**) Secreted DGX alone with assay buffer   (**B**) Secreted DGX with Non-raft liposomes
(**C**) Secreted DGX with Raft liposomes

In the western blot, signals in the first fraction (0-30% interface) signifies that DGX has affinity for both liposome composition that renders DGX buoyant and floats to the 0-30% interface upon ultracentrifugation. From the liposome floatation experiment it was inferred that the ECD of DGX posses affinity for lipid membranes.

III.3.7 Helical wheel depiction on 12 amino acid peptide region containing the pCBM1 in DmGluRA

The 12 amino acid peptide region (from residue 613 – 624 containing the pCBM1) in DmGluRA were plotted on a helical wheel. The hydrophobic patch consisting residues Leu^{615}, Tyr^{619}, Trp^{622}, and Lys^{621} were on one face of the helix that were capable of anchoring to the membrane. A few charged residues Q^{618} and K^{621} were also observed that might interact with the charged phospholipids. From such a distribution of the aminoacids on one face of the helical plot it was concluded that the 12 aminoacid peptide region was amphiphatic.
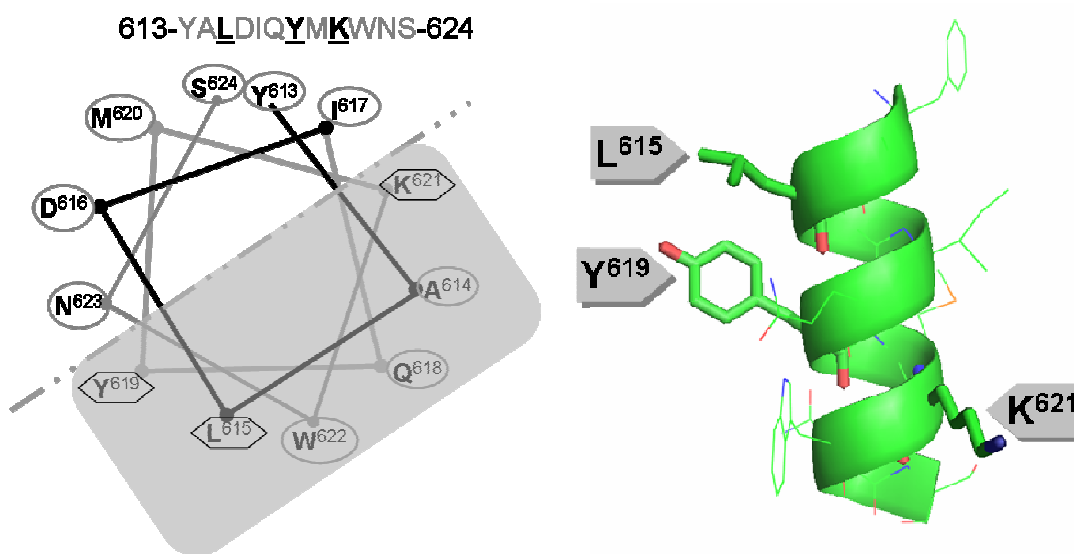
Fig. 46. Helical wheel depiction of the 12 amino acid region. Shows the distribution of amino acids typical of a amphipathic helix with the hydrophobic residues placed on one face containing the pCBM

III.3.8 CD spectrum analysis of the peptides

Two peptides were synthesized to study the effect of Raft liposomes on the conformational change induced upon interaction with the liposomes. The $Pep_{611-624}$ and $Pep_{602-624}$ peptide contained the residues ranging from 611 to 624 and 602 to 624 in DmGluRa respectively. About 50μM of the peptides ($Pep_{602-624}$ and $Pep_{611-624}$) were analyzed on the spectropolarimeter after incubation with 10mM liposomes of Raft composition in 50mM phosphate buffer pH 7.4. The spectrum for the data was interpreted after background correction obtained from the controls (such as reading from buffer alone and from the raft liposomes without peptide). The spectrum was plotted absorbance in x-axis against the ellipicity in the y-axis. CD spectra of $Pep_{602-624}$ and $Pep_{611-624}$ showed that there was no significant conformational change in the peptide upon its incubation with liposomes of raft compostition (DOPC:DPPC:Cholesterol, 30:30:40 mol%).

Pep₆₁₁₋₆₂₄ H-**SCYALDIQYMKWNS**-NH₂
Pep₆₀₂₋₆₂₄ H-**GLWPYADKLSCYALDIQYMKWNS**-NH₂

Fig. 47. CD spectrum analysis on peptides (pep602-624 and pep611-624) containing the cholesterol binding motif

III.3.9 Studies on DGXd12ct and DGXd12ct-GPI constructs in the RBV system

III.3.9.1 Recombinant virus production and expression of DGXd12ct and DGXd12ct-GPI constructs in the RBV system

In order to see the effect of removal of pCBM, further constructs were prepared by truncating by 12 amino acids containing the pCBM at the C-terminus of DGX. The DGXd12ct construct was prepared by truncating the 12 amino acids at the C-terminus. Like the DGXd12ct construct, DGXd12ct-GPI construct also lacked the pCBM1 but was tagged with a GPI-anchor at the C-terminus of DGXd12ct construct. The DGXd12ct and DGXd12ct-GPI constructs cloned in pVL1393 transfer vector were co-transfected into *Sf9* cells for recombinant virus production.

The usual procedure for recombinant baculovirus production was followed as mentioned in the materials and methods section. Expression tests on the clones were done on the infected *Sf9* cells by western blotting and detecting with anti-DGR antibody as primary antibody.

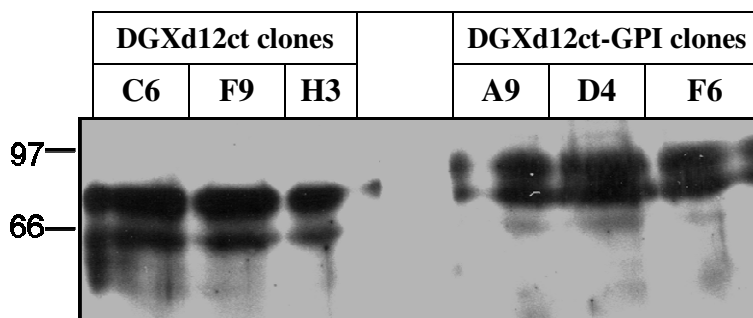| Construct Name	Truncation point	Theoretical Mol wt	C-term Tag	Titer value (Pfu/mL)
DGXd12ct	Cys 612	~ 69 kDa	-	3.66×10^8
DGXd12ct-GPI	Cys 612	~ 71 kDa	*flag*	5.48×10^8

Fig.48. Expression tests on clones of DGXd12ct and DGXd12ct-GPI for viral stock production. Three clones of each construct were selected for infection and the expression in total cells were analysed by Western blotting. In the Western blot, all 3 clones showed good expression for DGXd12ct and DGXd12ct-GPI.

[³H]-Glutamate binding trials on DGXd21ct and DGXd12ct-GPI expressed *Sf9* membranes

[³H]-Glutamate binding was carried out on DGXd12ct and DGXd21ct-GPI expressed and prepared *Sf9* membranes. The values were plotted with increasing concentration of unlabeled glutamate against the total counts measured from the bound [³H]-Glutamate. The model curve was a good fit and further it was inferred that the DGXd12ct membrane no binding was observed whereas DGXd12ct-GPI membranes had the similar affinity (6.3±1.9 µM) as that of the DmGluRA and its other truncated constructs as shown before (fig 42).
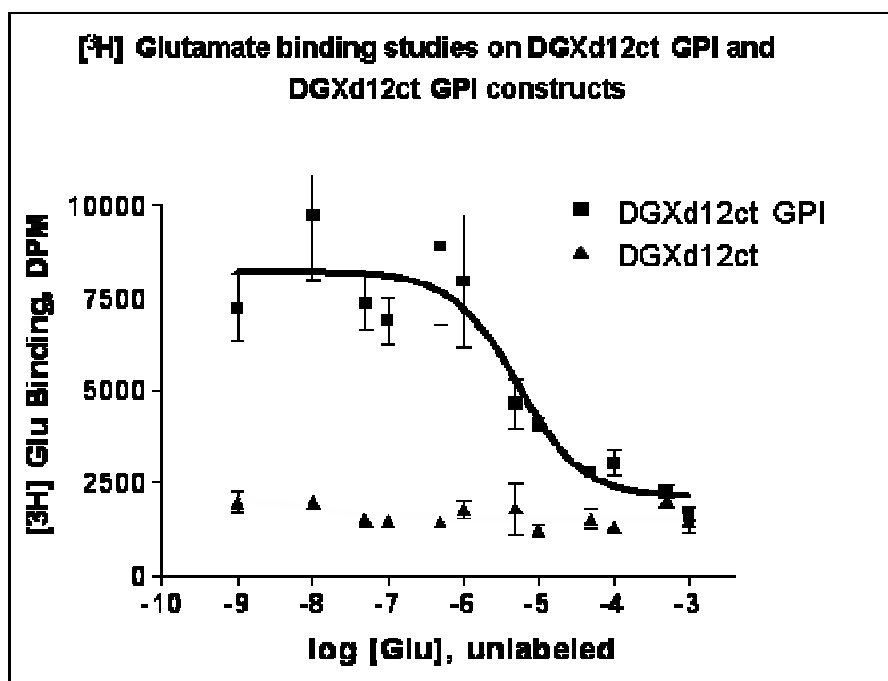

Fig. 49. Homologous competitive binding curve on DGXd12ct and DGXd12ct-GPI expressed-*Sf9* membranes. Competitive binding assay on DGXd12ct-GPI membranes showed the same affinity (IC_{50}=6.3±1.9 µM) as observed in the DGX, DGRTM1, DGRTM3, DGRTM5 and wild-type DmGluRA membranes. Total binding in DGXd12ct-GPI expressed *Sf9* membrane is 7140.7±1443.5 DPM and unspecific binding is 2808.7±327.2. No binding observed in case of membranes prepared from *Sf9* cells infected with DGXd12ct virus. Total binding was found to be 1971.7±291.6 DPM and unspecific binding is 1482.3±347.4. Curves represent the mean of independent experiments (n = 3 for DGXd12ct-GPI and n=1 for DGXd12ct).

From the binding curves, it can be concluded that the 12 amino acid pCBM containing peptide plays a majkor role in the activity of the receptor.

Discussion

X-ray crystallography and NMR have been the well-established techniques till date that are employed for the structure determination and characterisation of the proteins. The major limitation for solving a structure by x-ray crystallography is the amount and the quality of protein required for the crystallization trials. This is the primary reason for the slow pace of growth in the number of membrane protein structures solved. In recent years, several robust expression systems (prokaryotic and eukaryotic) have been developed; but the production of G-protein coupled receptors (GPCRs) in amounts that are sufficient for the structure characterization trials still remains a challenge. Certainly, it would be a difficult task to develop an expression system that contains all the necessary molecular mechanism to handle the protein expression of any kind. In recent years, interdisciplinary approaches have been applied to understand the protein characterization at molecular level with experimental data available and bioinformatics tools. The information so gathered significantly aids at various steps optimization of recombinant protein expression and purification.

Molecular modelling studies can be used as a tool to design cloning strategies for high secretion levels of the ligand binding extracellular domain (GABA$_B$1b) of the metabotropic GABA$_B$ receptor from *Rattus norvegicus*. Sequence analysis on the ECD of GABA$_B$1b receptor were predicted to be homologous to the *venus flytrap* domain of the periplasmic binding proteins (Olah et al., 1993). The crystal structure of the ECD of the metabotropic glutamate receptor (mGluR) belonging to the same class C GPCRs contains the *venus flytrap* of ECD in its structure. The crystal structure of mGluR was solved for the ECD in ligand (glutamate) bound and in un-bound state (Kunishima et al., 2000).

In the current study, a structure model of ECD of metabotropic GABA$_B$ receptor (GBR1bNT) was built using the structure coordinates of the ligand bound form of mGluR ECD (PDB code : 1EWK). The structure model obtained for GBR1bNT and the template (1EWK) was energy minimized under same conditions using the model_minimize and model_anneal (Rice and Brunger, 1994) modules of CNS package. During the energy minimization protocol, 15 representative energy

minimized structures were obtained. The models obtained were verified using Procheck program (Laskowski et al., 1993). The root mean square deviation (RMSD) between the template (1EWK) and the minimized structure was in the range of 1.85±0.05. The model thus obtained was useful to understand the structural features of GBR1bNT. Structure comparison of the ECD of mGluR and GBR1bNT showed that GBR1bNT contained features that might interfere with the expression and secretion of proteins such as the proline-rich region at the N-terminus.

In the current study, the ligand binding ECD of metabotropic GABA$_B$ receptor from *Rattus norvegicus* (GBR1bNT) was expressed and purified in insect cell system or recombinant virus system (RBV) and *E.coli*.

The advantages of using a RBV in overexpressing proteins are that since it is an eukaryotic system it possess similar glycosylation patterns like that of the mammalian system leading to expression of a functional protein. The system has a disadvantage of being time consuming and expensive but the other advantage is that the expression can be scaled up to large volumes once the recombinant virus is optimised for multiplicity of infection (MOI), recombinant protein expression and other kinetic parameters. Appropriate application of strategies has improved high-level expression of proteins in the RBV system.

GBR1bNT is a heterologous protein (from rat) to be expressed in the baculovirus system, so the native signal peptide was replaced with that of mellitin signal peptide, which is native to hymenopteran insect cells (Cagla). Mellitin is a secretory protein in the insect cells expressed in large quantities under the control of the mellitin signal peptide; moreover expression under the control of this peptide has shown to have improved the secretion of plant propain when expressed in the baculovirus system (Tessier et al., 1991).

Initially, the GBR1bNT was attempted to be expressed in the RBV system under the control of the mellitin signal peptide. Low secreted levels of purified GBR1bNT were obtained that was only detectable by silver staining. Bioinformatics and computational modelling approaches were applied to understand GBR1bNT at

sequence and structure level in order to analyze the poor secretion levels of GBR1bNT.

From the computational modelling studies of GBR1bNT, it is understood that GBR1bNT had a proline-rich domain immediately after the signal peptide region. This region was found to be unstructured and such a feature to be present at the start of the translation could be a problem in the proper folding of the protein. Previously, the 3D structure of ECD of frizzled receptor was solved by expressing the protein in the mammalian system with human growth hormone tagged at the N-terminus as the fusion partner (Dann et al., 2001). Also the chicken growth hormone (cGH) is known to be well expressed in the RBV system. With the following information a strategy was developed by preparing the pVL1393-cGH-GBR1bNT construct with cGH fused at the N-terminus of GBR1bNT to drive the expression. Tobacco etch virus cleavage site was included in the construct between cGH and GBR1bNT in order to obtain the GBR1bNT alone upon cleavage with TEV protease after purification. Another construct, pVL1393-cGH was prepared as a control over the cGH expression when expressed alone and when fused with GBR1bNT. Viral stocks are prepared and the protein expression levels are optimised.

In parallel another strategy of secretion of GBR1bNT under the control of the DmGluRA signal peptide (DGRsp) was planned and the required constructs were prepared. The rationale behind this approach is that in the previous studies (Eroglu, Phd thesis, 2002) on the overexpression of DmGluRA ECD yielded good quantities of the secreted protein in the same expression system. So, the idea was to see if GBR1bNT could be secreted under the control of DGRsp (pVL1393-DGRsp-GBR1bNT).

Since secretion method involving expression of GBR1bNT fused with cGH at N terminus involves two addional steps of cleavage and subsequent purification of the cleaved GBR1bNT, the strategy of expression under the control of DGRsp was attempted first. Under the control of DGRsp good amounts of secreted GBR1bNT were obtained upon purification on a Ni-sepharose column.

Although both mellitin and DGRsp are signal peptides of insect origin and native to the baculovirus system, the levels of secretion of GBR1bNT under the control of

DGRsp were higher in comparison to that of secretion under the control of mellitin signal peptide.

Such observations have been made in earlier reports also. The human t-PA was found to be poorly expressed in the baculovirus system. To improve the levels of expression, instead of native signal peptide the human t-PA was expressed and secreted under the control of cecropin B and 64K signal peptides which are native to the insect cells (Jarvis and Summers, 1989). The result showed no significant effect in the expression or secretion of this chimera t-PA on the expression of t-PA with the native signal peptides (cecropin B and 64K).

Thereby, the molecular mechanism behind the protein secretory pathway is unclear to derive a consensus for choosing a signal peptide to drive the expression of heterologous proteins in the insect cells.

In the current study the vectors pVL1393-DGRsp and pVL1393-cGH plasmids (does not contain GBR1bNT) have been designed such that any gene of interest can be directly cloned downstream of either the DmGluRA signal peptide (DGRsp) or cGH as N-terminus fusion partner. A Tobacco etch virus (TEV) protease recognition site has been included after DGRsp or cGH, so that the expressed protein of interest can be cleaved by TEV protease.

In the second part of the study, GBR1bNT expression was attempted in *E.coli*. *E.coli* system has a major disadvantage of being a prokaryotic system where post-translation modifications of protein are absent. But there are several other advantages for it being a expression system that is well studies, cost and time effective and ease of scaling up the expression. Several GPCRs have been expressed and purified in *E.coli* as inclusion bodies and have been shown functionally active (Baneres et al., 2005). Recently, the structure of the vasopressin receptor was solved by NMR by over-expressing the protein in *E.coli* (Tian et al., 2005).

The ECD of the metabotropic glutamate receptor for which the structure was solved (Kunishima et al., 2000) also undergoes glycosylation and was shown that receptor

was still functional without glycosylation upon expressing the protein with tunicamycin. GBR1bNT also undergoes glycosylation, so the over-expression in *E.coli* was attempted to study if functional protein was obtained. In a recent work, site-directed mutagenesis of the glycosylation sites in metabotropic $GABA_B1b$ receptor ($GABA_B1b$) have shown that the ECD of $GABA_B1bR$ can be functionally active without any glycosylation (Deriu et al., 2005).

In the present study, upon several trials of optimization of the expression and purification strategies, expression of pET15b-GST-GBR1bNT plasmid in Tuner cells of *E.coli* resulted in good expression of GST-GBR1bNT protein in soluble form, which was efficiently purified by GST sepharose column.

Radioligand binding studies on the purified GST-GBR1bNT bound to GST beads and crystallisation trials on the functional GBR1bNT would be a worthy attempt. On the other hand optimization of expression and purification of secreted form of DGRsp-GBR1bNT from insect cells that would be optimally glycosylated, may enable future studies of functional viability of the protein and subsequent crystallization for solving the 3D structure.

Solving structure can aid understanding of protein function to a great extent. On the other even in absence of detailed structural data, biochemical studies give us important information on protein function and its biological relevance. Only one GPCR's structure has been solved namely – Bovine rhodopsin.

The regulation of membrane proteins (or GPCRs) in the plasma membrane are not limited to the interactions within the residues of a protein or between protein-protein but also influenced by the lipid environment the protein is localized in. There are growing evidences about specific lipid or sterol requirement for the activity of membrane protein such as P-glycoprotein requires phosphatidyl choline and phosphatidyl ethanolamine for its activity (Sharom, 1997). The lac permease in *E.coli* requires cardiolipin for its conformational transition and ADP binding (Bogdanov et al., 1999). There are also crystal structures of membrane proteins reported where densities for lipids or sterols are observed interacting with the membrane protein.

The current study is focussed on relation between the DmGluRA affinity for its ligand glutamate and the local membrane composition. There are four putative cholesterol binding motifs (L/V-[X]$_{1-5}$-Y-[X]$_{1-5}$-R/K) in the transmembrane domain region of DmGluRA. During baculovirus expression studies it has been observed that Sf9 plasma membranes contain a rather low quantity of cholesterol and no phosphatidyl serine, whereas the phosphatidyl inositol is comparatively high. It has been shown that addition of cholesterol to the medium of infected Sf9 insect cells positively affected the properties resulting in an increase in high-affnity agonist binding sites for the recombinant oxytocin receptor (Gimpl et al., 1995).

Studies by (Eroglu et al., 2002) show that when DmGluRA was expressed in the rhabdomeres of the fly eye containing ergosterol it possessed 10 fold lower glutamate binding affinity than the insect cell membrane containing cholesterol. Modification of the membrane cholesterol content in the rhabdomeres upon treatment with MßCD-cholesterol complex and followed by glutamate binding studies surprisingly increased by 50 fold. These results show that cholesterol is a major requisite for DmGluRA to maintain its high affinity state. Cholesterol has been reported to be important for the activity of other membrane proteins such as P-glycoprotein, Ca2 + ATPase and Na+/K+-ATPase .

The presence of the 4 putative low consensus cholesterol binding motif (L/V-[X$_{1-5}$]-Y-[X$_{1-5}$]-R/K) on the transmembrane region DmGluRA raised the interest of investigating whether these motifs are involved in the regulation of the receptor. Truncation constructs of DmGluRA including one, two or three putative cholesterol binding motifs (pCBM) were made to study the role of the pCBM in maintaining the high affinity state of glutamate. Glutamate binding studies on the truncation constructs DGRTM1, DGRTM3 and DGRTM5 expressed in *Sf9* plasma membranes maintained the high affinity state. This result showed that DmGluRA does not require all of the transmembrane helices for binding glutamate. It was further observed that among the above mentioned three constructs, the DGRTM1 construct containing the glutamate binding extracellular domain, only one pCBM and one transmembrane helix could be the minimal construct that maintained the high affinity for glutamate.

In case of the DG14c construct, only small amount of protein was observed in the membrane preparation. Glutamate binding trials on the membrane preparations of DG14c failed to produce any signal leading to a possibility that the membrane preparation could be contaminated with membranes of the endoplasmic reticulum where the proteins are generally unfolded.

Binding studies were carried out on membrane preparations of SF9 cells infected with further truncated versions of the DmGluRA such as the DG14c construct (containing the extracellular domain lacking the cysteine rich domain) and DGX construct (containing the complete extracellular domain including one of the putative cholesterol binding motif at its C-terminus). The DGX protein was well expressed in the membranes and its affinity to bind glutamate as showed that the receptor is in the high affinity state.

Upon careful observation of expression of DGX and DG14c constructs secreted to the medium, it was noted that the DGX protein was secreted to the medium in considerable amounts as well as purifiable on a Ni-Sepharose column. Results obtained from studies on DGX construct in liposome floatation studies exhibited interaction of DGX with liposomes. It may be inferred that DGX construct has a hydrophobic patch that enables it to interact with the liposomes.

A 12 amino acid region from residue 613-624 of the DGX construct was subjected to a helical wheel depiction. The peptide distribution exhibited amphipathicity with long hydrophobic side chain residues along with the residues of pCBM on one face of the wheel and polar residues on the other face.

The results obtained from the experiments on the DGX construct, such as, the glutamate binding studies, liposome floatation studies and with the helical wheel depiction were interesting. This observation let us speculate that there could be a hydrophobic patch in the ECD of the DmGluRA that interacts with the lipid bilayer; the amphipathic peptide region containing the pCBM possessed the features of residues that are capable of anchoring or interacting with the lipid bilayer. Therefore it was inferred that this peptide region containing the pCBM could be involved in maintaining the high affinity state of the receptor by interacting with the lipid bilayer.

The DRM isolation studies on 1% Triton X-100 detergent extracted (at 4°C) membranes containing DGRTM1 showed that the DGRTM1 were associated with DRMs or rafts and possessed similar high affinity state to bind glutamate due to its association with DRMs as inferred in the case of DmGluRA (Eroglu et al., 2003). Both DGX and DGRTM1 constructs contained the pCBM and DGX differed from the DGRTM1 construct by lacking a transmembrane helix following the pCBM. The binding studies on DGX and DGRTM1 constructs show similar high affinity state to bind glutamate. Hence, it was assumed that DGX is also associated with DRMs.

It is an interesting observation that the ligand binding activity of DmGluRA is dependent on localization in DRM. In the present study, the high affinity glutamate binding activity of the receptor due to DRM association has been narrowed down to the region (1-624 of DmGluRA). This region contains one pCBM on an amphipathic 12 amino acid region, which implies that one single pCBM might be sufficient for maintaining the high affinity status of the receptor. The DGX acts as minimal construct that is capable of binding the ligand.

Binding studies with DGXd12ct exhibited no activity which indicates the important role of this 12 amino acid pCBM in ligand binding activity of DGX. Loss of activity may be attributed to either incapability of the DGXd12ct construct localising to raft which is necessary for functional viability of the receptor or inspite of localising to raft it loses the inherent activity. When binding study was performed using DGXd12ct-GPI construct containing a GPI anchor, the activity was restored. This gain of activity by incorporating GPI rules out the possibility that removing the 12 amino acids affects the inherent receptor activity. From these observations, it may be concluded that 12 amino acid region plays an important role raft formation that is essential for ligand binding activity of DGX. Further experiments are required to confirm this interesting observation of narrowing down the minimal requirement for raft formation and as a result ligand binding activity of DmGluRA to the 12 amino acid region.

As a futuristic prospective, site directed mutagenesis of the 12 amino acid region of DGX and performing ligand binding trials and photocholesterol crosslinking to these mutation construct will further narrow down the understanding of the receptor regulation to a residue level.

V. BIBLIOGRAPHY

Baneres JL, Mesnier D, Martin A, Joubert L, Dumuis A, Bockaert J (2005) Molecular characterization of a purified 5-HT4 receptor: a structural basis for drug efficacy. J Biol Chem 280:20253-20260.

Baude A, Nusser Z, Roberts JD, Mulvihill E, McIlhinney RA, Somogyi P (1993) The metabotropic glutamate receptor (mGluR1 alpha) is concentrated at perisynaptic membrane of neuronal subpopulations as detected by immunogold reaction. Neuron 11:771-787.

Becher A, White JH, McIlhinney RA (2001) The gamma-aminobutyric acid receptor B, but not the metabotropic glutamate receptor type-1, associates with lipid rafts in the rat cerebellum. J Neurochem 79:787-795.

Belrhali H, Nollert P, Royant A, Menzel C, Rosenbusch JP, Landau EM, Pebay-Peyroula E (1999) Protein, lipid and water organization in bacteriorhodopsin crystals: a molecular view of the purple membrane at 1.9 A resolution. Structure Fold Des 7:909-917.

Berg S, Edman M, Li L, Wikstrom M, Wieslander A (2001) Sequence properties of the 1,2-diacylglycerol 3-glucosyltransferase from Acholeplasma laidlawii membranes. Recognition of a large group of lipid glycosyltransferases in eubacteria and archaea. J Biol Chem 276:22056-22063.

Bettler B, Kaupmann K, Bowery N (1998) GABAB receptors: drugs meet clones. Curr Opin Neurobiol 8:345-350.

Beyer K, Nuscher B (1996) Specific cardiolipin binding interferes with labeling of sulfhydryl residues in the adenosine diphosphate/adenosine triphosphate carrier protein from beef heart mitochondria. Biochemistry 35:15784-15790.

Bogdanov M, Dowhan W (1995) Phosphatidylethanolamine is required for in vivo function of the membrane-associated lactose permease of Escherichia coli. J Biol Chem 270:732-739.

Bogdanov M, Dowhan W (1998) Phospholipid-assisted protein folding: phosphatidylethanolamine is required at a late step of the conformational maturation of the polytopic membrane protein lactose permease. Embo J 17:5255-5264.

Bogdanov M, Dowhan W (1999) Lipid-assisted protein folding. J Biol Chem 274:36827-36830.

Bogdanov M, Heacock PN, Dowhan W (2002) A polytopic membrane protein displays a reversible topology dependent on membrane lipid composition. Embo J 21:2107-2116.

Brown DA, London E (1998) Structure and origin of ordered lipid domains in biological membranes. J Membr Biol 164:103-114.

Burger, K., G. Gimpl, et al. (2000). "Regulation of receptor function by cholesterol." Cell Mol Life Sci 57(11): 1577-92.

Chen CC, Wilson TH (1984) The phospholipid requirement for activity of the lactose carrier of Escherichia coli. J Biol Chem 259:10150-10158.

Chini B, Parenti M (2004) G-protein coupled receptors in lipid rafts and caveolae: how, when and why do they go there? J Mol Endocrinol 32:325-338.

Chun M, Liyanage UK, Lisanti MP, Lodish HF (1994) Signal transduction of a G protein-coupled receptor in caveolae: colocalization of endothelin and its receptor with caveolin. Proc Natl Acad Sci U S A 91:11728-11732.

Conn PJ, Pin JP (1997) Pharmacology and functions of metabotropic glutamate receptors. Annu Rev Pharmacol Toxicol 37:205-237.

Cornelius, F. (2001). "Modulation of Na,K-ATPase and Na-ATPase activity by phospholipids and cholesterol. I. Steady-state kinetics." Biochemistry 40(30): 8842-51.

Couve A, Filippov AK, Connolly CN, Bettler B, Brown DA, Moss SJ (1998) Intracellular retention of recombinant GABAB receptors. J Biol Chem 273:26361-26367.

Dann CE, Hsieh JC, Rattner A, Sharma D, Nathans J, Leahy DJ (2001) Insights into Wnt binding and signalling from the structures of two Frizzled cysteine-rich domains. Nature 412:86-90.

de Cock H, Pasveer M, Tommassen J, Bouveret E (2001) Identification of phospholipids as new components that assist in the in vitro trimerization of a bacterial pore protein. Eur J Biochem 268:865-875.

de Weerd WF, Leeb-Lundberg LM (1997) Bradykinin sequesters B2 bradykinin receptors and the receptor-coupled Galpha subunits Galphaq and Galphai in caveolae in DDT1 MF-2 smooth muscle cells. J Biol Chem 272:17858-17866.

Delgado R, Barla R, Latorre R, Labarca P (1989) L-glutamate activates excitatory and inhibitory channels in Drosophila larval muscle. FEBS Lett 243:337-342.

Deriu D, Gassmann M, Firbank S, Ristig D, Lampert C, Mosbacher J, Froestl W, Kaupmann K, Bettler B, Grutter MG (2005) Determination of the minimal functional ligand-binding domain of the GABAB1b receptor. Biochem J 386:423-431.

Ding, J., A. P. Starling, et al. (1994). "Binding sites for cholesterol on Ca(2+)-ATPase studied by using a cholesterol-containing phospholipid." Biochemistry 33(16): 4974-9.

Dreja K, Voldstedlund M, Vinten J, Tranum-Jensen J, Hellstrand P, Sward K (2002) Cholesterol depletion disrupts caveolae and differentially impairs agonist-induced arterial contraction. Arterioscler Thromb Vasc Biol 22:1267-1272.

Drmota T, Novotny J, Gould GW, Svoboda P, Milligan G (1999) Visualization of distinct patterns of subcellular redistribution of the thyrotropin-releasing hormone receptor-1 and gqalpha /G11alpha induced by agonist stimulation. Biochem J 340 (Pt 2):529-538.

Duran A, Cabib E (1978) Solubilization and partial purification of yeast chitin synthetase. Confirmation of the zymogenic nature of the enzyme. J Biol Chem 253:4419-4425.

Easter A, Spruce AE (2002) Recombinant GABA(B) receptors formed from GABA(B1) and GABA(B2) subunits selectively inhibit N-type Ca(2+) channels in NG108-15 cells. Eur J Pharmacol 440:17-25.

Eroglu C, Brugger B, Wieland F, Sinning I (2003) Glutamate-binding affinity of Drosophila metabotropic glutamate receptor is modulated by association with lipid rafts. Proc Natl Acad Sci U S A 100:10219-10224.

Eroglu C, Cronet P, Panneels V, Beaufils P, Sinning I (2002) Functional reconstitution of purified metabotropic glutamate receptor expressed in the fly eye. EMBO Rep 3:491-496.

Fernandez-Ballester, G., J. Castresana, et al. (1994). "Role of cholesterol as a structural and functional effector of the nicotinic acetylcholine receptor." Biochem Soc Trans 22(3): 776-80.

Filippov AK, Couve A, Pangalos MN, Walsh FS, Brown DA, Moss SJ (2000) Heteromeric assembly of GABA(B)R1 and GABA(B)R2 receptor subunits inhibits Ca(2+) current in sympathetic neurons. J Neurosci 20:2867-2874.

Flower DR (1999) Modelling G-protein-coupled receptors for drug design. Biochim Biophys Acta 1422:207-234.

Foster DN, Proudman JA, Harmon SA, Foster LK (1997) Baculovirus-mediated expression of chicken growth hormone. Comp Biochem Physiol B Biochem Mol Biol 117:233-239.

Gimpl G, Fahrenholz F (2000) Human oxytocin receptors in cholesterol-rich vs. cholesterol-poor microdomains of the plasma membrane. Eur J Biochem 267:2483-2497.

Gimpl G, Klein U, Reilander H, Fahrenholz F (1995) Expression of the human oxytocin receptor in baculovirus-infected insect cells: high-affinity binding is induced by a cholesterol-cyclodextrin complex. Biochemistry 34:13794-13801.

Grisshammer R, Tate CG (1995) Overexpression of integral membrane proteins for structural studies. Q Rev Biophys 28:315-422.

Grunewald S, Schupp BJ, Ikeda SR, Kuner R, Steigerwald F, Kornau HC, Kohr G (2002) Importance of the gamma-aminobutyric acid(B) receptor C-termini for G-protein coupling. Mol Pharmacol 61:1070-1080.

Guzzi F, Zanchetta D, Cassoni P, Guzzi V, Francolini M, Parenti M, Chini B (2002) Localization of the human oxytocin receptor in caveolin-1 enriched domains turns the receptor-mediated inhibition of cell growth into a proliferative response. Oncogene 21:1658-1667.

Haasemann M, Cartaud J, Muller-Esterl W, Dunia I (1998) Agonist-induced redistribution of bradykinin B2 receptor in caveolae. J Cell Sci 111 (Pt 7):917-928.

Hagio M, Gombos Z, Varkonyi Z, Masamoto K, Sato N, Tsuzuki M, Wada H (2000) Direct evidence for requirement of phosphatidylglycerol in photosystem II of photosynthesis. Plant Physiol 124:795-804.

Hamm HE (1998) The many faces of G protein signaling. J Biol Chem 273:669-672.

Hawrot E, Xiao Y, Shi QL, Norman D, Kirkitadze M, Barlow PN (1998) Demonstration of a tandem pair of complement protein modules in GABA(B) receptor 1a. FEBS Lett 432:103-108.

Horn F, Vriend G, Cohen FE (2001) Collecting and harvesting biological data: the GPCRDB and NucleaRDB information systems. Nucleic Acids Res 29:346-349.

Houamed KM, Kuijper JL, Gilbert TL, Haldeman BA, O'Hara PJ, Mulvihill ER, Almers W, Hagen FS (1991) Cloning, expression, and gene structure of a G protein-coupled glutamate receptor from rat brain. Science 252:1318-1321.

Hunter GW, Negash S, Squier TC (1999) Phosphatidylethanolamine modulates Ca-ATPase function and dynamics. Biochemistry 38:1356-1364.

Igarashi J, Michel T (2000) Agonist-modulated targeting of the EDG-1 receptor to plasmalemmal caveolae. eNOS activation by sphingosine 1-phosphate and the role of caveolin-1 in sphingolipid signal transduction. J Biol Chem 275:32363-32370.

Ishizaka N, Griendling KK, Lassegue B, Alexander RW (1998) Angiotensin II type 1 receptor: relationship with caveolae and caveolin after initial agonist stimulation. Hypertension 32:459-466.

Iwata S, Ostermeier C, Ludwig B, Michel H (1995) Structure at 2.8 A resolution of cytochrome c oxidase from Paracoccus denitrificans. Nature 376:660-669.

Jarvis DL, Summers MD (1989) Glycosylation and secretion of human tissue plasminogen activator in recombinant baculovirus-infected insect cells. Mol Cell Biol 9:214-223.

Jordan P, Fromme P, Witt HT, Klukas O, Saenger W, Krauss N (2001) Three-dimensional structure of cyanobacterial photosystem I at 2.5 A resolution. Nature 411:909-917.

Joshi MK, Dracheva S, Mukhopadhyay AK, Bose S, Hendler RW (1998) Importance of specific native lipids in controlling the photocycle of bacteriorhodopsin. Biochemistry 37:14463-14470.

Ju H, Venema VJ, Liang H, Harris MB, Zou R, Venema RC (2000) Bradykinin activates the Janus-activated kinase/signal transducers and activators of transcription (JAK/STAT) pathway in vascular endothelial cells: localization of JAK/STAT signalling proteins in plasmalemmal caveolae. Biochem J 351:257-264.

Kadenbach B, Mende P, Kolbe HV, Stipani I, Palmieri F (1982) The mitochondrial phosphate carrier has an essential requirement for cardiolipin. FEBS Lett 139:109-112.

Kaupmann K, Huggel K, Heid J, Flor PJ, Bischoff S, Mickel SJ, McMaster G, Angst C, Bittiger H, Froestl W, Bettler B (1997) Expression cloning of GABA(B) receptors uncovers similarity to metabotropic glutamate receptors. Nature 386:239-246.

Kifor O, Diaz R, Butters R, Kifor I, Brown EM (1998) The calcium-sensing receptor is localized in caveolin-rich plasma membrane domains of bovine parathyroid cells. J Biol Chem 273:21708-21713.

Kifor O, Kifor I, Moore FD, Jr., Butters RR, Jr., Brown EM (2003) m-Calpain colocalizes with the calcium-sensing receptor (CaR) in caveolae in parathyroid cells and participates in degradation of the CaR. J Biol Chem 278:31167-31176.

Klein, U., G. Gimpl, et al. (1995). "Alteration of the myometrial plasma membrane cholesterol content with beta-cyclodextrin modulates the binding affinity of the oxytocin receptor." Biochemistry 34(42): 13784-93.

Kozak, S. L., S. E. Kuhmann, et al. (1999). "Roles of CD4 and coreceptors in binding, endocytosis, and proteolysis of gp120 envelope glycoproteins derived from human immunodeficiency virus type 1." J Biol Chem 274(33): 23499-507.

Krisch B, Feindt J, Mentlein R (1998) Immunoelectronmicroscopic analysis of the ligand-induced internalization of the somatostatin receptor subtype 2 in cultured human glioma cells. J Histochem Cytochem 46:1233-1242.

Kruse O, Hankamer B, Konczak C, Gerle C, Morris E, Radunz A, Schmid GH, Barber J (2000) Phosphatidylglycerol is involved in the dimerization of photosystem II. J Biol Chem 275:6509-6514.

Kuner, R., G. Kohr, et al. (1999). "Role of heteromer formation in GABAB receptor function." Science 283(5398): 74-7.

Kunishima N, Shimada Y, Tsuji Y, Sato T, Yamamoto M, Kumasaka T, Nakanishi S, Jingami H, Morikawa K (2000) Structural basis of glutamate recognition by a dimeric metabotropic glutamate receptor. Nature 407:971-977.

Lamb ME, Zhang C, Shea T, Kyle DJ, Leeb-Lundberg LM (2002) Human B1 and B2 bradykinin receptors and their agonists target caveolae-related lipid rafts to different degrees in HEK293 cells. Biochemistry 41:14340-14347.

Lange C, Nett JH, Trumpower BL, Hunte C (2001) Specific roles of protein-phospholipid interactions in the yeast cytochrome bc1 complex structure. Embo J 20:6591-6600.

Laskowski RA, Moss DS, Thornton JM (1993) Main-chain bond lengths and bond angles in protein structures. J Mol Biol 231:1049-1067.

Leclerc PC, Auger-Messier M, Lanctot PM, Escher E, Leduc R, Guillemette G (2002) A polyaromatic caveolin-binding-like motif in the cytoplasmic tail of the type 1 receptor for angiotensin II plays an important role in receptor trafficking and signaling. Endocrinology 143:4702-4710.

Lee AG (1998) How lipids interact with an intrinsic membrane protein: the case of the calcium pump. Biochim Biophys Acta 1376:381-390.

Li H, Papadopoulos V (1998) Peripheral-type benzodiazepine receptor function in cholesterol transport. Identification of a putative cholesterol recognition/interaction amino acid sequence and consensus pattern. Endocrinology 139:4991-4997.

Li H, Yao Z, Degenhardt B, Teper G, Papadopoulos V (2001) Cholesterol binding at the cholesterol recognition/ interaction amino acid consensus (CRAC) of the peripheral-type benzodiazepine receptor and inhibition of steroidogenesis by an HIV TAT-CRAC peptide. Proc Natl Acad Sci U S A 98:1267-1272.

Liang Y, Fotiadis D, Filipek S, Saperstein DA, Palczewski K, Engel A (2003) Organization of the G protein-coupled receptors rhodopsin and opsin in native membranes. J Biol Chem 278:21655-21662.

Luecke H, Schobert B, Richter HT, Cartailler JP, Lanyi JK (1999) Structure of bacteriorhodopsin at 1.55 A resolution. J Mol Biol 291:899-911.

Malitschek B, Schweizer C, Keir M, Heid J, Froestl W, Mosbacher J, Kuhn R, Henley J, Joly C, Pin JP, Kaupmann K, Bettler B (1999) The N-terminal domain of gamma-aminobutyric Acid(B) receptors is sufficient to specify agonist and antagonist binding. Mol Pharmacol 56:448-454.

Margeta-Mitrovic M, Jan YN, Jan LY (2000) A trafficking checkpoint controls GABA(B) receptor heterodimerization. Neuron 27:97-106.

Marinissen MJ, Gutkind JS (2001) G-protein-coupled receptors and signaling networks: emerging paradigms. Trends Pharmacol Sci 22:368-376.

Marshall FH, Jones KA, Kaupmann K, Bettler B (1999) GABAB receptors - the first 7TM heterodimers. Trends Pharmacol Sci 20:396-399.

Masu M, Tanabe Y, Tsuchida K, Shigemoto R, Nakanishi S (1991) Sequence and expression of a metabotropic glutamate receptor. Nature 349:760-765.

McAuley KE, Fyfe PK, Ridge JP, Isaacs NW, Cogdell RJ, Jones MR (1999) Structural details of an interaction between cardiolipin and an integral membrane protein. Proc Natl Acad Sci U S A 96:14706-14711.

Mentlein R, Held-Feindt J, Krisch B (2001) Topology of the signal transduction of the G protein-coupled somatostatin receptor sst2 in human glioma cells. Cell Tissue Res 303:27-34.

Nakanishi S (1994) Metabotropic glutamate receptors: synaptic transmission, modulation, and plasticity. Neuron 13:1031-1037.

Nalecz KA, Bolli R, Wojtczak L, Azzi A (1986) The monocarboxylate carrier from bovine heart mitochondria: partial purification and its substrate-transporting properties in a reconstituted system. Biochim Biophys Acta 851:29-37.

Navratil AM, Bliss SP, Berghorn KA, Haughian JM, Farmerie TA, Graham JK, Clay CM, Roberson MS (2003) Constitutive localization of the gonadotropin-releasing hormone (GnRH) receptor to low density membrane microdomains is necessary for GnRH signaling to ERK. J Biol Chem 278:31593-31602.

Nguyen, D. H. and D. Taub (2002). "CXCR4 function requires membrane cholesterol: implications for HIV infection." J Immunol 168(8): 4121-6.

Nollmann M, Gilbert R, Mitchell T, Sferrazza M, Byron O (2004) The role of cholesterol in the activity of pneumolysin, a bacterial protein toxin. Biophys J 86:3141-3151.

Okamoto T, Schlegel A, Scherer PE, Lisanti MP (1998a) Caveolins, a family of scaffolding proteins for organizing "preassembled signaling complexes" at the plasma membrane. J Biol Chem 273:5419-5422.

Okamoto T, Sekiyama N, Otsu M, Shimada Y, Sato A, Nakanishi S, Jingami H (1998b) Expression and purification of the extracellular ligand binding region of metabotropic glutamate receptor subtype 1. J Biol Chem 273:13089-13096.

Okamoto, T., A. Schlegel, et al. (1998). "Caveolins, a family of scaffolding proteins for organizing "preassembled signaling complexes" at the plasma membrane." J Biol Chem 273(10): 5419-22.

Olah GA, Trakhanov S, Trewhella J, Quiocho FA (1993) Leucine/isoleucine/valine-binding protein contracts upon binding of ligand. J Biol Chem 268:16241-16247.

O'Reilly, M., Luckow. (1994). Baculovirus expression vectors - A Laboratory Manual. Oxford.

Pagano A, Rovelli G, Mosbacher J, Lohmann T, Duthey B, Stauffer D, Ristig D, Schuler V, Meigel I, Lampert C, Stein T, Prezeau L, Blahos J, Pin J, Froestl W, Kuhn R, Heid J, Kaupmann K, Bettler B (2001) C-terminal interaction is essential for surface trafficking but not for heteromeric assembly of GABA(b) receptors. J Neurosci 21:1189-1202.

Palczewski K, Kumasaka T, Hori T, Behnke CA, Motoshima H, Fox BA, Le Trong I, Teller DC, Okada T, Stenkamp RE, Yamamoto M, Miyano M (2000) Crystal structure of rhodopsin: A G protein-coupled receptor. Science 289:739-745.

Pang, L., M. Graziano, et al. (1999). "Membrane cholesterol modulates galanin-GalR2 interaction." Biochemistry 38(37): 12003-11.

Panneels V, Eroglu C, Cronet P, Sinning I (2003) Pharmacological characterization and immunoaffinity purification of metabotropic glutamate receptor from Drosophila overexpressed in Sf9 cells. Protein Expr Purif 30:275-282.

Parmentier ML, Pin JP, Bockaert J, Grau Y (1996) Cloning and functional expression of a Drosophila metabotropic glutamate receptor expressed in the embryonic CNS. J Neurosci 16:6687-6694.

Pawson AJ, Maudsley SR, Lopes J, Katz AA, Sun YM, Davidson JS, Millar RP (2003) Multiple determinants for rapid agonist-induced internalization of a nonmammalian gonadotropin-releasing hormone receptor: a putative palmitoylation site and threonine doublet within the carboxyl-terminal tail Are critical. Endocrinology 144:3860-3871.

Percherancier, Y., B. Lagane, et al. (2003). "HIV-1 entry into T-cells is not dependent on CD4 and CCR5 localization to sphingolipid-enriched, detergent-resistant, raft membrane domains." J Biol Chem 278(5): 3153-61.

Pfaff T, Malitschek B, Kaupmann K, Prezeau L, Pin JP, Bettler B, Karschin A (1999) Alternative splicing generates a novel isoform of the rat metabotropic GABA(B)R1 receptor. Eur J Neurosci 11:2874-2882.

Pin, J. P., C. Joly, et al. (1994). "Domains involved in the specificity of G protein activation in phospholipase C-coupled metabotropic glutamate receptors." Embo J 13(2): 342-8.

Quiocho FA, Ledvina PS (1996) Atomic structure and specificity of bacterial periplasmic receptors for active transport and chemotaxis: variation of common themes. Mol Microbiol 20:17-25.

Rice LM, Brunger AT (1994) Torsion angle dynamics: reduced variable conformational sampling enhances crystallographic structure refinement. Proteins 19:277-290.

Rietveld AG, Koorengevel MC, de Kruijff B (1995) Non-bilayer lipids are required for efficient protein transport across the plasma membrane of Escherichia coli. Embo J 14:5506-5513.

Robbins MJ, Ciruela F, Rhodes A, McIlhinney RA (1999) Characterization of the dimerization of metabotropic glutamate receptors using an N-terminal truncation of mGluR1alpha. J Neurochem 72:2539-2547.

Robinson NC (1982) Specificity and binding affinity of phospholipids to the high-affinity cardiolipin sites of beef heart cytochrome c oxidase. Biochemistry 21:184-188.

Roettger BF, Rentsch RU, Pinon D, Holicky E, Hadac E, Larkin JM, Miller LJ (1995) Dual pathways of internalization of the cholecystokinin receptor. J Cell Biol 128:1029-1041.

Romano C, Miller JK, Hyrc K, Dikranian S, Mennerick S, Takeuchi Y, Goldberg MP, O'Malley KL (2001) Covalent and noncovalent interactions mediate metabotropic glutamate receptor mGlu5 dimerization. Mol Pharmacol 59:46-53.

Rothnie, A., D. Theron, et al. (2001). "The importance of cholesterol in maintenance of P-glycoprotein activity and its membrane perturbing influence." Eur Biophys J 30(6): 430-42.

Sambrook , J. a. R., D (2001). Molecular cloning - A laboratory manual. CSHL, CSHL press.

Scanlon, S. M., D. C. Williams, et al. (2001). "Membrane cholesterol modulates serotonin transporter activity." Biochemistry 40(35): 10507-13.

Schlame M, Rua D, Greenberg ML (2000) The biosynthesis and functional role of cardiolipin. Prog Lipid Res 39:257-288.

Schuster CM, Ultsch A, Schloss P, Cox JA, Schmitt B, Betz H (1991) Molecular cloning of an invertebrate glutamate receptor subunit expressed in Drosophila muscle. Science 254:112-114.

Scott DB, Blanpied TA, Swanson GT, Zhang C, Ehlers MD (2001) An NMDA receptor ER retention signal regulated by phosphorylation and alternative splicing. J Neurosci 21:3063-3072.

Sharom FJ (1997) The P-glycoprotein multidrug transporter: interactions with membrane lipids, and their modulation of activity. Biochem Soc Trans 25:1088-1096.

Shenoy-Scaria AM, Dietzen DJ, Kwong J, Link DC, Lublin DM (1994) Cysteine3 of Src family protein tyrosine kinase determines palmitoylation and localization in caveolae. J Cell Biol 126:353-363.

Shouffani, A. and B. I. Kanner (1990). "Cholesterol is required for the reconstruction of the sodium- and chloride-coupled, gamma-aminobutyric acid transporter from rat brain." J Biol Chem 265(11): 6002-8.

Simons K, Ikonen E (1997) Functional rafts in cell membranes. Nature 387:569-572.

Spiegel AM, Weinstein LS (2004) Inherited diseases involving g proteins and g protein-coupled receptors. Annu Rev Med 55:27-39.

Tanabe Y, Masu M, Ishii T, Shigemoto R, Nakanishi S (1992) A family of metabotropic glutamate receptors. Neuron 8:169-179.

Tanabe, Y., M. Masu, et al. (1992). "A family of metabotropic glutamate receptors." Neuron 8(1): 169-79.

Teixeira A, Chaverot N, Schroder C, Strosberg AD, Couraud PO, Cazaubon S (1999) Requirement of caveolae microdomains in extracellular signal-regulated kinase and focal adhesion kinase activation induced by endothelin-1 in primary astrocytes. J Neurochem 72:120-128.

Tian C, Breyer RM, Kim HJ, Karra MD, Friedman DB, Karpay A, Sanders CR (2005) Solution NMR spectroscopy of the human vasopressin V2 receptor, a G protein-coupled receptor. J Am Chem Soc 127:8010-8011.

Tlapak-Simmons VL, Baggenstoss BA, Clyne T, Weigel PH (1999) Purification and lipid dependence of the recombinant hyaluronan synthases from Streptococcus pyogenes and Streptococcus equisimilis. J Biol Chem 274:4239-4245.

Ushio-Fukai M, Hilenski L, Santanam N, Becker PL, Ma Y, Griendling KK, Alexander RW (2001) Cholesterol depletion inhibits epidermal growth factor receptor transactivation by angiotensin II in vascular smooth muscle cells: role of cholesterol-rich microdomains and focal adhesions in angiotensin II signaling. J Biol Chem 276:48269-48275.

van der Does C, Swaving J, van Klompenburg W, Driessen AJ (2000) Non-bilayer lipids stimulate the activity of the reconstituted bacterial protein translocase. J Biol Chem 275:2472-2478.

van der Heide T, Stuart MC, Poolman B (2001) On the osmotic signal and osmosensing mechanism of an ABC transport system for glycine betaine. Embo J 20:7022-7032.

Varsanyi M, Tolle HG, Heilmeyer MG, Jr., Dawson RM, Irvine RF (1983) Activation of sarcoplasmic reticular Ca2+ transport ATPase by phosphorylation of an associated phosphatidylinositol. Embo J 2:1543-1548.

Weiss, H. M. and R. Grisshammer (2002). "Purification and characterization of the human adenosine A(2a) receptor functionally expressed in Escherichia coli." Eur J Biochem 269(1): 82-92.

Wyse BD, Prior IA, Qian H, Morrow IC, Nixon S, Muncke C, Kurzchalia TV, Thomas WG, Parton RG, Hancock JF (2003) Caveolin interacts with the angiotensin II type 1 receptor during exocytic transport but not at the plasma membrane. J Biol Chem 278:23738-23746.

Yamaguchi T, Murata Y, Fujiyoshi Y, Doi T (2003) Regulated interaction of endothelin B receptor with caveolin-1. Eur J Biochem 270:1816-1827.

Zerangue N, Schwappach B, Jan YN, Jan LY (1999) A new ER trafficking signal regulates the subunit stoichiometry of plasma membrane K(ATP) channels. Neuron 22:537-548.